LEABHARLANN CHOLÁISTE NA TRÍONÓIDE, BAILE ÁTHA CLIATH | TRINITY COLLEGE LIBRARY DUBLIN
Ollscoil Átha Cliath | The University of Dublin

Terms and Conditions of Use of Digitised Theses from Trinity College Library Dublin

Copyright statement

All material supplied by Trinity College Library is protected by copyright (under the Copyright and Related Rights Act, 2000 as amended) and other relevant Intellectual Property Rights. By accessing and using a Digitised Thesis from Trinity College Library you acknowledge that all Intellectual Property Rights in any Works supplied are the sole and exclusive property of the copyright and/or other IPR holder. Specific copyright holders may not be explicitly identified. Use of materials from other sources within a thesis should not be construed as a claim over them.

A non-exclusive, non-transferable licence is hereby granted to those using or reproducing, in whole or in part, the material for valid purposes, providing the copyright owners are acknowledged using the normal conventions. Where specific permission to use material is required, this is identified and such permission must be sought from the copyright holder or agency cited.

Liability statement

By using a Digitised Thesis, I accept that Trinity College Dublin bears no legal responsibility for the accuracy, legality or comprehensiveness of materials contained within the thesis, and that Trinity College Dublin accepts no liability for indirect, consequential, or incidental, damages or losses arising from use of the thesis for whatever reason. Information located in a thesis may be subject to specific use constraints, details of which may not be explicitly described. It is the responsibility of potential and actual users to be aware of such constraints and to abide by them. By making use of material from a digitised thesis, you accept these copyright and disclaimer provisions. Where it is brought to the attention of Trinity College Library that there may be a breach of copyright or other restraint, it is the policy to withdraw or take down access to a thesis while the issue is being resolved.

Access Agreement

By using a Digitised Thesis from Trinity College Library you are bound by the following Terms & Conditions. Please read them carefully.

I have read and I understand the following statement: All material supplied via a Digitised Thesis from Trinity College Library is protected by copyright and other intellectual property rights, and duplication or sale of all or part of any of a thesis is not permitted, except that material may be duplicated by you for your research use or for educational purposes in electronic or print form providing the copyright owners are acknowledged using the normal conventions. You must obtain permission for any other use. Electronic or print copies may not be offered, whether for sale or otherwise to anyone. This copy has been supplied on the understanding that it is copyright material and that no quotation from the thesis may be published without proper acknowledgement.

Identification of factors involved in 3' end processing and transcription termination of histone mRNAs

A dissertation presented for the degree of Doctor of Philosophy, in the Faculty of Science, University of Dublin, Trinity College.

February 2011

by

Suzanne Martina Beggs

Department of Microbiology

Moyne Institute of Preventive Medicine

Trinity College Dublin

TRINITY COLLEGE
19 JUL 2011
LIBRARY DUBLIN
THESIS
9092

Declaration

I, Suzanne Martina Beggs, certify that the experimentation recorded herein represents my own work, unless otherwise stated in the text and has not been previously presented for a higher degree at this or any other University. This thesis may be lent or copied at the discretion of the Librarian.

Suzanne Beggs.

Suzanne Martina Beggs.

Summary

The production of core histone mRNAs is tightly regulated during the cell cycle in all eukaryotic cells. Histone mRNAs accumulate during the S-phase and are subsequently degraded upon entry into G2-phase of the cell cycle. This precise expression requires regulation at the level of gene transcription, transcript processing, nuclear export and RNA and protein degradation.

Previous research has shown that factors involved in the nuclear RNA surveillance system contribute to the biogenesis of histone mRNAs. Deletion of *RRP6*, a component of the nuclear exosome, leads to accumulation of *HTB1* mRNA during the S-phase and a delay in entry of cells into G2-phase. Additionally mutations in components of the TRAMP complex alter the steady state levels of histone mRNAs. In addition to their roles in degrading aberrant RNA transcripts, both TRAMP and the nuclear exosome are required for 3'end processing of non-polyadenylated snRNAs and snoRNAs following Nrd1p/Nab3p/Sen1p-mediated transcription termination.

This thesis sets out to explore the role of other factors in the non-coding, non-polyadenylated processing machinery in the regulation of histone mRNA levels in *Saccharomyces cerevisiae*. Focusing the on the components of the Nrd1p/Nab3p/Sen1p complex, we found that inactivation of Sen1p led to increased read-through beyond the 3' end processing sites of the yeast histone mRNA *HTB1*. This action of Sen1p was independent of Nrd1p and Nab3p. The identification of a role for factors required in the processing of non-polyadenylated RNAs in the biogenesis of yeast histone mRNAs prompted us to reinvestigate the polyadenylation status of these mRNAs. Using a novel hybrid selection and G-tailing procedure and subsequent cDNA cloning of *HTB1* mRNAs, we examined the length of the poly(A) and cleavage site usage in both asynchronous and cell cycle regulated cells. Our analysis of the polyadenylation status revealed that in asynchronous cells, histone mRNAs have shorter than average poly(A) tails and can be divided into three distinct populations, differing in poly(A) tail length. Inactivation of Sen1p and Rrp6p led to a decrease in the average poly(A) tail length of histone mRNA suggesting a role for these factors in the 3' end processing of histone mRNAs. Additionally, analysis of the asynchronous cells revealed five canonical cleavage sites present in wild type cells. Analysis of synchronised cells found that during the cell cycle, poly(A) tail length varies, with histone mRNAs in S-phase possessing very short poly(A) tails while those in G1-phase have longer poly(A) tails.

During G2-phase, histone mRNAs with two poly(A) tail lengths were detected – those with poly(A) tails of 25-50nts and those with no poly(A) tails. The discovery of histone mRNAs with no poly(A) tail coincided with the discovery of numerous non-canonical 3' ends located upstream of the stop *HTB1* stop codon. The involvement of components of the SCF ubiquitin ligase complexes, such as Skp1p and F-box proteins, which controls levels of many cell cycle regulated proteins in the biogenesis of histone mRNAs was also explored. The results indicate that mutations in Skp1p or F-box proteins do not affect transcription termination of histone mRNA but decreases in the steady state levels of *HTB1* mRNA were detected in some F-box mutants.

Taken together the research presented in this thesis demonstrates that histone mRNAs are distinct from the general pool of mRNAs in yeast cells and are regulated during the cell cycle by 3'end processing and polyadenylation.

Acknowledgements

My special thanks to my supervisor, Dr. Ursula Bond, for all of her help, support and advice over the past four years. A huge thank you to Tharappel C. James for his constant advice and encouragement and keeping me supplied with colourful lab equipment to brighten up my day. A special thank you to my fellow lab members, past and present – my bay-buddy Jimmy, Christina, Jane and Joanne, the one person who truly understood my need for organisation, I really couldn't have done this without you guys. Thank you for all the advice, encouragement and listening to me moan but most of all, thank you for all of the laughs. Best of luck to Will the newest member of the Bond lab.

Thank you to past and present members of the Dorman lab, especially Fitzy, Kelly, Heather, Shane, Andrew and Colin, for all their help, encouragement and sharing of knowledge on science and non-science related topics. I also wish to thank the members of the Foster lab, not only for making me an honorary "Fosterette" but for always letting me "borrow" whatever I needed. Your constant supplies of chocolate got me through some pretty tough days. I especially want to thank Emma for always being there when I needed a chat.

Thank you to everyone in the Moyne Institute, especially Gerry, Dave, Margaret, Myriam, Ronan and Stephen from the prep room and our executive officers; Jayne, Noreen and Caroline. I wish to thank my funding board, Science Foundation Ireland. Thank you for making this research possible.

A huge and special thank you to John, whose ability to make me always laugh got me through the bad science days. Your constant support and encouragement kept me going.

Finally, I wish to give my utmost special thanks to my Mum and Dad, and my brother Stephen, for their continuous love, encouragement and support. This would not have been possible without you.

Publications and Conference Communications

Publication:

Suzanne Beggs and Ursula Bond. (2011). "The PolyA Tail Length of Yeast Histone mRNAs varies during the Cell Cycle and is influenced by Sen1p and Rrp6p." *Accepted Nucleic Acid Research.*

Conference Communications:

Suzanne Beggs and Ursula Bond. The Role of *SEN1* in the Regulation of Histone mRNA Levels in *Saccharomyces cerevisiae.* Oral presentation at the Irish Fungal Meeting, University College Cork, June 2010.

Suzanne Beggs and Ursula Bond. The Role of *SEN1* in the Regulation of Histone mRNA Levels in *Saccharomyces cerevisiae.* Poster presentation at the Irish Fungal Meeting, University College Dublin, June 2009.

Suzanne Beggs, Ruth Canavan and Ursula Bond. The role of F-box proteins in the regulation of histone mRNA levels in *Saccharomyces cerevisiae.* Oral presentation at S.G.M. Autumn Meeting, Trinity College Dublin, September 2008.

Suzanne Beggs and Ursula Bond. The role of F-box proteins in the regulation of histone mRNA levels in *Saccharomyces cerevisiae.* Poster presentation at the Irish Fungal Meeting, N.U.I. Galway, June 2008.

Suzanne Beggs and Ursula Bond. The role of F-box proteins in the regulation of histone mRNA levels in *Saccharomyces cerevisiae.* Poster presentation at the British Yeast Group Meeting, N.U.I. Maynooth, March 2008.

Suzanne Beggs and Ursula Bond. The role of messenger RNA 3'-end formation and transcription termination in the cell cycle regulation of histone mRNAs. Poster presentation at the Irish Fungal Meeting, N.U.I. Maynooth. June 2007.

Index of Figures

Contents

Chapter 1

Introduction

1.1 Overview

A typical human diploid cell contains $3.1x10^9$ base pairs of deoxyribonucleic acid (DNA) which when unwound measures 1.2m in length. This large amount of DNA is tightly wrapped and compacted into an octameric complex through a series of interactions with a set of small proteins called histones. The octameric complex is called the nucleosome (Baxevanis and Landsman, 1998; Recht et al., 1996). Histones are positively charged proteins which facilitate the folding of DNA. Four types of histones have been described: H2A, H2B, H3 and H4, which organise as a single $(H3\text{-}H4)_2$ tetramer and two H2A-H2B dimers, around which 146 base pairs of DNA are wrapped to form the basic structural octamer of the nucleosome (Baxevanis and Landsman, 1997, 1998; Eriksson et al., 2005; Recht et al., 1996). The structure of the nucleosome is stabilised through an interaction with another histone, H1, which binds to the DNA in between the nucleosome core particles (Baxevanis and Landsman, 1997). The core histones of the nucleosome are highly conserved with 95% identity across all known H4 sequences. However histone H1 is only conserved in its central globular domain (Baxevanis and Landsman, 1998).

The level of compaction of DNA varies during the eukaryotic cell cycle. During interphase, chromatin is relatively decondensed and is distributed throughout the nucleus. As cells enter mitosis, chromatin condenses into chromatin structures which are relatively transcriptionally silent. As the cells undergo DNA replication, newly formed DNA must be repackaged into chromatin. As a result of this, the production of histones is tightly regulated to ensure that maximum production occurs in the S-phase of the cell cycle (Lycan et al., 1987; Marzluff et al., 2008; Xu et al., 1990).

During the cell cycle, low levels of histone mRNAs are detected during G1-phase of the cell cycle. Replication-dependent histone mRNAs accumulate upon entry into S-phase and are subsequently degraded rapidly upon entry into G2-phase of the cell cycle as a result of various critical control mechanisms at the levels of transcription, mRNA 3'-end formation and mRNA degradation. Cell cycle regulation of histone mRNAs leading to optimum expression during the S-phase is highly conserved between lower and higher eukaryotes. Despite the conservation of function, the mechanisms of histone mRNA biogenesis vary between the lower and higher eukaryotes. In particular,

histones in higher eukaryotes are non-polyadenylated while in lower eukaryotes such as the yeast *Saccharomyces cerevisiae*, histones are polyadenylated

This thesis aims to extend our knowledge of histone mRNA biogenesis in *S. cerevisiae* by investigating the role of a number of 3' end processing and transcription termination factors in the biogenesis of histone mRNAs. Given the differences in polyadenylation of histone mRNAs in lower and higher eukaryotes, we also sought to re-examine the 3'end cleavage and polyadenylation status of histone mRNAs in *S. cerevisiae*. Finally, the role of novel protein factors, in particular factors involved in the ubiquitin-mediated degradation of a number of cell cycle regulated proteins, in histone mRNA biogenesis was explored. This Introduction presents the background research into the general 3' end RNA processing and histone mRNA 3' end processing mechanisms within yeast and mammals. The 3' end processing and transcription termination machinery of non-polyadenylated RNAs is also described.

1.2 3' end processing of eukaryotic genes

The 3' end formation of eukaryotic messenger RNA precursors (pre-mRNA) is a fundamental step in gene expression of mature mRNAs and consists of two coupled nuclear reactions; a site-specific endonucleolytic cleavage event followed by polyadenylation of the newly formed 3' end (Dichtl and Keller, 2001; Viphakone et al., 2008; Zhao et al., 1999).

Cis-acting sequences in the vicinity of the 3' end cleavage site direct binding of a number of trans-acting factors to facilitate efficient and accurate 3' end processing and polyadenylation. While the trans-acting factors of pre-mRNA 3'end formation are highly conserved from yeast to mammals, the cis-acting sequences governing the reactions in the two organisms are different. The cis-acting and trans-acting factors involved in 3' end processing have been extensively studied using genetic, biochemical and two-hybrid analysis. In yeast, up to twenty factors have been identified as being involved in the 3' end processing of pre-mRNA while in mammals at least fourteen factors are required. The mechanism of 3' end cleavage and polyadenylation of mRNAs has recently been reviewed by (Mandel et al., 2008; Proudfoot, 2004; Zhao et

al., 1999) and is briefly summarised here. A summary of the cis-acting and trans-acting factors of mammals and yeast are shown in *Figure 1.1* and *Table 1.1*.

1.2.1 Cis-elements of cleavage and polyadenylation in higher and lower eukaryotes

In mammals, there are three primary sequence elements that define the cleavage and polyadenylation site and two auxiliary sequence elements that enhance and regulate the 3' end processing of pre-mRNA. The three primary elements are the highly conserved AAUAAA polyadenylation signal, the U-rich or GU-rich downstream element (DSE) and a dinucleotide CA cleavage site (*Figure 1.1A*). This sequence is often referred to as the poly(A) site as along with being the point of cleavage, it is also the point of polyadenylation. Two auxiliary sequences, consisting of the upstream U-rich element and another G-rich DSE have been identified in mammals (Dominski and Marzluff, 2007; Zhao et al., 1999). The polyadenylation signal (AAUAAA) usually lies approximately 13-15nt upstream of the cleavage site (Zhao et al., 1999). The DSE is generally located within 30nts of the cleavage site although it can often be found further downstream while the auxiliary upstream elements are located upstream of the polyadenylation signal (*Figure 1.1A*). The cleavage and polyadenylation site is positioned between the polyadenylation signal and the DSE (Mandel et al., 2008; Zhao et al., 1999).

The analysis of 3' end formation in the yeast *S. cerevisiae* has proved more complicated than in higher eukaryotes, mainly due to the lack of highly conserved sequence elements governing yeast mRNA 3' end formation. Three cis-acting sequences; the efficiency element (EE), the positioning element (PE) and the poly(A) site have been defined (*Figure 1.1B*). The efficiency element (EE) which usually consists of UA dinucleotides or U-rich stretches, is located upstream of the cleavage site but the distance from the cleavage site can vary (Mandel et al., 2008; Zhao et al., 1999). The positioning element (PE) contains a loosely conserved A-rich sequence and is located downstream of the EE and approximately 10-30 nucleotides upstream of the cleavage site. The cleavage/polyadenylation site consists of a consensus sequence $Py(A)_n$, where Py denotes pyrimidine. Conserved upstream and downstream U-rich elements (UUE

and DUE) are also involved in yeast 3' end formation (*Figure 1.1B*) (Mandel et al., 2008).

1.2.2 Trans-acting factors of cleavage and polyadenylation in higher and lower eukaryotes

In higher and lower eukaryotes, a large number of trans-acting factors, involved in cleavage and polyadenylation, have been identified by genetic, biochemical and two-hybrid analysis. The majority of trans-acting factors are highly conserved between higher and lower eukaryotes, however they are often found in different complexes (*Table 1.1*).

As shown in *Figure 1.1A*, cleavage of mammalian pre-mRNA requires five separate protein complexes; the cleavage and polyadenylation specificity factor (CPSF), the cleavage stimulation factor (CstF), cleavage factors I and II (CF I_m and CF II_m) and poly(A) polymerase (PAP). The components of each protein complex are shown in *Figure 1.1A* and listed in *Table 1.1*. An important milestone in recent years was the emergence of data which suggested that CPSF-73 of CPSF was the endonuclease responsible for the cleavage reaction (Dominski and Marzluff, 2007; Mandel et al., 2006; Millevoi and Vagner, 2010). The discovery of a metallo-β-lactamase domain and within this domain a β-CASP domain in CPSF-73 led to speculation that CPSF-73 was the endonuclease responsible for the 3' end cleavage reaction. Further evidence that CPSF-73 possessed endonucleolytic activity was provided by Mandel *et al.*, (2006) who demonstrated that bacterially expressed N-terminal portion of human CPSF-73 (amino acids 1-460) encompassing the metallo-β-lactamase and the β-CASP domains can cleave single stranded RNA substrates *in vitro*. Additionally cleavage of AAUAAA-containing pre-mRNAs was found to require zinc ions which is consistent with CPSF-73 being the endonuclease (Dominski and Marzluff, 2007; Mandel et al., 2006; Proudfoot, 2004). Although this data strongly suggests that CPSF-73 is the endonuclease responsible for the 3' end cleavage reaction, the final biochemical studies to prove its role have yet to be carried out.

Homologues of mammalian cleavage and polyadenylation factors are also found in yeasts, although they are often found in different complexes (*Table 1.1*). In yeast,

cleavage factor I (CF I) is required for cleavage. CFI consists of cleavage factor IA (CF IA), cleavage factor IB (CF IB) and cleavage factor II (CF II). Polyadenylation requires CF IA, polyadenylation factor I (PF I), poly(A) polymerase (PAP) and poly(A) binding protein (Pab1p) (*Figure 1.1B*) (Mandel et al., 2008; Proudfoot, 2004; Zhao et al., 1999). CF IA is a tetrameric factor consisting of Rna14p, Rna15p, Pcf11p and Clp1p while CF IB consists of Hrp1p. CF II consists of Yhh1p/Cft1p, Ydh1p/Cft2p, Ysh1p/Brr5p and Pta1p. PF I is a large complex consisting of eight subunits; Fip1p, Pfs2p, Yth1p, Mpe1p and the four CF II subunits. The combination of PF I and CF II has been termed as cleavage and polyadenylation factor (CPF) (Ohnacker et al., 2000). A number of additionally auxiliary protein factors have been linked to the CPF complex - Ref2p, Pti1p, Ssu72p, Glc7p, Swd2p and Syc1p (Gavin et al., 2002).

Within the CF IA complex, Rna15p binds specifically to the A-rich positioning element (PE) and has also been found to directly interact with Rna14p both *in vivo* and *in vitro* (Noble et al., 2004). The role of Rna14p and Rna15p of CF IA in cleavage and polyadenylation was first discovered through analysis of temperature sensitive mutations of genes encoding these proteins (Minvielle-Sebastia et al., 1991). Further studies demonstrated that Rna14p, Rna15p and Pcf11p were required for 3' end cleavage and proper transcription termination as inactivation of these genes at 37°C led to an accumulation of unprocessed read-through transcripts (Birse et al., 1998; Canavan and Bond, 2007).

The CF IB complex, consisting of Hrp1p, binds to the U-rich efficiency element (EE) and Rna14p acts to bridge Rna15p and Hrp1p (*Figure 1.1B*) (Gross and Moore, 2001; Mandel et al., 2008). In addition to interacting with Rna14p, Rna15p and Clp1p, Pcf11p can bind to the C-terminal domain (CTD) of the largest subunit of RNA Polymerase II through its CTD-interacting domain (Licatalosi et al., 2002). Pcf11p also interacts with CPF components, Ydh1p/Cft2p, Yhh1p/Cft1p, Ysh1p/Brr5p and Pta1p. Yhh1p/Cft1p binds to the poly(A) site and can interact with the CTD of RNA Polymerase II indicating that it is involved in direct interactions with the RNA substrate and the CTD of RNA Polymerase II (Dichtl et al., 2002). The Yhh1p/Cft1p and Ysh1p/Brr5p subunits have been shown to interact with Rna14p and Clp1p of CF IA. Ydh1p/Cft2p interacts with many CPF subunits, including Yhh1p/Cft1p, Ysh1p/Brr5p, Pta1p, Pfs2p and Ssu72p.

The PF I component Yth1p interacts with both Fip1p and the RNA transcript. This interaction is important for correct cleavage and poly(A) addition (Tacahashi et al., 2003). The Pfs2p protein of the PF I complex interacts with Rna14p, Ysh1p/Brr5p and Fip1p (Ohnacker et al., 2000). Fip1p also interacts physically with Pap1p, Yth1p and Rna14p suggesting that there is an important interaction between CF I, PF I and PAP (Helmling et al., 2001).

The CPF complex consists of fifteen polypeptides and its mechanism of assembly onto the RNA substrates is not clear. However through two-hybrid analysis, Pti1p, one of the auxiliary factors linked to the CPF complex, has been found to interact with Pta1p and Ref2p (Dheur et al., 2003). Ssu72p has also been found to interact with Pta1p (He et al., 2003).

Figure 1.1: Comparison of mammalian and yeast 3' end processing machinery. The cis-acting elements of both complexes are shown in black along the black line representing the pre-mRNA. **A.** Mammalian cis-acting and trans-acting elements of cleavage and polyadenylation. The components of the mammalian 3' end processing machinery are depicted as colour coded circles. Protein factors within each complex are depicted in the same colour; CstF subunits, blue, CPSF subunits, red, CF I_m subunits, purple, CF II_m subunits, green and PAP, pink. **B.** Yeast cis-acting and trans-acting elements of cleavage and polyadenylation. The components of the yeast 3' end processing machinery are depicted as colour-coded circles; CF IA subunits, blue, CF IB subunit, green, CF II subunits, red, PF I subunits, purple and PAP, pink. The yeast auxiliary protein factors are shown in yellow. Homologous proteins between the two 3' end processing machineries are described in Table 1.1.

A. Mammalian 3' end processing machinery

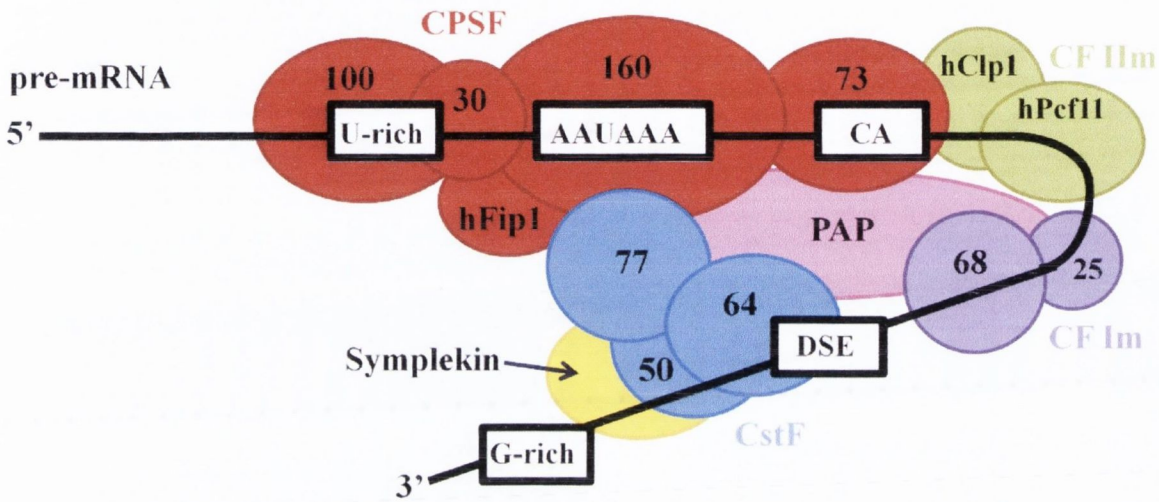

B. Yeast 3' end processing machinery

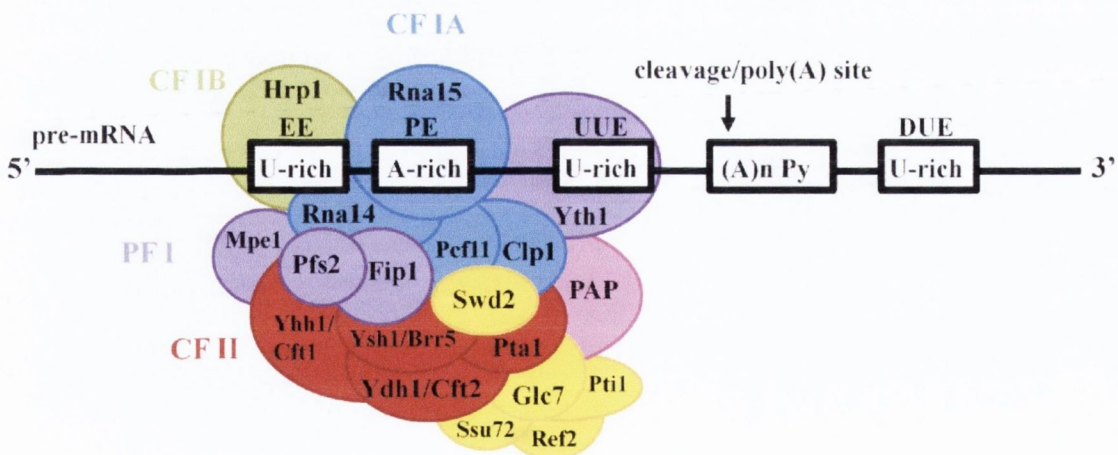

Table 1.1: Yeast pre-mRNA 3' end processing factors and their mammalian homologues

Yeast factor	Reaction step involved in	Yeast gene	Mammalian homologue	Mammalian factor	Function in yeast
CFIA	Cleavage and	*RNA14*	CstF-77	CstF	Forms a heterodimer with RNA15
	polyadenylation	*PCF11*	hPcf11	CF II_m	Binds to RNA14 and RNA15, Interacts with components of CFII
		CLP1	hClp1	CF II_m	Binds to PCF11, YSH1/BRR5 and YDH1/CFT2
		RNA15	CstF-64	CstF	Interacts with RNA14, Binds AE rich PE
	Polyadenylation	*PABI*	-	-	Binds to RNA15, Involved in poly(A) tail length control
CFIB	Cleavage	*HRP1/NAB4*	-	-	Interacts with RNA14 and RNA15, Crosslinks to AU-rich EE in RNA
CFII	Cleavage	*YHH1/CFT1*	CPSF-160	CPSF	Interacts with CTD of RNA Polymerase II
		YDH1/CFT2	CPSF-100	CPSF	ATP-dependent RNA binding
		YSH1/BRR5	CPSF-73	CPSF	Interacts with Clp1p, Pta1p
		PTA1	-	-	Interacts with phosphatase, Glc7p
PFI	Polyadenylation	*YHH1/CFT1*	CPSF-160	CPSF	Interacts with CTD of RNA polymerase II
		YDH1/CFT2	CPSF-100	CPSF	RNA binding is ATP-dependent
		YSH1/BRR5	CPSF-73	CPSF	Interacts with Clp1p, Pta1p, Fip1p

		PTA1	-	-	Interacts with phosphatase, Glc7p
		PAP1	PAP	PAP	Catalyses poly(A) tail extension, Interacts with FIP1
		MPE1	-	-	Interacts with other members of CPF and RNA14 of CFIA
		FIP1	hFip1	CPSF	Interacts with YTH1, RNA14 and PAP1
		PFS2	-	-	Interacts with YSH1/BRR5, FIP1 and RNA14
		YTH1	CPSF-30	CPSF	Interacts with FIP1, Binds to U-rich sequences (UUE and DUE) in RNA
Auxiliary factors of CPF	Cleavage and polyadenylation	*PTI1*	CstF-64	CstF	Interacts with Glc7p, Rna14p, Pcf11p and Pta1p
		SWD2	-	-	Interacts with proteins of CPF and PCF11 of CFIA
		SSU72	-	-	Interacts with PTA1, YDH1/CFT2 and Rpb2p of RNA Polymerase II
		GLC7	-	-	Interacts with PTA1
		REF2	-	-	Interacts with SWD2, Required for efficient 3' end processing of poorly identified poly(A) sites
		SYC1	-	-	Not required for 3' end processing but may negatively regulate 3' end processing possibly by competing with CTD of Brr5p

1.3 Interrelationships between mRNA 3' end formation and other processes

RNA Polymerase II plays a key role in gene expression and it mediates the recruitment of many factors involved in processing of the primary transcript including 5' capping, mRNA splicing and 3' end formation. For many years, researchers have focused on understanding the mechanisms of the individual mRNA transcription and processing reactions. Emerging information on the links between pre-mRNA processing and its associated factors has led researchers to view gene expression as a dynamic process with interactions occurring between transcription, mRNA processing and termination. These interactions are tightly co-ordinated and are ultimately required to ensure the final export of mature mRNAs. This next section outlines the current understanding of the communications between transcription, 3' end processing and termination.

1.3.1 Coupling of 3' end formation and transcription

The C-terminal domain (CTD) of the largest subunit of RNA Polymerase II, Rpb1p, consists of 26 heptad repeats with the sequence Tyr-Ser-Pro-Thr-Ser-Pro-Ser in *S. cerevisiae*. The mammalian CTD of RNA Polymerase II contains 52 heptad repeats with the same sequence although variants of the heptad repeat have been identified (Proudfoot, 2004). The CTD acts as a recruitment platform for transcription and mRNA processing factors. As a result, efficient capping, splicing and polyadenylation are dependent on the CTD (Noble et al., 2005). Using deletions in the CTD in an *rbp1-1* mutant background, Licatalosi *et al.*, (2002) demonstrated that the CTD was required for efficient 3' end cleavage of pre-mRNAs. They also observed shorter poly(A) tails in CTD deletion strains lacking the poly(A) nuclease (PAN) which is responsible for trimming the poly(A) tail in the nucleus (Licatalosi et al., 2002).

The key feature of the CTD is the presence of serines at positions 2, 5 and 7 in the heptad repeats. These serine residues are subject to phorphorylation by specific cyclin-associated kinases. In mammals, Cdk7, a component of TFIIH, phosphorylates serine 5 of the CTD at the promoter and recruit the capping enzyme, guanylyltransferase (Akhtar et al., 2009; Glover-Cutter et al., 2009; Kim et al., 2009a). A second kinase, Cdk9, plays a role in negatively regulating transcription initiation. As RNA Polymerase

II switches from initiation to elongation, serine 5 becomes dephosphorylated by Rtr1p phosphatase and there is a concomitant phosphorylation of serine 2 by Cdk9/P-TEFb (Bur1p and Ctk1p in *S. cerevisiae*) which promotes efficient elongation and subsequently termination (Buratowski, 2009; Kim et al., 2009b; Komarnitsky et al., 2000). Levels of serine 2 phosphorylation are modulated by the serine 2 phosphatase Fcp1p, which leads to a gradual increase in phosphorylated serine 2 as RNA polymerase II moves farther away from the promoter (Kim et al., 2009b). Phosphorylation of serine 7 has been shown to be involved in snRNA-processing but has yet to be shown to be involved in mRNA processing (Egloff et al., 2007). Several other CTD phosphatases have been identified in *S. cerevisiae,* including Scp1p and Ssu72p, which may play a direct role in RNA Polymerase II elongation/termination and the recycling of RNA Polymerase II for re-initiation of transcription (Buratowski, 2009; Proudfoot, 2004). During transcription, the binding of 3' end processing factors to the CTD is dependent on the phosphorylation status of the CTD (Vasiljeva et al., 2008). Direct contact between yeast cleavage and polyadenylation factors such as Pcf11p of CF IA, Hrp1p of CF IB, Yhh1p/Cft1p of CPF and the phosphorylated CTD has been demonstrated both biochemically and genetically (Licatalosi et al., 2002; Proudfoot, 2004).

The protein Pcf11p which is a component of CF IA, plays an essential role in the recruitment of other components of CF IA (Rna14p, Rna15p and Clp1p) and CF IB (Hrp1p/Nab4p) to the CTD via its N-terminal CTD-interaction domain (CID). The CID of Pcf11p interacts with the serine 2 phosphorylated form of RNA Polymerase II, consistent with CF IA playing a role in termination (Amrani et al., 1997; Proudfoot, 2004). Pta1p, Ydh1p/Cft2p and Fip1p of CPF have also been found to interact directly with the CTD of RNA Polymerase II (Kyburz et al., 2003).

1.3.2 Coupling of 3' end formation and termination

The final stage in the transcription process, termination, is critical for successful gene expression as it allows for the release of transcripts from the site of transcription and the release of RNA Polymerase II from the DNA template. This facilitates the recycling of RNA Polymerase II back to the promoter for further rounds of transcription (Proudfoot

et al., 2002). The mechanism of termination requires the recognition of polyadenylation sites and pause sites.

A link between 3' end processing and transcription termination was first discovered in mammals by (Whitelaw and Proudfoot, 1986) and in yeast by Birse *et al.*, (1998) using transcription run-on analysis in temperature sensitive mutants of CF IA components, *rna14*, *rna15* and *pcf11*. These studies revealed that inhibition of 3' end cleavage by incubation at the non-permissive temperature resulted in a decrease in transcription termination and an accumulation of read-through transcripts in all three mutants (Birse et al., 1998).

Recently a role for the CTD of RNA Polymerase II in transcription termination has been described. Using truncation mutants of the mammalian CTD of RNA Polymerase II, Park *et al.*, (2004) demonstrated that the CTD was not required for RNA Polymerase II poly(A) dependent pausing but was required for the release of RNA Polymerase II from the transcript (Park et al., 2004). Additionally, Zhang *et al.*, (2005) demonstrated that mutations in the CTD of RNA Polymerase II led to inaccurate transcription termination.

As mentioned above, several proteins involved in 3' end processing have been shown to interact with the CTD of RNA Polymerase II. Mutations in the CID of Pcf11p and Yhh1p/Cft1p have also been found to cause defects in transcription termination in yeast (Dichtl et al., 2002; Zhang et al., 2005). This suggests that both the CTD of RNA Polymerase II and the CID of Pcf11p play important roles in transcription termination. In *Drosophila* cells, dPcf11p appears to act as a bridge between the RNA Polymerase CTD and the nascent RNA. dPcf11p can inhibit transcription at low but not high nucleotide concentrations, suggesting that dPcf11p dismantles paused RNA Polymerase II complexes in metazoan cells (Zhang and Gilmour, 2006).

Two models have been proposed to account for termination of RNA Polymerase II on transcribed genes (*Figure 1.2*). The "torpedo" model (*Figure 1.2A*) proposes that upon cleavage of the pre-mRNA, the 5' phosphate on the released downstream RNA is exposed to the 5'-3' exonuclease Rat1p/Xrn2p. Rat1p/Xrn2p rapidly digests the unstable pre-mRNA transcript until it reaches the RNA Polymerase II. This triggers transcription termination through physical interaction with RNA Polymerase I (Kim et al., 2004; West et al., 2004). Pcf11p, interacts with Rat1p and it is thought that Rat1p

acts as the "torpedo" and Pcf11p acts as the terminator. Alternatively the "anti-terminator" or "allosteric" model (*Figure 1.2B*), proposes that as RNA polymerase II passes the polyadenylation signal (AAUAAA) there is a decrease in the processivity of the Polymerase. This causes the release of the DNA template, the RNA template and other factors (Ghazal et al., 2009; Kim et al., 2006a; Lykke-Andersen and Jensen, 2007; Rondon et al., 2009). Pcf11p also has the ability to dismantle transcription elongation complexes *in vitro*, possibly by bridging the nascent RNA and RNA Polymerase II CTD. This action of Pcf11p supports the "anti-terminator" termination model (Buratowski, 2005). Since both models have experimental support, it is likely that termination can occur by more than one mechanism and one pathway may dominate over the other in particular gene contexts (Kim et al., 2006a).

Transcription termination appears to be triggered by the pausing of RNA Polymerase II once it has transversed the polyadenylation signal. Identification of the cis-acting sequences responsible for the pausing of RNA Polymerase II has been difficult due to the lack of a consensus sequences within the pause sites. However, transcription termination pause sites have been identified downstream of a number of mammalian genes. The best characterised pause site is the MAZ (G_5AG_5) site which is located downstream of the human C2 complement gene. *In vitro* studies have demonstrated that four MAZ binding sites, positioned downstream of a synthetic poly(A) site, promote efficient 3' end cleavage and polyadenylation, while mutation of these MAZ sites abolishes the process (Gromak et al., 2006; Yonaha and Proudfoot, 1999).

Another sequence positioned 800bp downstream of the poly(A) site has also previously been shown to be essential for transcription termination of the human β-globin gene. RNA transcribed from the human β-globin gene encodes a co-transcriptional cleavage (CoTC) activity which contributes to termination. This site appears to act as an additional cleavage site on the pre-mRNA downstream of the poly(A) site (Dye and Proudfoot, 1999; Gromak et al., 2006) The 5'-3' exoribonuclease, Xrn2p, degrades the RNA transcript downstream of the CoTc site and in doing so promotes transcription termination (Dye and Proudfoot, 1999; Gromak et al., 2006; Kim et al., 2006a).

Figure 1.2: Models for termination by RNA Polymerase II. The proposed models for transcription termination by RNA Polymerase II demonstrate coupling between transcription, termination and 3' end processing. **A.** The torpedo model. After cleavage (lightning bolt), the 5'-3' exonuclease Rat1p (pink star) attaches to the 5' phosphate of the downstream transcript and begins digesting the remaining RNA (black line) until it reaches the RNA Polymerase II complex (blue oval), triggering terminate. The green hexagon denotes the 5' cap. **B.** The anti-terminator model. RNA Polymerase II is in its active form during elongation (blue oval). When the RNA Polymerase II passes the poly(A) site (AAUAAA), it is modified to a non-processive form, causing termination and release of RNA Polymerase II. The dotted line represents the degraded downstream RNA.

A. Torpedo model

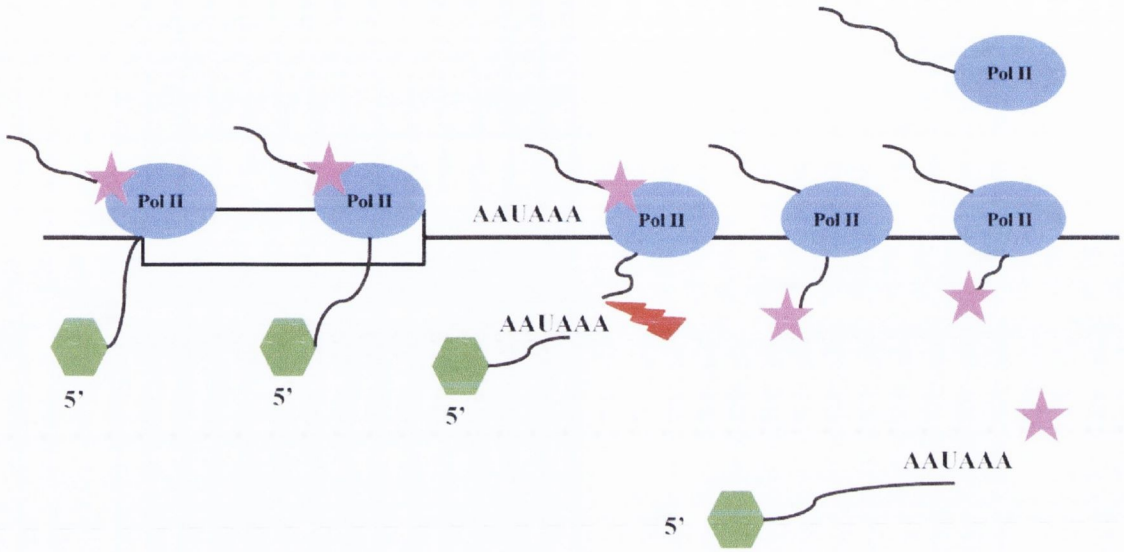

B. Anti-terminator model

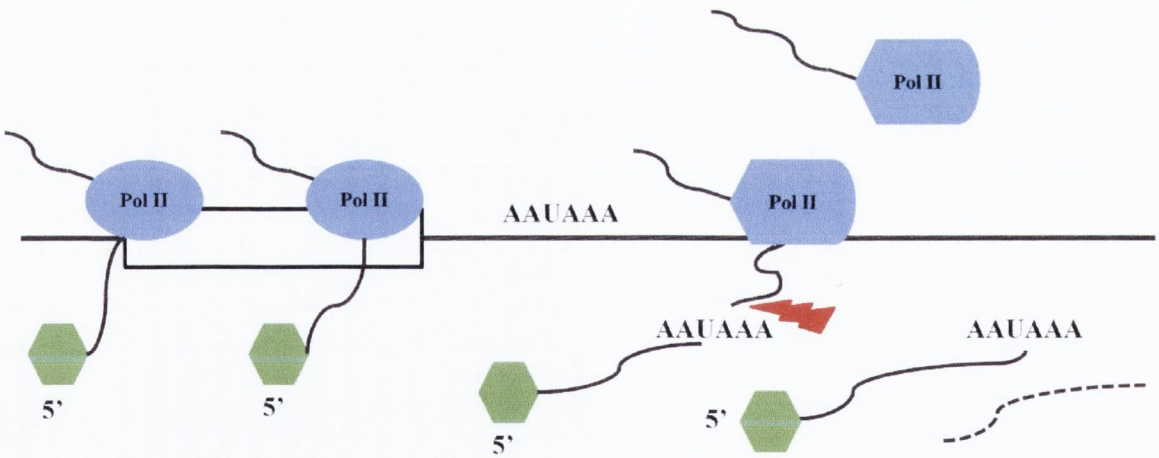

1.4 Formation of 3' ends of histone mRNAs and cell cycle regulation of histone mRNAs

In higher eukaryotes histone mRNAs belong to a small sub-set of mRNAs that are non-polyadenylated. Instead histone mRNAs contain a conserved stem-loop structure at the 3' end of the mRNA and 3' end formation requires a unique processing machinery which is quite distinct from the general 3' end cleavage and polyadenylation machinery. However a recent study by (Narita et al., 2007) has shown that the absence of Negative Elongation Factor (NELF) and Cap Binding Complex (CBC) leads to the aberrant production of polyadenylated histone mRNAs indicating that there is an aberrant fail-safe poly(A) site present at the 3' end of mammalian histone mRNAs (Narita et al., 2007). Mammalian histone gene expression is regulated at both the transcriptional and post-transcriptional level. Harris *et al.*, (1991) found that there was a 35-fold increase in histone mRNA levels during the S-phase of the cell cycle. Histone mRNAs are rapidly degraded as cells enter the G2-phase of the cell cycle resulting from changes in transcription, post-transcriptional processing and mRNA stability (Harris et al., 1991). In lower eukaryotes, histone mRNAs are polyadenylated and lack the stem-loop structure at the 3'end. Despite these differences, yeast histone mRNAs in both higher and lower eukaryotes are cell cycle regulated. The divergence in structure but the conservation of function in histone mRNA 3' end processing between higher and lower eukaryotes presents an evolutionary paradox. This next section outlines the current knowledge of mammalian and yeast histone mRNA processing.

1.4.1 Mammalian histone mRNA 3' end formation

In mammals, formation of mature histone mRNAs requires a single endonucleolytic cleavage, which is directed by two conserved cis-acting sequence elements, a stem-loop structure, which is located upstream of the cleavage site and a purine-rich histone downstream element (HDE), which is located 10 to 15 nucleotides downstream of the cleavage site (*Figure 1.3*) (Bond and Yario, 1994; Bond et al., 1991; Davila Lopez and Samuelsson, 2008; Dominski and Marzluff, 1999; Sullivan et al., 2009).

The stem-loop, which consists of a six base stem and a four nucleotide loop, is recognised by a protein called the stem-loop binding protein (SLBP) (Dominski and

Marzluff, 1999; Mullen and Marzluff, 2008; Pandey et al., 1991; Sullivan et al., 2009). Using foot-printing experiments, William and Marzluff, (1995) found that mutations in the stem-loop structure and/or sequences flanking the stem-loop structure caused a reduction in the binding affinity of SLBP, both *in vivo* and *in vitro* (Williams and Marzluff, 1995). The SLBP has also been shown to be required for histone pre-mRNA processing (Pandey et al., 1991) but also accompanies the histone mRNA to the cytoplasm were it is required for histone mRNA translation (Dominski and Marzluff, 2007; Mullen and Marzluff, 2008; Williams and Marzluff, 1995). Research has also found that the SLBP plays a direct role in histone mRNA stability through interaction with Upf1p, a factor involved in translation termination and nonsense-mediated decay (NMD) (Kaygun and Marzluff, 2005; Mullen and Marzluff, 2008).

The histone downstream element (HDE) is located 10 nucleotides downstream of 3' end cleavage site. In sea urchins, the consensus sequence for the HDE is GAAAGA and has previously been shown to be complementary to 3-8 nucleotides of sea urchin U7 snRNA (Birnstiel, 1988; Cho et al., 1995; Pandey et al., 1991). The U7 small nuclear ribonucleo-protein (U7 snRNP) (*Figure 1.3*), is a low-abundance particle present in about 10^4 copies per mammalian nucleus (Dominski and Marzluff, 1999; Sullivan et al., 2009). Subsequent studies revealed a similar complementarity between human histone mRNAs and U7 snRNP and the discovery that disruption of the base pairing leads to a reduction of 3' end processing *in vivo* (Bond et al., 1991). Bond *et al.*, (1991), demonstrated that by introducing a series of mutations in the mouse H2A-614 gene that disrupted the base-pairing between the HDE and the U7 snRNP, a reduction in processing *in vitro* is observed. Further research found that reducing the distance between the HDE and the 3' end cleavage site affected the cleavage site specifically (Scharl and Steitz, 1996). The binding of the SLBP to the stem-loop stabilises the binding of the U7 snRNP to the HDE (Davila Lopez and Samuelsson, 2008). Research has found that the 100kDa zinc finger protein, ZFP-100, acts as a bridging factor to stabilise the binding of the U7 snRNP to the HDE by interacting with both the SLBP and to Lsm11 of U7 snRNP (*Figure 1.3*) (Dominski and Marzluff, 2007).

While mostly consisting of unique factors, the histone 3' end processing machinery shares a number of proteins with the 3' end cleavage and polyadenylation machinery, including CPSF-73, CPSF-100, symplekin and possibly hFip1, all of which interact with the SLBP or the U7 snRNP (*Figure 1.3*). Although direct evidence has not yet

been shown, the endonuclease CPSF-73 is thought to be responsible for the cleavage reaction as it can be cross-linked to the cleavage site (Davila Lopez and Samuelsson, 2008; Dominski and Marzluff, 2007; Mandel et al., 2006; Marzluff et al., 2008). CPSF-100 is also involved in the cleavage reaction. Symplekin, a component of an essential heat labile factor (HLF), is also required for histone 3' end processing (Dominski and Marzluff, 2007; Millevoi and Vagner, 2010).

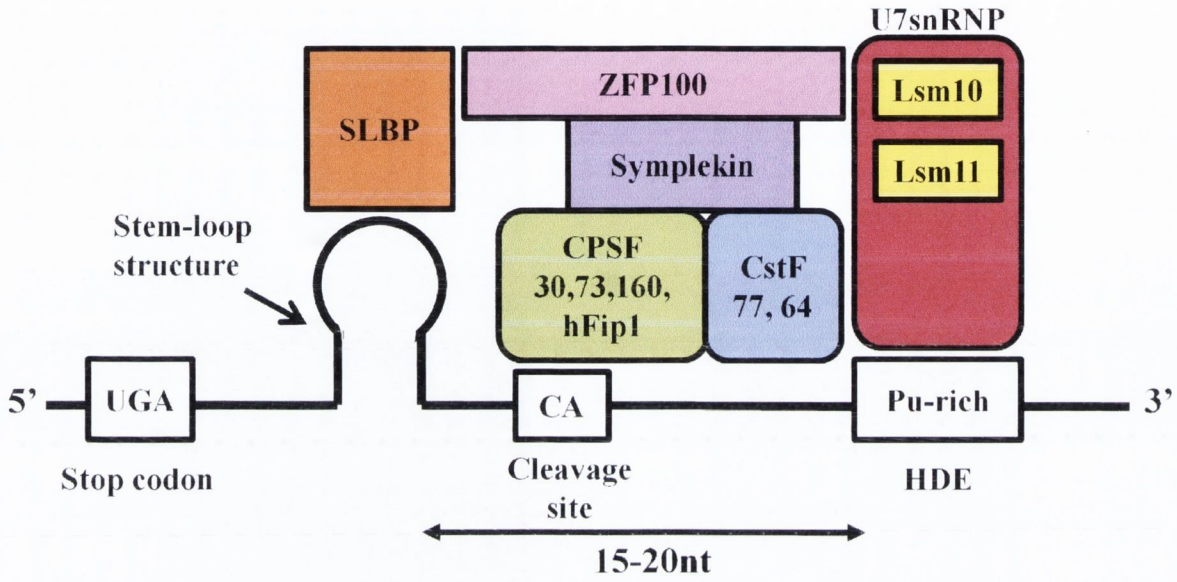

Figure 1.3: Schematic drawing of the 3' end of mammalian histone mRNA. The histone downstream element (HDE) binds with the U7 snRNP and the stem-loop binding protein binds to the stem-loop structure. Lsm11 and Lsm10 are both components of U7 snRNP. The zinc-finger binding protein 100 (ZFP100) interacts with both the SLBP and Lsm10. The proteins which are known to interact or are predicted to interact with the histone pre-mRNA complex are shown. These include CPSF-30, CPSF-73, CPSF-160, hFip1, CstF-77, CstF-64 and Symplekin. Figure adapted from (Millevoi and Vagner, 2010).

1.4.2 Mammalian histone mRNA levels during the cell cycle

1.4.2.1 Transcriptional regulation

During the cell cycle, mammalian histone gene expression is regulated through a number of individual elements. The histone gene promoter can be divided into three regions; the core promoter (CP), the subtype-specific consensus elements (SSCS) and the distal activating domain (DAD). The CP region consists of the essential RNA Polymerase II initiating sequences such as the TATA box. Mutations in the TATA box have been found to abolish the transcription of histone genes (Grunstein, 1992). The SSCS consist of a conserved CCAAT sequence and are involved in the control of histone synthesis during the S-phase as mutations in SSCS elements have been shown to disturb the efficiency of transcription during the S- phase of the cell cycle (LaBella et al., 1988; Sive et al., 1986). The distal activating domain (DAD) consists of upstream promoter elements which allow for constitutive transcription throughout the cell cycle. No core consensus promoter sequence element controlling cell cycle regulation has been identified.

1.4.2.2 Post-transcriptional regulation

Both mRNA degradation and 3' end processing are involved in the post-transcriptional cell cycle regulation of histone mRNAs (Harris et al., 1991). Maximum 3' end processing of mammalian histone mRNAs occurs during the S-phase of the cell cycle. The SLBP is cell cycle regulated. In Chinese hamster ovary cells, SLBP accumulates in late G1-phase and early S-phase and is degraded at the end of S-phase (Mullen and Marzluff, 2008). Unlike SLBP, U7 snRNP levels remain constant throughout the cell cycle (Bond and Yario, 1994). Levels of symplekin decrease during G1-phase, suggesting that symplekin may also be cell cycle regulated (Kolev and Steitz, 2005). Mullen and Marzluff, (2008) recently discovered that mammalian histone mRNA degradation involves the addition of short oligo(U) tract to the 3' end of the RNA. This oligo(U) tract is recognised by the Lsm1-7 complex, which then initiates degradation of the histone mRNA through recruitment of the decapping complex. The decapping complex, which consists of Dcp1p and Dcp2p, removes the 5' cap so degradation of the

mRNA transcript can occur in the 5'-3' direction by Xrn1 (Chowdhury et al., 2007; Mullen and Marzluff, 2008; Wilusz and Wilusz, 2008).

1.4.3 Yeast histone mRNA 3' end formation

In lower eukaryotes, such as *S. cerevisiae*, histone mRNAs do not possess a stem-loop structure but like histones in higher eukaryotes, are cell cycle regulated. Fahrner *et al.*, (1980) purified yeast histone mRNA for the first time and demonstrated that the histones H2A, H2B, H3 and H4 are polyadenylated yet histone mRNAs are poorly retained on oligo dT columns (Campbell and Bond, unpublished data). While much is known about the cell cycle regulation of mammalian histone mRNAs and the cis-acting and trans-acting factors involved in this process, much less is known about the regulation of these mRNAs in yeasts and other lower eukaryotes.

1.4.4 Yeast histone mRNA levels during the cell cycle

1.4.4.1 Transcriptional control mechanism

The core histones in *S. cerevisiae* are encoded by four divergently transcribed gene pairs, *HTA1-HTB1*, *HTA2-HTB2*, *HHT1-HHF1* and *HHT2-HHF2*. The *HTA1-HTB1* and *HTA2-HTB2* gene pairs carry genes for histones H2A and H2B, while *HHT1-HHF1* and *HHT2-HHF2* loci carry genes for histone H3 and H4 (Eriksson et al., 2005; Sutton et al., 2001). Studies of the core histones have identified a consensus sequence of (G/A)TTCCN$_6$TTCNC which is present in the promoter region of the histones. This conserved sequence has been termed the upstream activating sequence (UAS). Multiple copies of the UAS have been identified in the core histones with both *HTA1* and *HHT1* containing four UAS sequences and six possible UAS sequences identified in *HTA2* and *HHT2* (Eriksson et al., 2005). The putative histone acetyltransferse protein, Spt10p, binds specifically to the UAS sequences identified in all four core histones. In *Δspt10* strains, chromatin was found to be incorrectly assembled. It has been suggested that Spt10p acts indirectly on other genes through its regulation of histone genes (Eriksson et al., 2005). UAS sequences play both positive and negative roles. In their positive role, UAS sequences control the activation of transcription and cell cycle periodicity.

However, UAS sequences can also mediate the repression of transcription in G1- and G2-phase of the cell cycle (Eriksson et al., 2005; Osley and Lycan, 1987).

During the cell cycle, mRNA from the core yeast histone genes accumulates at S-phase through transcriptional activation at G1-/S-phase. As cells enter early G1-, G2- and M-phases, the expression of histone mRNA is repressed by the action of several trans-acting factors (Sutton et al., 2001). These trans-acting factors include Hir1p, Hir2p and Asf1p. *HIR1* and *HIR2* genes are negative regulators of the cell cycle. Hir2p, in conjunction with both Hir2p and Hir3p, was found to cause transcription repression of a *HTA1-lac* reporter gene (Spector et al., 1997). Asf1p is a highly conserved protein which through yeast two-hybrid analysis has been found to interact with Hir1p. Asf1p is also a repressor of transcription and plays a role in the cell cycle (Sutton et al., 2001), however, its mechanism of repression is unclear.

1.4.4.2 Post-transcriptional control mechanism

In the early 1980s, experimental proof for the tight regulation of histone mRNAs at a transcriptional and post-transcription level emerged. Hereford *et al.*, (1981) demonstrated that H2A and H2B mRNA levels accumulate in the S-phase of the cell cycle and coincided with DNA synthesis (Hereford et al., 1981). Lycan *et al.*, (1987) investigated the role of post-transcriptional regulation in the control of histone gene expression. Using the H2B-lacZ gene fusion, which contains 80 amino acids of the H2B 5' coding region, they demonstrated that the histone gene fusion did not show the cell cycle accumulation pattern of the normal H2B gene. This indicated that the 5' end of the histone H2B was not responsible for the S-phase accumulation and that the 3' end may play a role (Lycan et al., 1987). In 1990, Xu *et al.* investigated the contribution of the 3' end of histone genes to the cell cycle regulation of histone mRNAs. In this study, a plasmid was constructed consisting of the bacterial neomycin phosphotransferase II gene fused upstream of the last 17 amino acids of the *HTB1* coding sequence and the 3' untranslated sequence. The fusion gene was placed under the control of the GAL1 promoter. The *neo-HTB1* transcript, emanating from the fusion gene showed a cell cycle regulation pattern similar to wild type *HTB1* gene. The deletion of 66 to 103bp of the 3' untranslated portion of *HTB1* resulted in the loss of the cell cycle regulation (Xu et al., 1990).

Campbell *et al.*, (2002) identified a sequence element located approximately 110nts downstream of the 3' end cleavage sites of *HTB1* gene that influences cell cycle regulation of *neo-HTB1* mRNA. This purine-rich sequence element was termed the distal downstream element (DDE) and lies in the region of transcription termination. Mutations in the DDE led to a delay in the accumulation of the *neo-HTB1* mRNA in the S-phase and a lack of mRNA turnover in the G2-phase. This study also found that the DDE binds to protein factor(s) which may play a possible role in stabilising the pre-mRNA during the cell cycle (Campbell et al., 2002). In a follow up study, Canavan and Bond (2007) demonstrated that the CF IA components, Rna14p, Rna15p and Pcf11p, were required for the biogenesis of histone mRNA, suggesting that yeast histone mRNAs are processed by the general 3' end processing and polyadenylation machinery.

1.5. 3' end processing of non-polyadenylated RNAs

1.5.1 Transcription termination of non-polyadenylated RNAs

RNA Polymerase II also transcribes non-coding non-polyadenylated RNAs such as small nuclear RNA (snRNA), small nucleolar RNA (snoRNA) and cryptic unstable transcripts (CUTs) of 300-600nts in length (Morlando et al., 2002; Rondon et al., 2009; Vasiljeva et al., 2008). CUTs result from widespread transcription throughout the genome, possibly representing the largest share of hidden transcripts in the genome (Azzouz et al., 2009a). 3' end processing and transcription termination of these RNAs requires the Nrd1p/Nab3p/Sen1p termination complex, the TRAMP complex and the nuclear exosome (Grzechnik and Kufel, 2008; Gudipati et al., 2008; Wilusz and Wilusz, 2008).

The Nrd1p/Nab3p/Sen1p termination complex consists of two RNA binding proteins, Nrd1p and Nab3p, and a 5'-3' ATP dependent helicase, Sen1p (Azzouz et al., 2009a; Steinmetz and Brow, 1996, 1998). The amino terminus of Nrd1p contains a C-terminal interacting domain (CID) which binds RNA Polymerase II (Steinmetz and Brow, 1998). The CID of Nrd1p has sequence similarity to Pcf11p, a component of CFIA (Steinmetz et al., 2001). However unlike Pcf11p, Nrd1p preferentially binds to C-terminal domain (CTD) of RNA Polymerase II phosphorylated at Ser5 (Vasiljeva et al., 2008). Nrd1p interacts genetically with Ctk1p (Steinmetz et al., 2001). Co-immunoprecipitation

experiments have shown that Nab3p interacts physically with Nrd1p forming a heterodimer with a 1:1 stoichiometry (Carroll et al., 2007). Both Nrd1p and Nab3p have RNA recognition motifs (RRMs) which function to bind specific RNA sequences, 5'-GUAA/G-3' for Nrd1p and 5'-UCUU-3' for Nab3p (Carroll et al., 2004; Vasiljeva and Buratowski, 2006; Vasiljeva et al., 2008) that are often found in close proximity to each other (Carroll et al., 2004). Mass spectrometry indicates that Nrd1p interacts with components of both the exosome (Rrp6p, Rrp44p and Rrp4p) and the TRAMP complex (Trf4p and Air2p) as well with the poly(A) binding protein 1 (Pabp1) (Vasiljeva and Buratowski, 2006; Vasiljeva et al., 2008).

Sen1p, an essential nuclear protein, belongs to the 5'-3' ATP-dependent helicase I family which can unwind both DNA and RNA substrates (Ursic et al., 2004). Sen1p has been found to co-purify with factors required for the capping and cleavage/polyadenylation of mRNAs and the capping and maturation of snRNAs (Ursic et al., 2004). The N-terminal region of Sen1p interacts with the CTD of Rpb1p, the largest subunit of RNA Polymerase II, and an internal segment of Rad2p, a single stranded DNA endonuclease (Ursic et al., 2004). Sen1p also interacts with Rnt1p - a member of the RNase III family of double-stranded RNA endonucleases, Glc7p - a component of CPF and Nab3p – component of the Nrd1p/Nab3p/Sen1p complex (Finkel et al., 2010). Previous research has found that interactions between Nrd1p and Nab3p are crucial for the recruitment of the termination complex. This led Vasiljeva *et al.*, (2008) to suggest that the combination of Nrd1p binding to CTD of RNA Polymerase II phosphorylated at Ser5 and the RNA sequence recognition by Nrd1p and Nab3p channels particular RNAs into this termination and processing pathway (Vasiljeva et al., 2008).

3' end processing of transcripts via the Nrd1p/Nab3p/Sen1p pathway requires both the TRAMP and nuclear exosome complexes. TRAMP contains a poly(A) polymerase, Trf4p or Trf5p, a putative RNA binding protein, Air1p or Air2p, and the DEVH-box helicase Mtr4p (Houseley et al., 2007; LaCava et al., 2005). The poly(A) polymerases Trf4p and Trf5p contain a catalytic domain in their N-terminus but unlike conventional nuclear poly(A) polymerase, they lack a recognisable RNA-binding domain (Vanacova et al., 2005). The TRAMP complex is conserved in all eukaryotes (Houseley et al., 2007).

The exosome is a conserved multi-subunit 3'-5' exoribonuclease complex that plays a central role in RNA processing pathways both in the cytoplasm and in the nucleus. The exosome is made up of nine catalytically inactive core polypeptides with six subunits (Rrp42p, Rrp43p, Rrp45p, Rrp46p, Mtr3p and a phosphorolytic RNase, Rrp41p) related to RNase P, and three putative RNA-binding proteins, Csl4p, Rrp4p and Rrp40p. These core components are found in both the nucleus and the cytoplasm. Rrp40p is constitutively associated with a processive hydrolytic exoribonuclease, Rrp44p, which is the only active nuclease of the yeast core exosome (Azzouz et al., 2009a; Callahan and Butler, 2010; Lemay et al., 2010; Milligan et al., 2005). In the nucleus, the core exosome is associated with two additional proteins – Rrp6p and Rrp47p. Rrp6p provides hydrolytic activity to the nuclear exosome but can also function independently of the core exosome. Rrp47p is a nucleic acid binding protein which cooperates with Rrp6p (Azzouz et al., 2009a; Callahan and Butler, 2010; Lemay et al., 2010; Milligan et al., 2005). In general, activity of the exosome is regulated through association with co-factors such as Ski7p and the Ski2p, Ski3p and Ski8p complex in the cytoplasm or the TRAMP complex in the nucleus (Azzouz et al., 2009a; Callahan and Butler, 2010; Milligan et al., 2005).

3' end processing of snoRNAs, snRNAs and CUTs proceeds through the recognition of Nrd1/Nab3 binding sites at the 3' end of the RNA which triggers transcription termination. A short poly(A) tail is added to the free 3'OH by Trf4p/Trf5p. The poly(A) tail is then recognised by the nuclear exosome which proceeds to digest the newly adenylated substrate (*Figure 1.4*) (Houseley et al., 2007; Wilusz and Wilusz, 2008). Following transcription termination by the Nrd1p/Nab3p/Sen1p complex, transcripts can be either trimmed back to a defined 3' end cleavage site through the action of TRAMP/exosome or be fully degraded in a 3' – 5' direction. The molecular mechanism controlling the decision of TRAMP/exosome complex to trim or degrade the transcript is currently not fully understood but the presence of Nrd1 binding sites in some transcripts appears to favour trimming. It has been suggested that these Nrd1 binding sites block the continued 3' – 5' exosome activity of the exosome (*Figure 1.4*). Vasiljeva *et al.*, (2008) demonstrated that Nrd1p through its interaction with Trf4p, stimulates degradation of non-polyadenylated RNA by the nuclear exosome and in some cases blocks 3'-5' degradation by the nuclear exosome via selected Nrd1p binding sites (Houseley et al., 2007; Vasiljeva et al., 2008).

The complete degradation of other transcripts such as CUTs, depends on the position of RNA Polymerase II relative to the transcription start site (Gudipati et al., 2008; Villa et al., 2008). Nrd1p terminators, located within a window of less than 1kb from the transcription start site, elicit Nrd1p/Nab3p/Sen1p dependent termination and ensuing degradation. After this threshold transcripts are poorly recognised by the Nrd1p/Nab3p/Sen1p complex (Villa et al., 2008). While most CUTs polyadenylated by Trf4p and degraded by the nuclear exosome (Gudipati et al., 2008), some CUTs are exported to the cytoplasm and associate with polyribosomes before being degraded in this compartment (Villa et al., 2008).

Figure 1.4: Interactions of the Nrd1p/Nab3p/Sen1p, TRAMP and exosome complexes with non-polyadenylated RNA. Following transcription of a cluster of Nrd1/Nab3 binding sites (grey ovals), the Nrd1p/Nab3p/Sen1p complex is proposed to recruit the TRAMP complex and the exosome. The Nrd1p/Nab3pSen1p complex promotes transcription termination of CUTs, snRNAs and snoRNAs causing the transcript to become adenylated by Trf4p. Mtr4p recruits Rrp6p and the exosome complex which in turn trims the newly added poly(A) tail. Unknown factors (dark grey circles) are thought to bind to the sn/snoRNA, preventing the exosome from completely degrading the sn/snoRNA transcripts. These factors do not bind to CUT transcripts so the exosome completely degrades the transcript. The orange line represents the DNA and light grey circles represent nucleosomes. Figure was adapted from (Houseley et al., 2007).

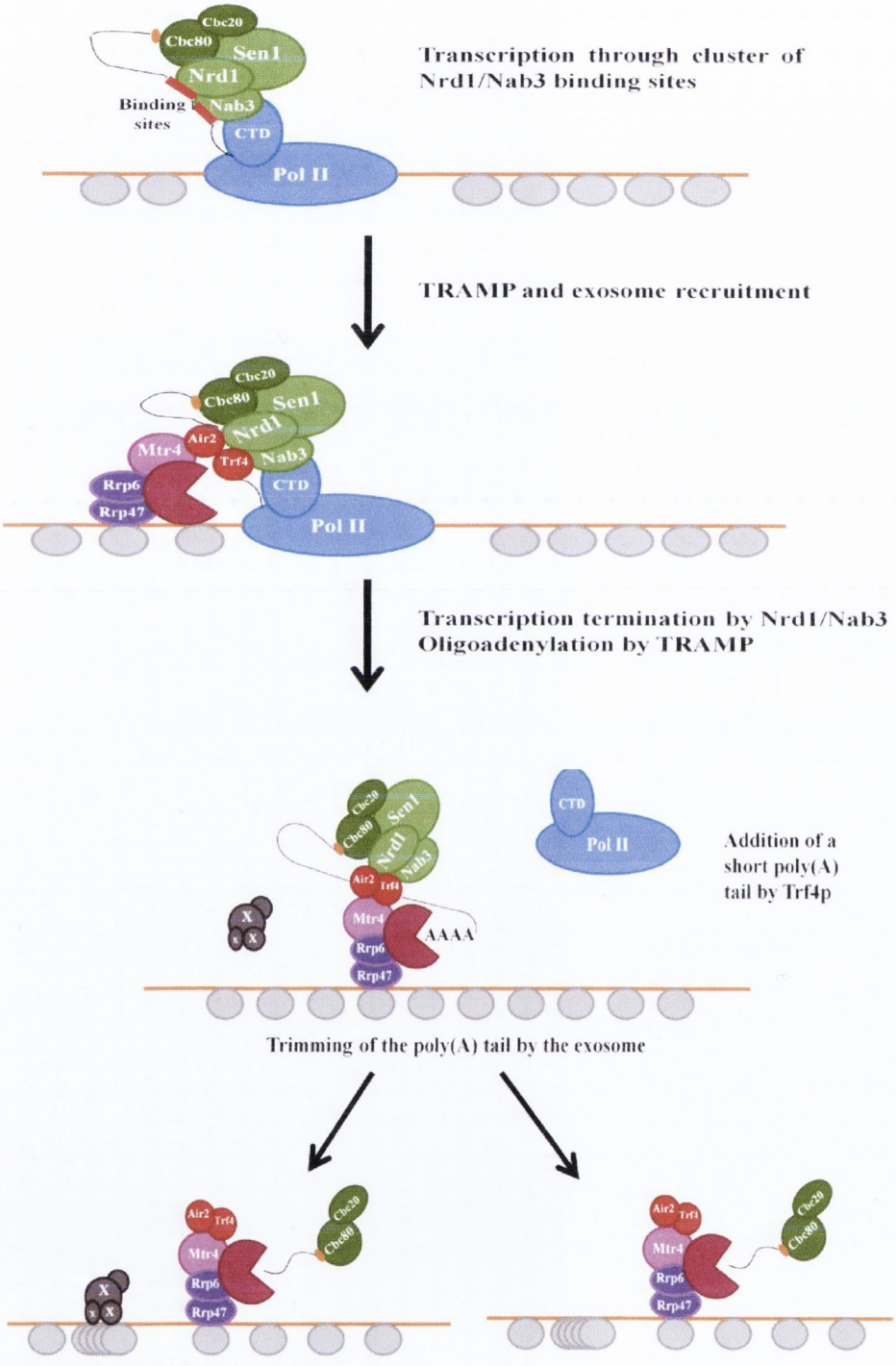
Cbc20
Cbc80
Sen1
Nrd1
Binding sites
Nab3
CTD
Pol II
Transcription through cluster of Nrd1/Nab3 binding sites
TRAMP and exosome recruitment
Air2
Mtr4
Trf4
Rrp6
Rrp47
Transcription termination by Nrd1/Nab3
Oligoadenylation by TRAMP
AAAA
Addition of a short poly(A) tail by Trf4p
Trimming of the poly(A) tail by the exosome
Complete degradation of sn/snoRNA transcripts by the exosome is halted by the presence of unknown factors thus allowing for the maturation of snRNA and snoRNA
Complete degradation of CUTs by the exosome

1.5.2 Components of the non-polyadenylated RNA processing machinery are involved in mRNA processing

The Nrd1p/Nab3p/Sen1p termination complex has also been implicated in the regulation of a subset of mRNAs via polyadenylation-independent transcription termination (Lykke-Andersen and Jensen, 2007). The best characterised example of this is *NRD1* RNA itself. A series of Nrd1p and Nab3p binding sites situated in the 5'end of the transcript direct auto regulation through transcription termination-coupled RNA degradation similar to what is described for CUTs (Arigo et al., 2006; Lykke-Andersen and Jensen, 2007).

Steinmetz and Brow, (2006), conducted a global "ChIP-on-chip" analysis on the genomic occupancy of RNA Polymerase II in a Sen1p temperature-sensitive yeast strain. This revealed read-through transcription in genes encoding short transcripts such as snRNAs, snoRNAs, CUTs and short mRNAs (<600nts). In this study, Sen1p was shown to be critical for termination of a subset of short protein encoding genes including *CYC1*, *IES5*, *SOD1*, *RPL43B* and *FPR1* (Steinmetz et al., 2006b). These mRNAs are polyadenylated but it is as yet unclear whether Sen1p is working independently of Nrd1p and Nab3p or if the complex as a whole is acting together with the mRNA cleavage and polyadenylation machinery (Steinmetz et al., 2006b).

Ciais *et al.*, (2008) found that the 3'UTR of *CTH2* pre-mRNA contains numerous potential binding sites for Nrd1p (10 binding sites) and Nab3p (24 binding sites) and that 3'extended *CTH2* pre-mRNA accumulated in strains with mutations in the TRAMP4 complex and the Nrd1p/Nab3p/Sen1p termination complex. This led them to predict that the Nrd1p/Nab3p/Sen1p complex binds the nascent CTH2 transcript and recruits the TRAMP4 complex and the nuclear exosome. The exosome then rapidly degrades the pre-mRNA after transcription termination generates a free 3' end (Ciais et al., 2008).

1.5.3 Components of the non-polyadenylated RNA processing machinery are involved in histone mRNA processing

While yeast histone mRNAs are known to be polyadenylated and to require components of the 3' end processing and polyadenylation machinery, specifically CF IA, for their 3'

end processing, recent data has uncovered a role for components of the non-polyadenylated processing pathway in the biogenesis and regulation of histone mRNAs. Canavan and Bond, (2007) demonstrated that Rrp6p, a component of the exosome, contributes to the cell cycle regulation of histone mRNAs. Deletion of *RRP6* led to the continued accumulation of the histone mRNA *HTB1* during the S-phase of the cell cycle leading to delayed exit of cells from S- into G2-phase (Canavan and Bond, 2007).

A role for the TRAMP complex in histone mRNA regulation has also been identified (Reis and Campbell, 2007). In this study it was discovered that Asf1p, a histone H3/H4 chaperone which is important for nucleosome assembly *in vivo* during DNA replication, repair and transcription, and Rad53p which monitors histone protein levels and targets excess soluble histone for degradation, are both required for viability in a *Δtrf4* strain. Trf4p was also found to have strong synthetic interactions with Asf1p and Hir1p, a transcriptional co-repressor which is required for the regulation of histone expression (Reis and Campbell, 2007). In addition to those findings, they also discovered that the levels of replication-dependent histones are specifically up-regulated in *trf4-ts trf5Δ* cells and that deletion of *TRF4* in a *RRP6* deletion strain is synthetically lethal. Trf4p and Trf5p were also found to be able to maintain appropriate histone mRNA levels in the absence of Air1/2p suggesting that there may be other RNA-binding proteins that mediate Trf4p interactions with specific substrates that lead to the up-regulation of histone mRNA (Reis and Campbell, 2007). Through their findings, Reis and Campbell, 2007 hypothesised that Trf4/5p might be involved in a post-transcriptional mechanism, either directly or indirectly on histone mRNAs, for maintaining the proper balance of histone transcripts. They proposed that the TRAMP complex acts as a failsafe mechanism to control levels of histone mRNA (Reis and Campbell, 2007).

1.5.4 The regulation of non-polyadenylated RNAs by known cleavage and polyadenylation factors

The finding that some polyadenylated mRNAs can be processed by the Nrd1p/Nab3p/Sen1p termination pathway suggests interplay or cross-communication between the 3' end cleavage and polyadenylation pathway and the Nrd1p/Nab3p/Sen1p pathway might be occurring. Many similarities exist between the two 3' end processing pathways (Steinmetz et al., 2001). Firstly, both pathways require recognition elements

on the nascent transcript to direct RNA 3' end maturation and to prevent RNA Polymerase II from reading through the normal termination region. Secondly, both pathways contain transcription termination proteins (Pcf11p and Nrd1p) which contain CID motifs and interact directly with RNA Polymerase II (Steinmetz et al., 2001). Finally both pathways share a number of common proteins such as Hrp1p, Ssu72p, Pti1p, Rna15p and Ref2p (Carroll et al., 2004).

1.6 Objectives of this study

The aim of this research was to explore further the 3' end formation and transcription termination of histone mRNA and to identify proteins required in these processes. With the emergence of evidence that factors of both the exosome and the TRAMP complex contribute to the biogenesis of histone mRNAs, the role of other factors in the non-coding, non-polyadenylated processing machinery was explored. Specifically the aims of this thesis were to examine the role of the Nrd1p/Nab3p/Sen1p complex in 3' end processing and transcription termination of histone mRNA. Given the facts that both TRAMP and the exosome appear to play important roles in histone mRNA biogenesis, a second aim of the study was to re-examine the polyadenylation status of yeast histone mRNAs and finally to identify other proteins required for histone mRNA biogenesis.

The data presented in this thesis revealed that Sen1p contributes to the transcription termination of histone mRNAs. This effect was independent of Nrd1p and Nab3p confirming previous findings for an independent role of Sen1p. Our analysis of the polyadenylation status revealed that in asynchronous cells, histone mRNAs have shorter than average poly(A) tails and can be divided into three distinct populations, differing in poly(A) tail length. Inactivation of Sen1p and Rrp6p led to a decrease in the average poly(A) tail length of histone mRNA suggesting a role for these factors in the 3' end processing of histone mRNAs. This analysis also identified five canonical cleavage sites present in wild type cells, three of which have previously been identified by (Campbell et al., 2002; Miura et al., 2006). The length of the poly(A) tail and cleavage site usage during the cell cycle was also investigated. These results show that poly(A) tail length varies during the cell cycle, with histone mRNAs in S-phase possessing very short poly(A) tails while those in G1-phase have longer poly(A) tails. During G2-phase, histone mRNAs with two poly(A) tail lengths were detected – those with

poly(A) tails of 25-50 nts and those with no poly(A) tails. The discovery of histone mRNAs with no poly(A) tail coincided with the discovery of numerous non-canonical 3' ends located upstream of the *HTB1* stop codon.

Finally the involvement of components of the SCF ubiquitin ligase complexes, such as Skp1p and F-box proteins, which controls levels of many cell cycle regulated proteins, in the transcription termination of histone mRNAs was also explored. The results indicate that mutations in Skp1p or F-box proteins does not affect transcription termination of histone mRNA.

Chapter 2

Materials and Methods

2.1 Yeast strains and growth conditions

Saccharomyces cerevisiae strains used in this study are listed in Table 2.1. Yeast strains were cultured at 22, 25 or 30°C in YEPD medium (1% (w/v) yeast extract, 2% (w/v) bacto peptone, 2% (w/v) dextrose) to an optical density at 660 nm (OD_{660nm}) of between 0.6 and 1.8. For temperature sensitive mutant strains, cultures were grown to an OD_{660nm} value of 0.8 at 22 or 25°C. Cells were harvested by centrifugation at 8,000 rpm for 10 mins at room temperature in a Sorvall SS-34 rotor, resuspended in half the original volume of preheated media and incubated at 37°C for 2 hr.

Yeast strains containing plasmids were cultured in synthetic complete agar medium [2% (w/v) agar, 2% (w/v) glucose, 6.7% (w/v) yeast nitrogen base without amino acids and ammonium sulphate, supplemented with 0.5% (w/v) ammonium sulphate and amino acids to give a final concentration of 14 mg/ml yeast synthetic drop-out medium, 10 mg/ml of adenine, lysine, tryptophan, leucine, histidine and 2.5 mg/ml of uracil]. Leucine was omitted from the media for strains harbouring plasmids with a LEU gene.

2.2 Bacterial strains and growth conditions

The *Escherichia coli* strain, XL1 –blue supercompetent (*recA1 endA1 gyrA96 thi- 1 hsdR17 supE44 relA1 lac[F' proAB lac^{q}ZΔM15 Tn10(Tet^r)]*, *Stratagen,)* was used for plasmid propagation. *E. coli* cells transformed with plasmids were grown in Luri-Bertani media (LB; 1% (w/v) tryptone, 0.5% (w/v) yeast extract and 10 mM NaCl) overnight at 37°C, with carbenicillin and/or kanamycin added to final concentrations of 50 µg/ml.

Table 2.1: Yeast strains used in this study.

Strain	Genotype	Source
BY4741	*MATa; his3D1; leu2D0; met15D0; ura3D0*	Euroscarf
BY4742	*MATα ; his3D1; leu2D0; lys2D0; ura3D0*	Euroscarf
BY4743	*MATa/MATα; his3D1/his3D1; leu2D0/leu2D0; met15D0/MET15; LYS2/lys2D0; ura3D0/ura3D0*	Euroscarf
YNL311C	*BY4741; Mat a; his3D1; leu2D0; met15D0; ura3D0; YNL311c::kanMX4*	Euroscarf
YDR219C	*BY4741; Mat a; his3D1; leu2D0; met15D0; ura3D0; YDR219c::kanMX4*	Euroscarf
YBR280C	*BY4741; Mat a; his3D1; leu2D0; met15D0; ura3D0; YBR280c::kanMX4*	Euroscarf
YLR368W	*BY4741; Mat a; his3D1; leu2D0; met15D0; ura3D0; YLR368w::kanMX4*	Euroscarf
YLR097C	*BY4741; Mat a; his3D1; leu2D0; met15D0; ura3D0; YLR097c::kanMX4*	Euroscarf
YIL046W	*BY4743; Mat a/α; his3D1/his3D1; leu2D0/leu2D0; lys2D0/LYS2; MET15/met15D0; ura3D0/ura3D0; YIL046w::kanMX4/YIL046w*	Euroscarf
YJL149W	*BY4741; Mat a; his3D1; leu2D0; met15D0; ura3D0; YJL149w::kanMX4*	Euroscarf
YFL009W	*BY4743; Mat a/a; his3D1/his3D1; leu2D0/leu2D0; lys2D0/LYS2; MET15/met15D0; ura3D0/ura3D0; YFL009w::kanMX4/YFL009w*	Euroscarf
YJR090C	*BY4741; Mat a; his3D1; leu2D0; met15D0; ura3D0; YJR090c::kanMX4*	Euroscarf
YNL230C	*BY4741; Mat a; his3D1; leu2D0; met15D0; ura3D0; YNL230c::kanMX4*	Euroscarf
YLR224W	*BY4741; Mat a; his3D1; leu2D0; met15D0; ura3D0; YLR224w::kanMX4*	Euroscarf
YDR131C	*BY4741; Mat a; his3D1; leu2D0; met15D0; ura3D0; YDR131c::kanMX4*	Euroscarf
YJL204C	*BY4741; Mat a; his3D1; leu2D0; met15D0; ura3D0; YJL204c::kanMX4*	Euroscarf
YML088W	*BY4731; Mat a; leu2D0; met15D0; ura3D0; YML088w::kanMX4*	Euroscarf

YMR258C	*BY4741; Mat a; his3D1; leu2D0; met15D0; ura3D0; YMR258c::kanMX4*	Euroscarf
YOR080W	*BY4741; Mat a; his3D1; leu2D0; met15D0; ura3D0; YOR080w::kanMX4*	Euroscarf
W303	*MATa ; leu2-3_112; ura 3-52; trp 1Δ2; his3-11; ade2-1; kan1-100*	Euroscarf
skp1-3	*his3-D200, lys2-801, ade2-101, leu2-D1, ura3-52, trp1-D63, skp1-3::LEU2(@CHROM 4)*	Rashid Abdulle ST Judes, Memphis
skp1-4	*his3-D200, lys2-801, ade2-101, leu2-D1, ura3-52, trp1-D63, skp1-4::LEU2(@CHROM 4)*	Rashid Abdulle ST Judes, Memphis
Δrrp6	*MATa, his3, leu2, ura3, ade2, trp1, rrp6::KANr*	Libri, D., CNRS
rna14-3/Δrrp6	*MATa, leu2-3_112, ura3-1, trp1-1, his3-11_15, ade2-1, can1-100, rna14-3, rrp6::KAN*	Libri, D., CNRS
46a	*MATa cup1Δ ura3 his3 trp1 lys2 ade2 leu2*	David Brow, Madison, Wisconsin
46α	*MATα cup1Δ ura3 his3 trp1 lys2 ade2 leu2*	David Brow, Madison, Wisconsin
46a sen1-E1597K	*MATa cup1Δ ura3 his3 trp1 lys2 ade2 leu2 sen1-E1597K*	David Brow, Madison, Wisconsin
46α nrd1-5	*MATα cup1Δ ura3 his3 trp1 lys2 ade2 leu2 nrd1-V368G*	David Brow, Madison, Wisconsin
46α nab3-11	*MATα cup1Δ ura3 his3 trp1 lys2 ade2 leu2 nab3:: KANMX [pRS313-nab3-11(F371L, P374T)]*	David Brow, Madison, Wisconsin
46α ssu72-G33A	*MATα cup1Δ ura3 his3 trp1 lys2 ade2 leu2 ssu72-G33A*	David Brow, Madison, Wisconsin
46α hrp1-5	*MATα cup1Δ ura3 his3 trp1 lys2 ade2 leu2 hrp1-5:: HIS3 [pRS315-hrp1-L205S(LEU2)]*	David Brow, Madison, Wisconsin
46a rpb11-E108G	*MATa cup1Δ ura3 his3 trp1 lys2 ade2 leu2 rpb11-E108G*	David Brow, Madison, Wisconsin

2.3 Transformation of bacteria with plasmid DNA

2.3.1 Preparation of competent cells

Competent cells where prepared as described by the supplier *New England Biolabs*. Briefly, an overnight culture of the *Escherichia coli* strain, XL1–blue supercompetent was sub-cultured into LB broth and grown to an optical density of 0.4-0.6 at 37°C, 200 rpm. The cells were centrifuged at 5,000 rpm for 5 mins at 4°C and the pellet was resuspended in 1/2.5 of the original volume in ice-cold TFB1 (30 mM KOAc, 100 mM RbCl, 10 mM $CaCl_2$, 50 mM $MnCl_2$ and 15% glycerol at pH 5.8). The sample was placed on ice for 5 mins and then pelleted at 5,000 rpm for 5 mins at 4°C. The pellet was resuspended in 1/25 of the original volume of ice-cold TFB2 (10 mM MOPS, 75 mM $CaCl_2$, 10 mM $RbCl_2$ and 15 % glycerol). The suspension was kept on ice for 15-60 mins and then aliquoted into 200µl samples and kept at – 70°C until usage.

2.3.2 Transformation of bacteria with plasmid DNA

Competent cells were thawed on ice and 50 ng of plasmid DNA or 20µl of ligation mix (see section 2.16.3) was added to the cells. Following an one hour incubation on ice, the suspension was heat shocked for 45 secs at 42°C and placed on ice for 2 mins. 1ml of preheated LB broth was added to transformation and the cells were grown with vigorous aeration at 37°C for 1 hr. 250µl of the transformed cells was plated on LB plates containing 50 µg/ml carbenicillin.

2.4 Transformation of yeast with plasmid DNA

DNA plasmids were introduced into the yeast strains using the lithium acetate procedure (Ito et al., 1983). The yeast cells were grown overnight to an OD_{660nm} of 1.0 – 1.5 and then 1ml of culture was centrifuged at 13,200 rpm for 2 min. The supernatant was removed and the cells were washed twice in 0.1M lithium acetate. The cells were centrifuged at 13,200 rpm for 1 min. 240µl of 35 % polyethylene glycol (PEG) (w/v) was added to the cell pellet and mixed vigoursly to resuspend. To this, 36µl of 1M lithium acetate was added and the solution was mixed thoroughly. Salmon sperm DNA

(1 mg/ml) was heated to 95°C for 10 mins and then quickly chilled on ice. 1µg of plasmid DNA was added to 100µg of the carrier DNA and the solution was made up to 360µl with SDW, all of which was added to the cell pellet solution. The solution was mixed thoroughly by vortexing and incubated at 42°C for a minimum of 1 hr. Following incubation, the tubes were centrifuged at 13,200 rpm for 1 min and the supernatant was discarded. 1ml of pre-warmed YEPD (30°C) was added to the pellet and the mixture was vortexed. The cells were allowed to recover at 30°C for 3- 6 hrs and the cells were collected by centrifugation at 13,200 rpm for 1 min. The pellet was resuspended in 150µl of SDW and the whole suspension was plated on synthetic complete agar medium minus leucine. The transformants were selected within 2-3 days.

2.5 Isolation of plasmid DNA from bacteria

Genelute™ plasmid miniprep kit (*Sigma*) was used to extract plasmid DNA from 5mls of *E. coli*. The cells were harvested by pelleting 5mls of cell culture for 5 mins at 13,200 rpm. The bacterial pellets were resuspended in 200µl of resuspension solution and then 200µl of lysis solution. The microcentrifuge tubes were inverted gently 9-10 times until the solution became viscous. The cell debris was precipitated by adding 350µl of neutralisation buffer. The tubes were inverted and centrifuged at 13,200 rpm for 10 mins. The cleared lysate was added to a DNA binding column which was then centrifuged for 1 min at 13,200 rpm. The column was washed with 700µl of wash solution and the centrifugation step was repeated. A further spin of 13,200 rpm for 2 mins was performed to remove any residual wash buffer and the column was transferred to a fresh tube. 100µl of SDW was added to the column and this was allowed to stand at room temperature for 5 mins. A final centrifugation step at 13,200 rpm for 1 min was performed to collect the plasmid. The solutions were provided by *Sigma*.

2.6 Isolation of high molecular weight yeast DNA

Cells were grown to an OD_{660nm} of 0.4 – 0.6 and pelleted at 13,200 rpm for 5 min. Cells were resuspended in 500µl SDW and transferred to a microcentrifuge tube. Cells

were pelleted for 5 mins at 13,200 rpm, the supernatant was decanted and the pellet was resuspended in the residual growth media by briefly vortexing. 200µl of a solution containing 2% Triton X-100, 1% SDS, 100 mM NaCl, 10 mM Tris pH 8.0 and 1 mM EDTA was added to the cells. To this 200µl of phenol, pH 8.0/chloroform and 0.3g of 425 – 600 µM acid washed glass beads was added and the solution was vortexed vigorously for 3 mins. 200µl of TE buffer was added and the solution was centrifuged at 13,200 rpm for 7 mins. The aqueous layer was removed and the phenol/chloroform was repeated. The aqueous layer was removed and placed in a fresh microcentrifuge tube to which 1ml of 100% ethanol was added. The solution was mixed by inversion and centrifuged at 13,200 rpm for 15 min.

The resulting pellet was resuspended in 400µl of 1X TE buffer and 30 µg of RNase A was added. The solution was incubated at 37°C for 15 mins after which a phenol/chloroform extraction was repeated. The final aqueous layer was supplemented with 10µl of 4M ammonium acetate, 1ml of 100% ethanol and 3µl glycogen and placed at -70°C for 1 hr. Samples were centrifuged for 20 mins at 13,200 rpm and the DNA pellet was washed in 70% ethanol. Following a short drying period, the pellet was resuspended in 50µl TE buffer.

2.7 Calculation of nucleic acid concentrations

A UV/vis spectrometer (*Biophotometer/Genesys 10uv ThermoSpectronic*) was used to determine the concentration of RNA and DNA samples at an absorbance of 260 nm (A_{260}). The samples were diluted 1:500 in dH_2O and the optical density at 260 nm was measured using quartz cuvette. The concentration of nucleic acid was determined using the conversion factors below:

OD_{260}nm value of 1 equals: 50 µg/ml double stranded

40 µg/ml single stranded RNA.

2.8 Southern hybridisation analysis

PCR products were separated on a 2% Tris-boric acid, EDTA (TBE) (89 mM Tris-base, 88 mM Boric Acid, 0.02 mM EDTA) agarose gel containing 0.5 µg/ml ethidium bromide. The PCR fragments were identified by a brief exposure to UV intensity light.

Prior to transfer of the DNA to membrane, the agarose gel was soaked in 0.25M HCl for 15 mins to depurinate the DNA, then rinsed twice in sterile water. The gels were then denatured (0.5 M NaOH, 1.5 M NaCl) for 15 mins and finally rinsed in sterile water before transfer. The DNA was transferred to a nylon membrane (*Biodyne®B 0.45µ, Pall Corporation*), by capillary transfer using 20X SSC (3M NaCl, 0.3M sodium citrate, pH 7.0) for a minimum of 12 hrs. Nucleic acids were cross-linked to the membrane using a UV light (program C3 setting, 150 mJoule, Genelinker, *Bio-Rad*). Membranes were pre-hybridised in a solution containing 7% SDS, 5X SSC, 2% blocking buffer (10% casein (*Sigma*) in 1X MAB [1X Maleic Acid Buffer (0.1 M maleic acid, 0.15 M NaCl, pH 7.5)], 0.1% N-lauroylsarcosine and 50 mM sodium-phosphate (pH 7.0) for 60 mins at 68°C. A fresh aliquot of hybridisation buffer containing 5 ng of digoxygenin-UTP DNA probe (prepared as described in section 2.10.6) was added and membranes were incubated overnight at 68°C in a hybridisation oven. Following hybridisation, the membranes were washed twice for 15 mins in 2X washing solution (2X SSC, 0.1% SDS) at room temperature, followed by two washes in 0.5X washing solution (0.5X SSC, 0.1% SDS) for 15 mins at 50°C. Membranes were then washed in washing buffer (1X MAB, 0.3% (v/v) tween® 20) for 5 mins at room temperature. The membrane was blocked in blocking buffer (1X MAB with 1% (w/v) casein) for 60 mins, followed by incubation with antibody solution (anti-DIG-alkaline phosphate (*Roche*), diluted 1:10,000 in blocking buffer), for 30 mins. Two more stringent washes were carried out with wash buffer for 15 mins at room temperature. The membrane was immersed in detection buffer (100 mM NaCl, 100 mM Tris-HCl, pH9.5) for 5 mins at room temperature. This was followed by chemiluminescent detection with CDP-star (0.25 mM, *Sigma*). The membranes were then exposed to X-ray film (Hyperfilm, *Amersham Biosciences*).

2.9 RNA analysis

2.9.1 RNA isolation by the hot-phenol method

The hot-phenol method, developed by Krieg, was used to isolate total RNA with some modifications (Krieg, 1996). Cells were harvested (10-50ml, OD_{600nm} = 0.6 – 1.8) by centrifugation at 8,000 rpm for 10 mins at 4°C in a Sorvall SS-34 rotor. Pellets were washed twice with 10ml of sterile distilled water (SDW) and then resuspended in 500µl of AE buffer (10 mM EDTA and 50 mM Sodium acetate, pH 5.3), 50µl of 10% SDS (w/v) and 550µl of pre-warmed AE buffered-phenol (pH 5.3, 65°C). The extract was vortexed for 60 sec at maximum speed. Tubes were incubated for 30 min at 65°C, with vigorous vortexing for 10 sec every 5 mins. The debris and organic phase was separated from the upper aqueous phase by centrifugation at 14,000 rpm for 5 mins at 4°C. The upper aqueous phase was recovered and re-extracted twice more, first with 500µl of pre-warmed AE buffered-phenol (pH 5.3, 65°C), and second, 450 µl of chloroform. The RNA was precipitated by adding 0.1 vol of 3M sodium acetate (pH 5.3) and 2.5 vol of 100% (v/v) ethanol at -70°C for 45 mins. Samples were centrifuged at 14,000 rpm for 30 mins at 4°C, washed with 70% (v/v) ethanol and following a short drying period, the pellets were resuspended in 50µl DEPC-treated SDW.

2.9.2 Tris-acetate EDTA agarose gel electrophoresis

RNA was separated on 1% (w/v) Tris-acetate EDTA (TAE) (5 mM Tris-base, 0.05M EDTA, pH 8.0 and 0.01M glacial acetic acid) agarose gels. RNA samples of the desired concentration were precipitated at –70°C with 0.1 vol sodium acetate, pH 5.3, and 2.5 vol 100% ethanol. RNA pellets were resuspended in a denaturing loading buffer (1µg DEPC-treated SDW, 3.5µl formaldehyde, 10µl formamide, 2µl 10X MOPS buffer (200 mM MOPS, 300 mM sodium citrate, pH 7.0), 3.5µl formaldehyde gel loading buffer (0.1% bromophenol blue, 0.1% xylene cyanol, 50% (w/v) glycerol and 10 mM EDTA, pH8.0)) and incubated at 65°C for 15 mins to denature the RNA. Gels were electrophoresised at 40 V in 1X TAE buffer. The gels were subsequently blotted as described in section 2.9.3.

2.9.3 Northern analysis

RNA was transferred from the TAE agarose gel to a nylon filter membrane as described in section 2.8. Hybridisations were carried out as described in section 2.8 and processed as described in section 2.8.

2.9.4 Northern stripping

Membranes were washed in water twice for 10 mins and then incubated in stripping solution (DEPC-treated SDW and 0.1% SDS (w/v)) for 60 mins at 68°C in a hybridisation oven. The solution was changed after 30 mins and a fresh aliquot of stripping solution was added. Following stripping, the membranes were rinsed in water followed by 2 x SSC. The membranes were then hybridised in hybridisation solution (7% SDS, 5X SSC, 2% blocking buffer, 0.1% N-lauroylsarcosine and 50 mM sodium-phosphate (pH 7.0)) for 90 mins and the digoxygenin-UTP DNA probe was later added in hybridisation solution and the membranes were incubated overnight at 68°C.

2.10 Polymerase chain reaction, amplification of DNA and cDNA

2.10.1 Purification of RNA

To remove any contaminating DNA, RNA samples were incubated with 0.02U RNasin® ribonuclease inhibitor, 1X DNase I buffer (40 mM Tris-HCl (pH 8.0), 10 mM $MgSO_4$ and 1 mM $CaCl_2$) and 5U DNase I (*Promega Inc.* Madison, WI) in a final volume of 65µl at 37°C for 60 mins. Following digestion, the samples were incubated at 65°C for 10 mins to deactivate the enzyme. The RNA was precipitated by adding 0.1 vol of 3M sodium acetate (pH 5.3) and 2.5 vol of 100% (v/v) ethanol at -70°C for 45 mins. Samples were centrifuged at 14,000 rpm for 30 mins at 4°C and the supernatant was removed. The RNA pellets were then washed in 70% (v/v) ethanol and following a short drying period, the pellets were resuspended in 50µl DEPC-treated SDW.

2.10.2 Reverse transcription of RNA

DNase-treated RNA samples (2μg) were reversed transcribed in a reaction mixture containing 1X M-MLV RT buffer (*Promega*), 1.25 mM NTP mix (containing UTP, ATP, GTP and CTP), 500 nM transcript-specific reverse primer, 0.01U RNasin® ribonuclease inhibitor (*Promega*) and 0.5μl of M-MLV Reverse Transcriptase RNase H (*Promega*). The final volume was 20μl. Samples were incubated at 70°C for 5 mins, 4°C for 5 mins, 25°C for 10mins and 42°C for 60 mins, followed by inactivation at 70°C for 15 mins.

2.10.3 Amplification of DNA and cDNA by polymerase chain reaction (PCR)

PCR reactions were carried out in a final volume of 25μl containing 0.25 mM dNTPs, 1X thermophilic DNA buffer (10 mM Tris-HCl (pH 9.0), 50 mM KCl and 0.1% Triton X-100, *Promega Inc.* Madison, WI), 1.5 mM $MgCl_2$, 0.04U Taq polymerase (*NEB Bioline*), 400 nM forward primer, 400 nM reverse primer and 2-10 ng of the desired DNA template or 2μl of the cDNA (prepared as outlined in section 2.10.2) using a GeneAmp® PCR System 2700 machine. The primers used are listed in Table 2.2. The reaction was performed using the following amplification parameters which consisted of an initial denaturation of 95°C for 5 mins, 30 cycles of denaturation at 95°C for 30 secs, annealing at an appropriate temperature for 1 min, extension at 72°C for 45 secs and one round of final extension at 72°C for 7 mins. For semi-quantitative RT-PCR, reactions were carried out as described above except that 0.1μl of cDNA template was used and only 20 rounds of amplification were carried out. 5μl of PCR sample was added to 2μl of loading dye buffer (0.25% bromophenol blue, 0.25% xylene cyanol FF and 50% glycerol) and these were subsequently electrophoresised on a 2% Tris-boric EDTA (TBE) (89 mM Tris-base, 88 mM Boric Acid, 0.02 mM EDTA) agarose gel with 1X TBE running buffer.

The *Wallace rule* (i) was used to calculate the melting temperature (T_m) for short oligonucleotides (< 20 nucleotides). A, T, G and C refer to the base composition of the oligonucleotides (Wallace, 1979).

$$\text{(i)}\quad T_m = 2(A + T) + 4(G + C)$$

The annealing temperature was set at 5 – 10°C below the T_m value.

2.10.4 Real-time reverse transcription-PCR (Real-time RT-PCR)

Quantitative real-time RT-PCR was performed using a Rotor-gene RG-3000 machine (*Corbett Research*) with SYBR Green I dye. The 13.5µl reaction contained 7.5µl of Power SYBR Green PCR Master Mix (*Applied Biosystems*), together with 1µl of template (cDNA), 180 nM forward primer and 180 nM reverse primer. The primers used for amplification of *HTB1*, *ACT1* and 5.8S rRNA cDNA are listed in Table 2.2. The amplification protocol consisted of an initial denaturation step of 94°C for 10 mins, followed by 40 amplification cycles at 94°C for 15 secs, 55°C for 60 secs and 72°C for 60 secs.

Initially, serial dilutions of the template where prepared and the reactions were carried out in order to give a linear range of data points. The efficiency of the reaction (Eff) was determined by plotting the data on a graph with a fitted line to determine the slope. The formula $Eff = (10^{-1/slope})-1$ was used.

The fluorescence data was analysed by quantitative analysis to calculate the threshold value, C_t. This involves comparing the C_t values of the samples of interest with a control sample. The C_t values of both the control and the samples of interest are normalized to an appropriate housekeeping gene (5.8S rRNA). The Pfaffl relative quantification method was used to calculate the gene expression levels. Here, HTB1_Endo Levels = $1.96^{(control\ Ct - mutant\ Ct)}$ where 1.96 is the fold increase of *HTB1* product per round of replication. 5.8S rRNA Levels = $1.72^{(control\ Ct - mutant\ Ct)}$ where 1.76 is the fold increase of 5.8S rRNA product per round of replication. The level of gene expression was then normalised using the following calculation: *HTB1* mRNA / 5.8S rRNA.

2.10.5 Colony polymerase chain reaction

Colonies were picked using pipette tips and resuspended in 10µl of 20 mM NaOH at incubated at 95°C for 10 mins. The colony PCR was carried out in a volume of 25 µl, containing 0.25 mM dNTPs, 1X thermophilic DNA buffer (10 mM Tris-HCl (pH 9.0), 50 mM KCl and 0.1% Triton X-100, *Promega Inc. Madison, WI*), 1.5 mM $MgCl_2$, 0.04U Taq polymerase (*NEB Bioline*), 400 nM forward primer, 400 nM reverse primer and 2 µl of the template. The amplification conditions consisted of an initial

denaturation of 95°C for 5 min, 30 cycles of denaturation at 95°C for 30 secs, annealing at an appropriate temperature for 1 min, extension at 72°C for 45 secs and one round of final extension at 72°C for 7 mins.

2.10.6 Amplification of digoxygenin-UTP labelled DNA probes

A standard PCR amplification procedure was used to prepare digoxygenin-UTP labelled DNA probes, with the exception that the dNTP mix was replaced by digoxygenin-UTP probe mix (1.86 mM dATP, dCTP, dGTP, 1.3 mM dTTP and 0.65 mM alkali-labile DIG-11-UTP, pH 7, *Roche*).

2.10.7 Dot blotting of digoxygenin-UTP labelled DNA probes

Serial dilutions of the digoxygenin-UTP labelled DNA probe were spotted onto a piece of nylon membrane. Once the probe had dried, the membrane was washed briefly in washing buffer (1X MAB, 0.3% (v/v) tween® 20) at room temperature and then incubated in blocking buffer (1X MAB with 1% (w/v) casein) for 30 mins. The blocking buffer was removed and the membrane was incubated with antibody solution (Anti-DIG-alkaline phosphate, diluted 1:10,000 in blocking buffer) for 30 mins. The membranes were washed twice in washing buffer (1X MAB, 0.3% (v/v) tween® 20) for 15 mins. Chemiluminescence was detected with CDP-star (0.25 mM, *Sigma*) in detection buffer (100 mM NaCl, 100 mM Tris-HCl, pH 9.5) by exposure o X-ray film (Hyperfilm, *Amersham Biosciences*).

2.11 Synchronisation of yeast cells by the α_1-pheromone mating factor

The yeast cells were grown in YEPD medium to an OD_{660nm} of 0.4 – 0.6. The α_1-mating factor (TRP-HIS-TRP-LEU-GLN-LEU-LYS-PRO-GLY-GLN-PRO-MET-TYR) was added to give a final concentration of 2 μg/ml and the culture was incubated for up to 3 hrs. Cells were deemed arrested when 90% of the cells demonstrated a characteristic "schmooed" cell appearance. The α_1- mating factor was then removed by centrifugation and the cells were subsequently washed twice in sterile distilled water.

Pellets were resuspended in the original volume of pre-warmed YEPD. Samples (200ml) were collected at 15 mins intervals, centrifuged at 4,000 rpm for 5 mins and frozen a –70°C.

2.12 Flow cytometry analysis of cell cycle progression

Cells were synchronised with α_1- mating factor as described in section 2.11. One ml of cells (~1.0 x10^7 cells/ml) was removed at 15 min intervals and following centrifugation the pellets were fixed with 95% (v/v) ethanol and stored at 4°C for up to 3 days. The samples were then washed in water and resuspended in 50 mM sodium citrate, pH 7.0. The cells were sonicated for 10 secs at a setting of 5 amplitude microns on a SoniPrep sonicator (*MSE*). RNase A in 50 mM sodium citrate was added to a final concentration of 0.25 mg/ml and the cells were incubated at 50°C for 2 hrs. Proteinase K was then added to a final concentration of 1 mg/ml and the cells were incubated for a further 2 hrs at 50°C. Following centrifugation and removal of the supernatant, propidium iodide was added to a final concentration of 16 µg/ml. Cell sorting was carried out on a Beckman Coulter Exics XL FACs Analysis machine using the following settings:

FS	420 V	10 gain
SS	597 V	75 gain
FL1	663 V	1 gain
FL2	1282 V	1 gain
FL3	1127 V	5 gain
FL4	915 V	1 gain

The data was analysed using WinMDE software.

FACs analysis of asynchronous was carried out using the same parameters. Cell populations were gated to quantify the number of 1n and 2n cells.

2.13 Generation of *HTB1* poly(A) cDNA library

2.13.1 Purification and isolation of *HTB1* mRNA

2 mg of total RNA was DNase treated as described in section 2.10.1 followed by a Proteinase K (200µg) treatment at 50°C for 1 hr. To inactivate the Proteinase K, a phenol/chloroform (1:1) extraction was carried out and the RNA was precipitated by adding 0.1 vol of 3 M sodium acetate (pH 5.3) and 2.5 vol of 100% (v/v) ethanol at -70°C for 45 mins. Samples were centrifuged at 14,000 rpm for 30 mins at 4°C, washed with 70% (v/v) ethanol and following a short drying period, the pellets were resuspended in 500µl dH_2O.

The sample was denatured by incubation at 65°C for 10 mins. The HTB1 biotinylated primer (see Table 2.2) and 20X SSC were added at a final concentration of 600 nM and 75 mM respectively and the solution was allowed to return to room temperature. The solution was then resuspended in pre-washed streptavidin-paramagnetic beads (1 mg/ml) and left at room temperature for a further 10 mins with gentle inversion every 1-2 mins. The beads were captured using a magnetic stand and the supernatant was collected and placed in a microcentrifuge tube. The beads were washed four times with 300 µl of 0.5X SSC with the beads being recaptured each time. Following the final wash, the bound *HTB1* mRNA was eluted from the beads using 250µl of dH_2O at 65°C. The eluted mRNA was frozen at – 70°C overnight and then lyophilised. The lyophilised product was resuspended in 25µl of dH_2O.

2.13.2 G-tailing of isolated *HTB1* mRNA by poly(A) polymerase

The purified *HTB1* mRNA was G-tailed using Yeast Poly(A) Polymerase (*USB*, Ohio). The G-tailing reaction was carried out in a final volume of 25µl, containing 1X poly(A) polymerase reaction buffer (20 mM Tris-HCl (pH 7.0), 50 mM KCl, 0.7 mM $MnCl_2$, 0.2 mM EDTA, 100 µg/ml, acetylated BSA and 10 % glycerol), 0.5 mM rGTP, 750U of Yeast Poly(A) Polymerase (*USB*, Ohio) and 10µl of purified *HTB1* mRNA. The reaction was incubated at 37°C for 30 mins and was then loaded onto a silica column. The G-tailed purified *HTB1* mRNA was eluted from the column using 30µl dH_2O and the whole sample was used to make cDNA as described in section 2.10.2 using the

AnchorC reverse primer (see Table 2.2) in a reaction volume of 60µl. 2µl of the cDNA was amplified in a 25µl reaction containing 0.25 mM dNTPs, 1X thermophilic DNA buffer (10 mM Tris-HCl (pH 9.0), 50 mM KCl and 0.1% Triton X-100, *Promega Inc.* Madison, WI), 1.5 mM $MgCl_2$, 0.04U Taq polymerase (*NEB Bioline*), 400 nM HTB1 For$^{1\text{-}22}$ primer and 400 nM AnchorC reverse primer (see Table 2.2). The reaction was performed using the following amplification parameters which consisted of an initial denaturation of 95°C for 5 mins, 30 cycles of denaturation at 95°C for 30 secs, annealing at 60°C for 1 min, extension at 72 °C for 45 secs and one round of final extension at 72°C for 7 mins. A TOPO TA cloning kit (*Invitrogen*) was used to clone the cDNA library as per manufacturers' instructions (*Figure 2.1*). After an overnight incubation, the resulting clones were replica plated onto on LB plates containing 50µg/ml of carbenicillin and kanamycin and re-incubated overnight. The clones were screened by direct colony PCR as in section 2.10.5, using M13 forward and reverse primers (see Table 2.2). PCR products in the expected size range of >550 nts were further analysed. The positive clones were subsequently inoculated into overnight cultures of LB media containing 50µg/ml of carbenicillin and kanamycin. PCR amplification was carried the extracted plasmids using M13 and HTB1 forward and reverse primers (see Table 2.2) to further confirm the presence of the *HTB1* insert.

2.14 Sequencing

All sequencing reactions were carried out by GATC, Germany. Direct sequencing from poly(A) tail cloned plasmids were carried out using M13 forward and reverse primers (Table 2.2). For sequencing of RT-PCR products, gene specific primers used in the reaction were used. Plasmids used in sequencing reactions were isolated as described in section 2.5.

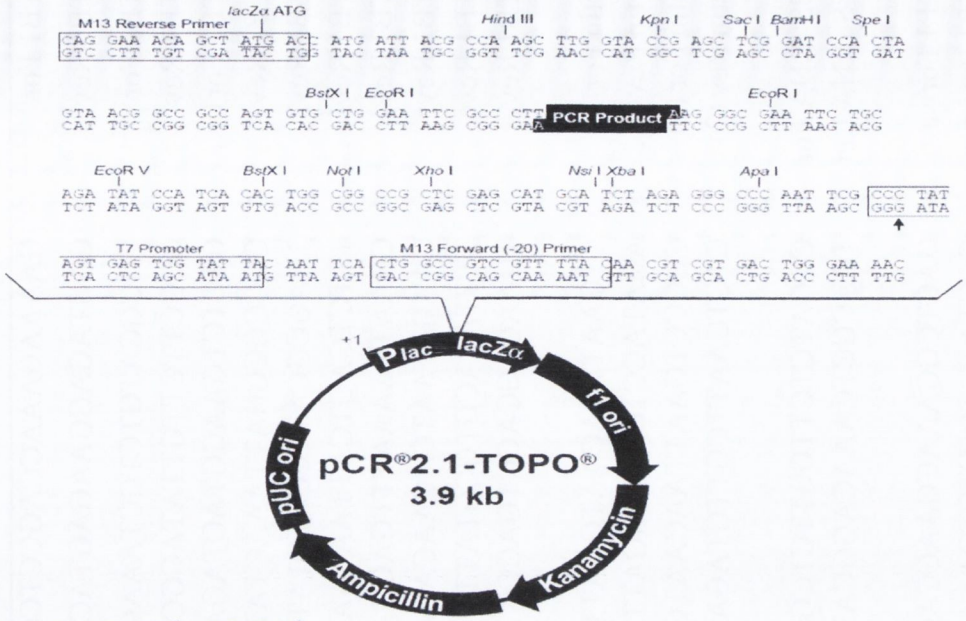

Comments for pCR®2.1-TOPO®
3931 nucleotides

LacZα fragment: bases 1-547
M13 reverse priming site: bases 205-221
Multiple cloning site: bases 234-357
T7 promoter/priming site: bases 364-383
M13 Forward (-20) priming site: bases 391-406
f1 origin: bases 548-985
Kanamycin resistance ORF: bases 1319-2113
Ampicillin resistance ORF: bases 2131-2991
pUC origin: bases 3136-3809

Figure 2.1: Map of the pCR2.1-TOPO plasmid. The pCR2.1-TOPO plasmid (*Invitrogen*) was used to clone the selected *HTB1* products >550nts at the PCR site which is flanked by EcoR1 restriction sites. The location of the M13 forward and reverse primers is shown.

Table 2.2: Oligonucleotides used in this study.

Oligonucleotides	Sequences 5' - 3'	Nucleotide position
HTB1 For$^{16-32}$	GAAAAGAAACCAGCCTCC	16-32, Coding sequence
HTB1 Rev$^{368-388}$	GAGTAGAGGAAGAGTACTTGG	368-388, Coding sequence
HTB1 For$^{1-22}$	GGCGCATGTCTGCTAAAGCCGAAAAG	1-22, Coding sequence
HTB1 Rev$^{252-270}$	GCGCTTCTTGTTATACGCAGCC	252-270, Coding sequence
HTB1 For1	GTCTCTGAAGGTACTAGAGCTG	343-351 nts relative to the ATG in HTB1 sequence
HTB1 Rev1	GGCCGCGGATTAAACTATTATACAA	473-489 nts relative to the ATG in HTB1 sequence
HTB1 Rev2	TAAGCGCATTCCCTCTATGAGAC	551-573 nts relative to the ATG in HTB1 sequence
HTB1 Rev3	TTTCTGAGTCATTAATAAGCAACACTA	620-646 nts relative to the ATG in HTB1 sequence
HTB1 Rev4	CGAATTAAAATTTGAGGAAAAATCTAGTA	705-733 nts relative to the ATG in HTB1 sequence
HTB1 Rev5	GAAGTTAATCACAACAGAGGGTT	788-810 nts relative to the ATG in HTB1 sequence
HTB1 Rev6	TTTTATACGTGCGTATTCTATTGTTCA	870-896 nts relative to the ATG in HTB1 sequence
HTB1 Rev7	TGAAGTGCAGCTGACGATC	979-997 nts relative to the ATG in HTB1 sequence
Actin For	CTGAATTAACAATGGATTCTGGTA	(-11)- (+13) nts relative the ATG site in ACT1 sequence
Actin Rev	AGATACCTCTCTTGGATTGAGCTT	172-195 nts relative the ATG site in ACT1 sequence
Actin For (2)	CCGCCTGAATTAACAATGGATTCTGAGG	((-11)-9)-(313-316) nts relative the ATG site in ACT1 sequence
Actin Rev (2)	CTCTCAATTCGTTGTAGAAGGT	572-594 nts relative the ATG site in ACT1 sequence
5.8S rRNA For	CGGATCTCTTGGTTCTCGC	
5.8S rRNA Rev	TGACGCTCAAACAGGCATG	
SKP1 Forward	GACTCGGAAACGAACCACAAAAGC	154-177 nts relative to the ATG in SKP1 sequence
SKP1 Reverse	GCCTATCTTGCTCTGAAATGGCGC	631-654 nts relative to the ATG in SKP1 sequence

HHF1 For	CCGAACACGCCAAGAGAAAGACTG	221-244 nts relative to the ATG in HHF1 sequence
HHF1 Rev1	CCGGCTATAATACACTCATATTTGTAG	386-410 nts relative to the ATG in HHF1 sequence
HHF1 Rev3	CCGGCGAAATTATTCCATCAT	564-587 nts relative to the ATG in HHF1 sequence
HHF1 Rev5	GCGCCTGCTTTTCTTGTC	736-753 nts relative to the ATG in HHF1 sequence
HHT1 For	CACGCCAAGCGTGTCACTATCC	340-361 nts relative to the ATG in HHT1 sequence
HHT1 Rev1	CAACTGTTAAAGAACCCAGTAAACC	481-505 nts relative to the ATG in HHT1 sequence
HHT1 Rev3	CTTTAACCACATGGAAAGCCA	648-668 nts relative to the ATG in HHT1 sequence
HHT1 Rev5	CAAGTCTATTGACAAGTGGTTCTTC	806-830 nts relative to the ATG in HHT1 sequence
HTA1 For	GCCAAAGAAGTCTGCCAAGGCTACC	354-378 nts relative to the ATG in HTA1 sequence
HTA1 Rev1	CAATGGAGAAGCAGTTTAGTTCC	431-453 nts relative to the ATG in HTA1 sequence
HTA1 Rev3	GTGCCCAATGAACCTAAACAG	596-616 nts relative to the ATG in HTA1 sequence
HTA1 Rev5	GGGCGAATAAGGACAGAAGC	760-779 nts relative to the ATG in HTA1 sequence
HTB2 For	CCTGGTGAATTGGCTAAACATGCC	319-342 nts relative to the ATG in HTB2 sequence
HTB2 Rev1	GACCCTTCCAATCATATCTGGACAAG	481-506 nts relative to the ATG in HTB2 sequence
HTB2 Rev3	GCACCAAACTGCTCAAGATAAGATCG	690-715 nts relative to the ATG in HTB2 sequence
HTB2 Rev5	GCCCATTAAAGAGCACTTTACACAG	845-869 nts relative to the ATG in HTB2 sequence
TDH3 For	CGACAACGAATACGGTTACTCTACC	936-960 nts relative to the ATG in TDH3 sequence
TDH3 Rev1	GCGCATCAAGAAAAAACACAAAGC	1108-1132 nts relative to the ATG in TDH3 sequence
TDH3 Rev2	CTAAAATTTCACTCAGCATCCACAAT	1191-1216 nts relative to the ATG in TDH3 sequence
TDH3 Rev3	CCTGGCGGAAAAAATTCATTTG	1276-1297 nts relative to the ATG in TDH3 sequence
TDH3 Rev4	GCACGCAAATATAGGCATGATTT	1358-1380 nts relative to the ATG in TDH3 sequence
TDH3 Rev5	CTTATCTTGGCGCGTACATTT	1441-1461 nts relative to the ATG in TDH3 sequence

TDH3 Rev6	CCGGCCACTCAGATTTTGTTAT	1526-1542 nts relative to the ATG in TDH3 sequence
TDH3 Rev7	GGGAAGAAATGAGGATTGAGCGAG	1633-1656 nts relative to the ATG in TDH3 sequence
ACT1 For	CCATGAAGGTCAAGATCATTGCTCC	1279-1303 nts relative the ATG site in ACT1 sequence
ACT1 Rev1	GAGGTACATACATAAACATACGCGC	1450-1474 nts relative the ATG site in ACT1 sequence
ACT1 Rev2	GTCAGTGCTTAAACACGTCTTTTCC	1537-1561 nts relative the ATG site in ACT1 sequence
ACT1 Rev3	CGTAGAAAAGGGAGAGACAAAACAC	1597-1621 nts relative the ATG site in ACT1 sequence
ACT1 Rev4	GATCATATGATACACGGTCCAATGG	1709-1733 nts relative the ATG site in ACT1 sequence
HTB1 Reverse Biotinylated	GCTTGAGTAGAGGAAGAGTACTTGGTAACAG	362-392, Coding sequence
Oligo C primer	CGAGGACTCGAGCTCAAGCCCCCCCCCCCCCCC	
M13 Forward	TGTAAAACGACGGCCAGT	
M13 Reverse	CAGGAAACAGCTATGACC	
E. coli 16S rRNA For	GCATAACGTCGCAAGACCAAAGAGG	
E. coli 16S rRNA Rev	CCCTCCGTATTACCGCGGCTGC	

Chapter 3

The role of the Nrd1p/Nab3p/Sen1p complex in the 3- end processing and transcription termination of histone mRNAs

3.1 Introduction

Histone mRNA biogenesis requires factors from both the general cleavage and polyadenylation pathway and the non-polyadenylation pathway. Previously Rna14p, Rna15p and Pcf11p of CF IA have been shown to be required for 3' end cleavage and proper transcription termination of histone mRNAs as inactivation of these genes at 37°C led to an accumulation of unprocessed read-through histone *HTB1* transcripts (Birse et al., 1998; Canavan and Bond, 2007). Additionally, Canavan and Bond, (2007) demonstrated that *RRP6*, a component of the nuclear exosome, contributes to the cell cycle regulation of histone mRNAs. Deletion of *RRP6* led to continued accumulation of the histone mRNA *HTB1* during the S-phase of the cell cycle leading to delayed exit from S-phase into G2-phase (Canavan and Bond, 2007).

In a recent study by Reis and Campbell, (2007), a role for the TRAMP complex in histone mRNA biogenesis was uncovered. The authors found that the histone H3/H4 chaperone, Asf1p and Rad53p, which monitor histone protein levels, were both required for viability in a *Δtrf4* strain. *TRF4* was found to have strong synthetic interactions with *ASF1* and *HIR1*, a transcriptional co-repressor which is required for the regulation of histone expression. Additionally, they discovered that the levels of replication-dependent histones are specifically up regulated in *trf4-ts trf5Δ* cells and that deletion of *TRF4* in a *RRP6* deletion strain is synthetically lethal (Reis and Campbell, 2007).

A recent study by Kuehner and Brow, (2008) identified a number of Sen1p interacting proteins which include Hrp1p of CF IB, Ssu72p of CPF and Rpb11p, a component of RNA Polymerase II. These proteins have also been found to be components of the 3' end processing machinery of both polyadenylated RNA and non-polyadenylated RNA (Dheur et al., 2005; Sheldon et al., 2005; Steinmetz and Brow, 2003). The finding that some polyadenylated mRNAs can be processed by the Nrd1p/Nab3p/Sen1p termination pathway (Rondon et al., 2009), together with the discovery of roles for factors from the mRNA processing pathway in the 3' end processing and transcription termination of non-polyadenylated RNAs, suggests substantial cross communication between the 3' end processing and transcription termination machinery of both polyadenylated and non-polyadenylated RNAs.

Since both the TRAMP and exosome complexes have been shown to be involved in histone mRNA biogenesis and are known to interact with the Nrd1p/Nab3p/Sen1p complex, the role of the individual components of the Nrd1p/Nab3p/Sen1p complex in the regulation of histone mRNA levels in *S. cerevisiae* was investigated. Additionally the role of factors common to both pathways in the regulation of histone mRNA levels was also explored.

3.2 Results

3.2.1 The individual components of the Nrd1p/Nab3p/Sen1p complex do not significantly alter the steady state levels of histone mRNA

In order to determine whether the individual components of the Nrd1p/Nab3p/Sen1p termination complex alter the steady state levels of histone mRNA, total RNA was isolated from yeast strains carrying temperature-sensitive mutations of the components of the Nrd1p/Nab3p/Sen1p complex (Table 2.1). Briefly, the temperature sensitive strains were grown in YEPD to an optical density (OD_{600nm}) value of 0.8 ($1x10^7$ cells) at 25°C. Following centrifugation, the cultures were divided in two and resuspended in YEPD pre-warmed to either 25°C or 37°C. Both cultures were re-incubated at their respective temperatures for a further 2 hours (Chapter 2, section 2.1). Total RNA was isolated and Northern blot analysis was performed as described in Chapter 2, section 2.9.3.

Figure 3.1 shows the RNA from the individual temperature sensitive mutants of the Nrd1p/Nab3p/Sen1p termination complex and their wild-type counterparts probed for *HTB1*. At the permissive temperature (25°C), the steady state levels of *HTB1* mRNA present in the wild-type strains appear approximately the same as those in the mutant strains (*Figure 3.1B*, compare lanes 1 to 6). A slight reduction in the steady state levels of *HTB1* mRNA was observed for the wild-type strains and each of the mutant strains following incubation at 37°C (*Figure 3.*1, lanes 7 to 12). This reduced level of *HTB1* mRNA in wild-type cells incubated at 37°C has previously been observed (Canavan and Bond, 2007) and may reflect reduced transcription or more rapid turnover of histone mRNAs at 37°C. At the non-permissive temperature the level of *HTB1* mRNA in *nrd1-5* and *sen1* appeared slightly reduced compared to the wild-type parental strain (*Figure 3.1B*, lanes 8, 9 and 10). In *nab3-11*, histone mRNAs appeared similar to its parental wild-type strain (*Figure 3.1B*, lane 11). The results suggest that the individual components of the Nrd1p/Nab3p/Sen1p complex do not appear to significantly alter histone mRNA steady state levels.

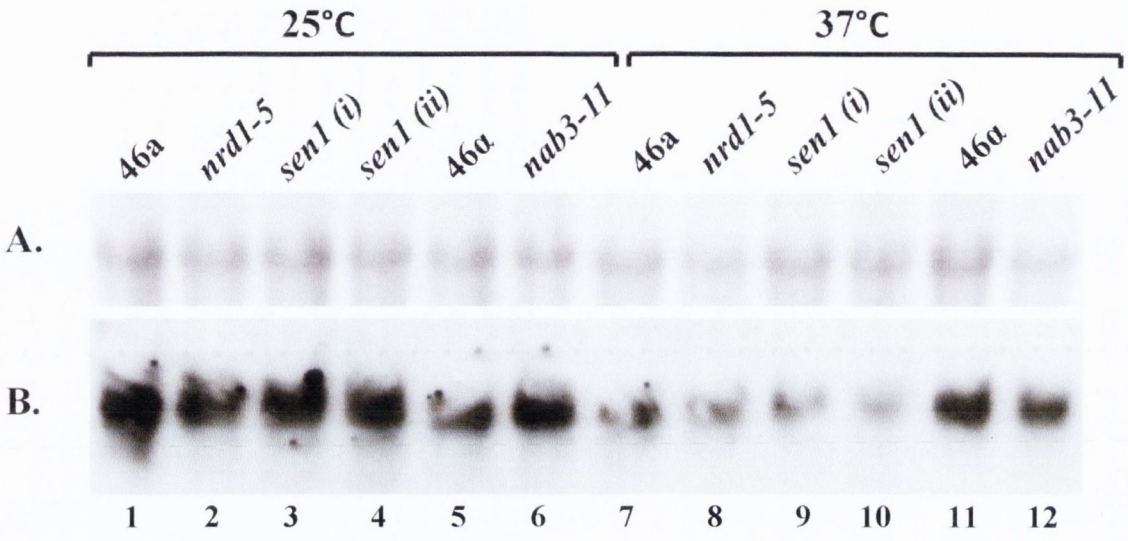

Figure 3.1: Northern blot analysis of *HTB1* mRNA with the individual temperature-sensitive components of the Nrd1p/Nab3p/Sen1p complex. Total RNA, 30μg, was isolated from the strains 46a (wild-type); *nrd1-5*; *sen1*; 46α (wild-type) and *nab3-11* at the permissive temperature (25°C) and following inactivation for 2hrs at the non-permissive temperature (37°C). **A.** Ethidium bromide stained gel showing the ribosomal RNAs. rRNA was used as a control of equal loading of the gel. **B.** The blot was hybridised with the *HTB1* probe.

Since Northern blot analysis is considered a semi quantitative technique, the steady-state levels of *HTB1* mRNA in the individual temperature sensitive mutants of the components of the Nrd1p/Nab3p/Sen1p complex were also quantified by real-time reverse transcription PCR (RT-PCR) (Chapter 2, section 2.10.4). To ensure that the RNA used was not contaminated with DNA, a negative control was set up for each reaction without the Reverse Transcriptase. Reactions were carried out in triplicate and a melt curve was included in each experiment (data not shown).

Initially, the correct concentrations of primers needed for the real-time RT-PCR was determined by carrying out a series of real-time RT-PCR reactions with varying concentrations of either the *HTB1* or 5.8S rRNA. The latter primer pair was used as an internal control to allow for variations in total RNA concentrations between samples. The primer concentration resulting in the least amount of primer dimers (2.5pmole/µl for *HTB1* and 1pmole/µl for 5.8S rRNA primers) were chosen and used in all subsequent reactions (data not shown).

The efficiencies of amplification using the *HTB1* and 5.8S rRNA primers were calculated in order to determine the true fold increase of the products after each cycle. The primer efficiencies of the *HTB1* and 5.8S rRNA were determined by varying the concentration of cDNA in the real-time RT-PCR reaction and then plotting the average Ct values (the cycle at which there is a significant detectable increase in fluorescence above background) for each cDNA concentration against the log of the amount of cDNA used (*Figure 3.2*). The efficiency of the primers was found to be 96% for the *HTB1* primers and 72% for the 5.8S rRNA primers i.e. the *HTB1* and 5.8S rRNA primers replicate the PCR products at a rate of 1.96 and 1.72 respectively for each real-time cycle.

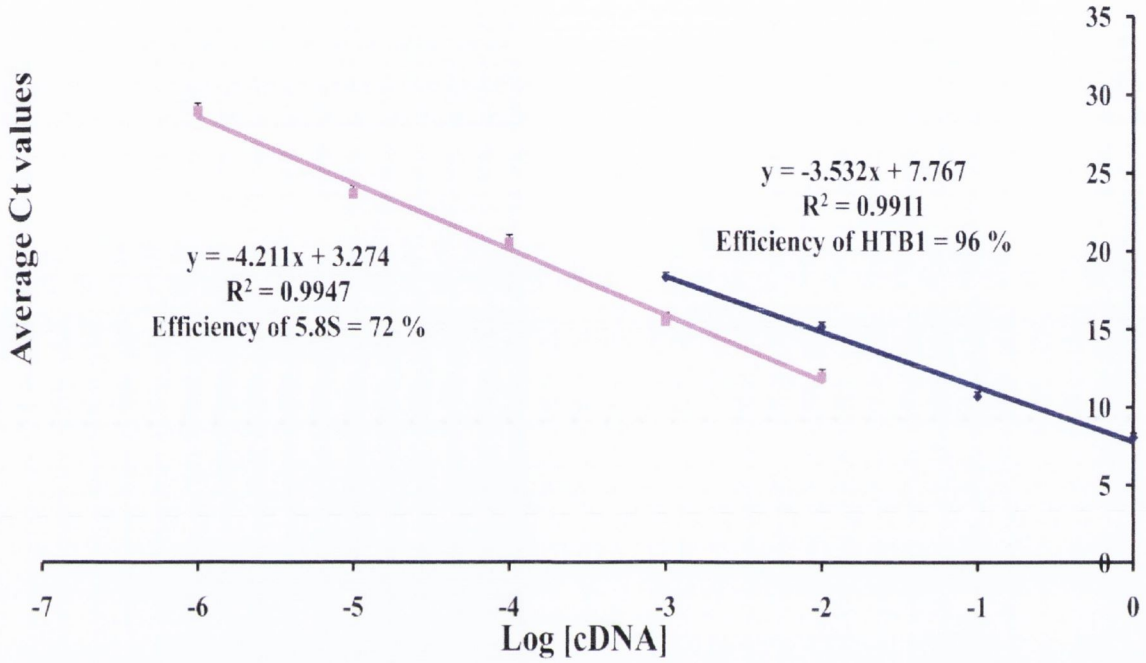

Figure 3.2: Primer efficiencies of the HTB1_Endo and 5.8S rRNA primers. The primer efficiencies of the HTB1_Endo (navy) and 5.8S rRNA primers (pink) were determined by varying the concentration of cDNA in the real-time RT-PCR reaction and plotting the average Ct values for each cDNA concentration against the log of the amount of the cDNA used.

Real-time RT-PCR analysis was carried out for RNA isolated from each temperature sensitive mutant and the wild-type strains as described in Chapter 2, section 2.10.4. Using the calculations discussed in Chapter 2, section 2.10.4, the Ct values were used to calculate the level of *HTB1* expression at the non-permissive temperature, 37°C.

The level of expression of the mutant strains was compared to those of the wild-type strains and the results were plotted. The ratio of *HTB1* to 5.8S rRNA was set at 1.0 for the wild-type strain and all mutant strains were compared to this. The experiment was carried out a total of three times and the average expression levels of *HTB1* mRNA for the individual components of the Nrd1p/Nab3p/Sen1p complex were calculated from the accumulated data sets (*Figure 3.3*). The trend observed in the Northern blot analysis were no significant decrease in the levels of *HTB1* mRNA expression was observed for each of the individual components of the Nrd1p/Nab3p/Sen1p termination complex upon inactivation at the non-permissive temperature was also observed by real-time RT-PCR. At the non-permissive temperature, *nrd1-5* shows a slight decrease in *HTB1* mRNA expression (*Figure 3.3*). While an increase in the levels of *HTB1* mRNA expression was also observed for *nab3-11*, this increase was not statistically significant. The observations from both Northern blot analysis and real-time RT-PCR demonstrate that inactivation of the individual components of the Nrd1p/Nab3p/Sen1p termination complex exert no significant effect on the steady state levels of *HTB1* mRNA.

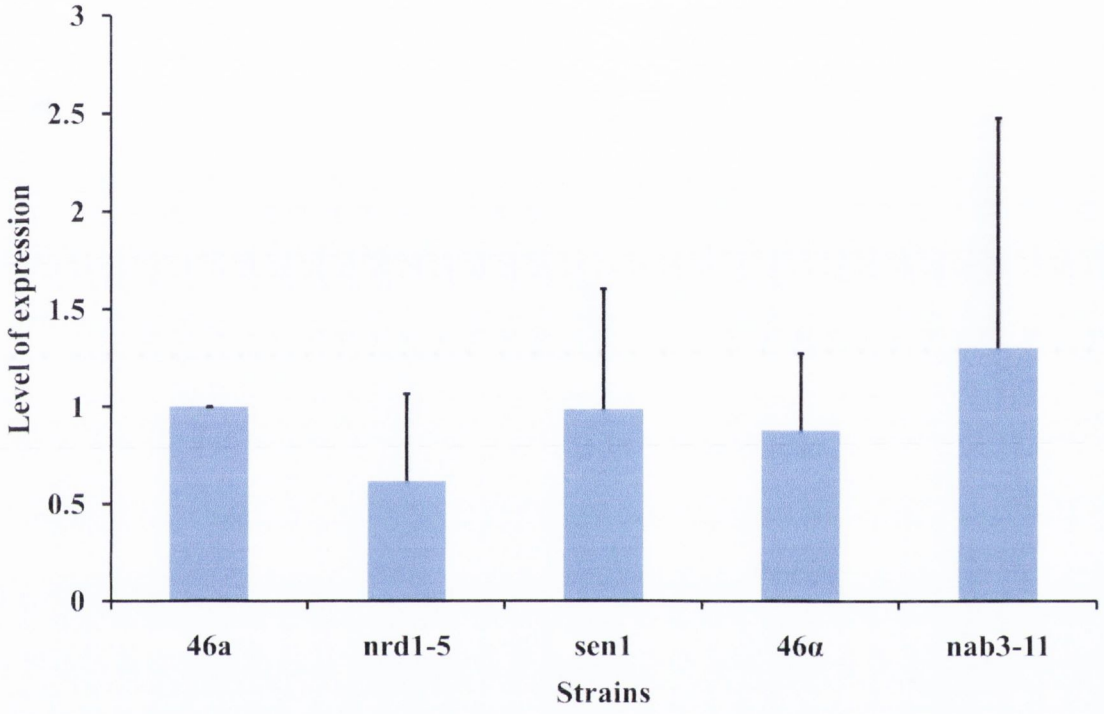

Figure 3.3: Comparison of the steady state levels of *HTB1* mRNA at 37°C by real-time RT-PCR. 2μg of total RNA from the individual components of the Nrd1p/Nab3p/Sen1p complex which had undergone inactivation at 37°C for 2hrs was reverse transcribed with *HTB1* and 5.8S rRNA primers and subsequently underwent real-time RT-PCR. The level of *HTB1* mRNA expression was calculated for each mutant and compared to the *HTB1* mRNA expression of the wild-type, 46a, which was set at 1.

3.2.2 Sen1p is involved in transcription termination of *HTB1* mRNA and works independently of Nrd1p and Nab3p

Both the Northern blot and real-time RT-PCR analysis suggested that the individual components of the Nrd1p/Nab3p/Sen1p complex did not significantly alter the steady state levels of histone mRNA. To determine if any of the components of the Nrd1p/Nab3p/Sen1p termination complex contribute to transcription termination of histone mRNAs, the *nrd1-5, sen1* and *nab3-11* temperature sensitive strains were inactivated as described in section 3.2.1 and total RNA was isolated (Chapter 2, section 2.1). To capture any unprocessed primary transcripts that have not been cleaved and polyadenylated at the correct 3'-end of the mRNA, RT-PCR was carried out using reverse primers spanning the region downstream of the correct 3'-end cleavage site of the *HTB1* mRNA (see *Figure 3.4A*). The cDNA products were amplified using a common forward primer (*Figure 3.4A* and Chapter 2, Table 2.2). If 3' end processing occurs normally, then a product emanating from reverse primer 1, which is located upstream of the known cleavage sites as defined by (Campbell et al., 2002; Miura et al., 2006) should be observed. However, if cleavage and polyadenylation have not occurred, RNA read-through products downstream of the poly(A) site are expected. In order to confirm the predicted sizes of the fragments to be generated by RT-PCR, PCR reactions were first carried out using S288c genomic DNA (*Figure 3.4B*, lanes 1 to 7).

Figure 3.4A: Schematic diagram of the *HTB1* gene and the location of the primers used for RT-PCR. The location of the primers used for cDNA synthesis (Rev1–Rev7) are shown, as is the forward primer (For1) used for PCR amplification of the cDNAs. The open reading frame 1-397 is designated by a black rectangle. The expanded nucleotide sequence shows the location of the major 3' end cleavage sites for *HTB1* (*) as previously been identified by (Campbell et al., 2002; Miura et al., 2006). **B.** PCR amplification of the *HTB1* fragments and their predicted sizes by PCR. DNA fragments spanning the 3' end of the *HTB1* gene were amplified in PCR reactions using S288c genomic DNA as template. A common forward primer (HTB1 For1) was used in each reaction (see Figure 3.4A). The sequence of the primers and their location on the *HTB1* gene are shown in Table 2.2. Lane 1; Rev1 (147nts), Lane 2; Rev2 (231nts), Lane 3; Rev3 (309nts), Lane 4; Rev4 (392nts), Lane 5; Rev5 (468nts), Lane 6; Rev6 (554nts), Lane 7; Rev7 (646nts) and Lane M; molecular weight marker. The expected sizes of the PCR products (nts) are shown in brackets.

A. Location of primers used in assay.

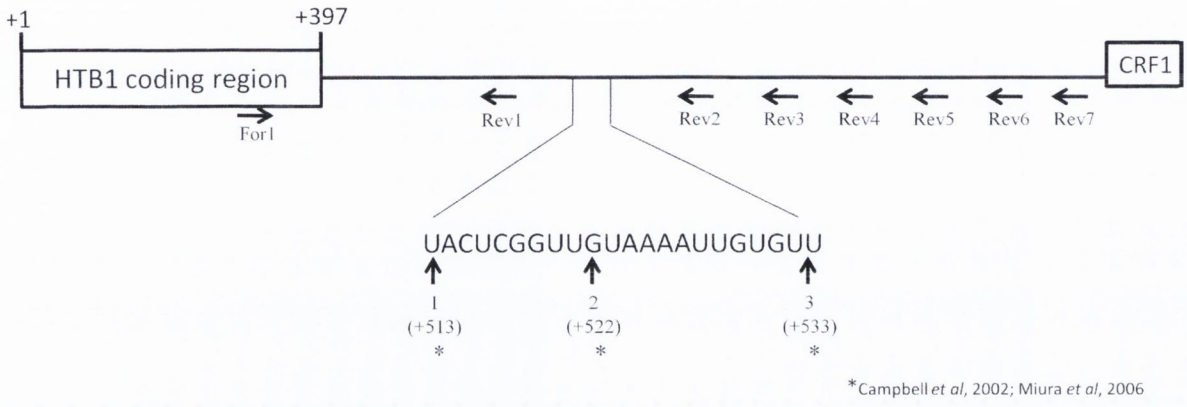

*Campbell *et al*, 2002; Miura *et al*, 2006

B. PCR amplification control using DNA.

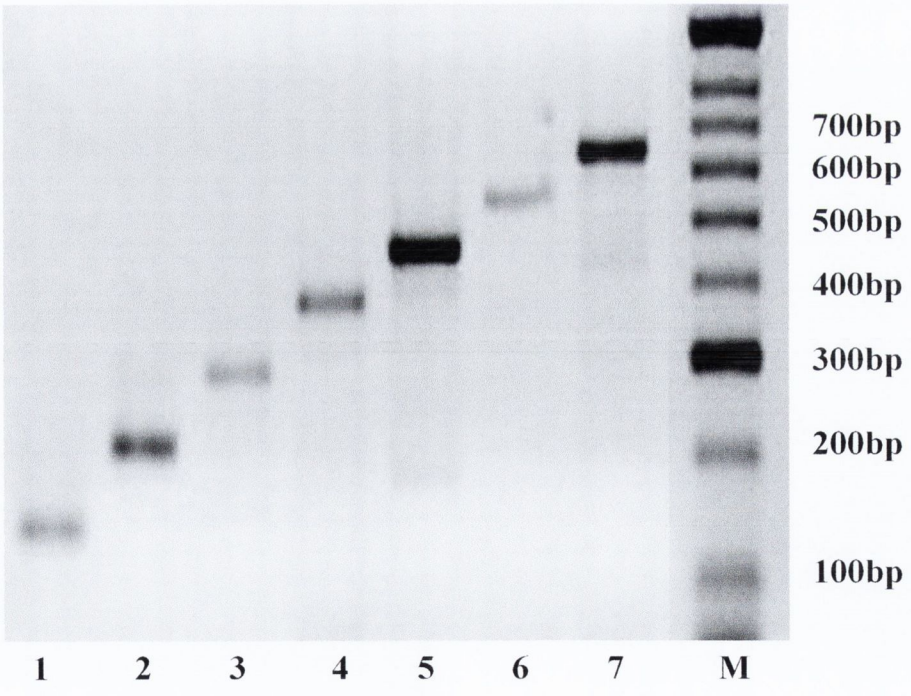

Previous studies have demonstrated that transcription termination is inhibited in the temperature sensitive strain *rna14-3/Δrrp6* (Birse et al., 1998; Canavan and Bond, 2007). Therefore as a positive control for the read-through assay, RT-PCR was carried out using total RNA isolated from the temperature sensitive strain. cDNA was prepared as described in Chapter 2, section 2.10.2 and PCR amplification was carried out using a common forward primer and seven reverse primers spanning the downstream region of the correct 3'-end cleavage site of the *HTB1* mRNA (*Figure 3.4A*). As shown in *Figure 3.5A*, at 22°C, the RNA is correctly processed and a product is detected with reverse primer 1 (lane 1). A small amount of read-through product was detected with HTB1 reverse 2 (lane 2). A band of 304nts was also observed with reverse primer 2 and through DNA sequencing was shown to be 99% identical to the yeast *HKA* gene and 98% identical to the *NIN1* gene, a subunit of the 19S regulatory particle of the 26S proteasome lid. The band observed in lane 5 does not represent a genuine HTB1 RT-PCR product as sequence analysis identifies it as *YKL006w*, the N-terminally acetylated component of the 60S ribosomal subunit. At 37°C, read-through products are detected with six of the reverse primers (*Figure 3.5B,* lanes 1-6). To ensure that the RNA used was not contaminated with DNA, a negative control was set up for each reaction without Reverse Transcriptase (*Figure 3.5A* and *B,* lane 8). The results demonstrate that disruption of cleavage and polyadenylation leads to read-through RNA as a result of inhibition of transcription termination, demonstrating the feasibility of this assay for detecting such transcripts.

Figure 3.6A demonstrates the results observed for the RT-PCR reaction carried out on the wild-type strain, 46a, at the permissive temperature (25°C) and the non-permissive temperature (37°C). PCR products were obtained with reverse primer 1 (*Figure 3.6A,* lane 1) and a very low amount of product of the correct size (231nts) was observed with reverse primer 2 (lane 2, denoted by *) representing a small amount of read-through primary transcript, indicating that the majority of *HTB1* transcripts are correctly cleaved and polyadenylated at both the permissive and non-permissive temperature. The strong artefactual band of 304nts was also observed in lane 2.

As with the wild-type strains, in *nrd1-5* correctly processed RNA was detected with reverse primer 1 (*Figure 3.6B,* lane 1). A small amount of read-through transcripts (231nts) was observed with reverse primer 2 (lane 2). The 304nts artefactual band was also evident with this primer. At the non-permissive temperature, no read-through

transcripts were evident (*Figure 3.6B*, lanes 2 to 7). This same pattern was observed for Nab3-11p at both the permissive and non-permissive temperatures (*Figure 3.6C*), indicating that inactivation of either Nab3p or Nrd1p has no effect on transcription termination and 3' end processing of histone mRNA.

However for the temperature sensitive strain *sen1*, a different pattern was evident. At the permissive temperature, as with the other strains, RT-PCR products were observed with reverse primer 1 (*Figure 3.6D*, lane 1). At the non-permissive temperature, read-through products were detected for reverse primers 2 to 5 (*Figure 3.6D*, lanes 2-5). The read-through products (indicated by * in *Figure 3.6D*) were isolated and DNA sequenced, confirming them as histone H2B specific transcripts. These results were confirmed with five independent RNA samples. A number of bands not of the predicted size for *HTB1* products were also observed in lanes 2-5. To identify *HTB1* specific products, Southern blotting was performed on the RT-PCR products of *sen1* at both temperatures using digoxygenin-labelled DNA probe spanning the downstream region of *HTB1* from For1 to Rev7, *Figure 3.4A*. As shown in *Figure 3.7*, only read-through products of the correct size were detected for reverse primers 1 to 5 indicating that the other bands were non-specific. This experiment was repeated twice using independent RT-PCR samples of *sen1* at the non-permissive temperature. The non-specific PCR products evident in *Figure 3.6D* reflect the limited quantity of substrate (primary transcripts) present in the reaction. Sequencing of these PCR products indicate that they originate from rRNA and other genes which are unrelated to histone genes (data not shown) and may reflect the high A-T content of the primers. The results from the *sen1* RT-PCR analysis indicate the inactivation of the Sen1p at 37°C effects the transcription termination of *HTB1* mRNA.

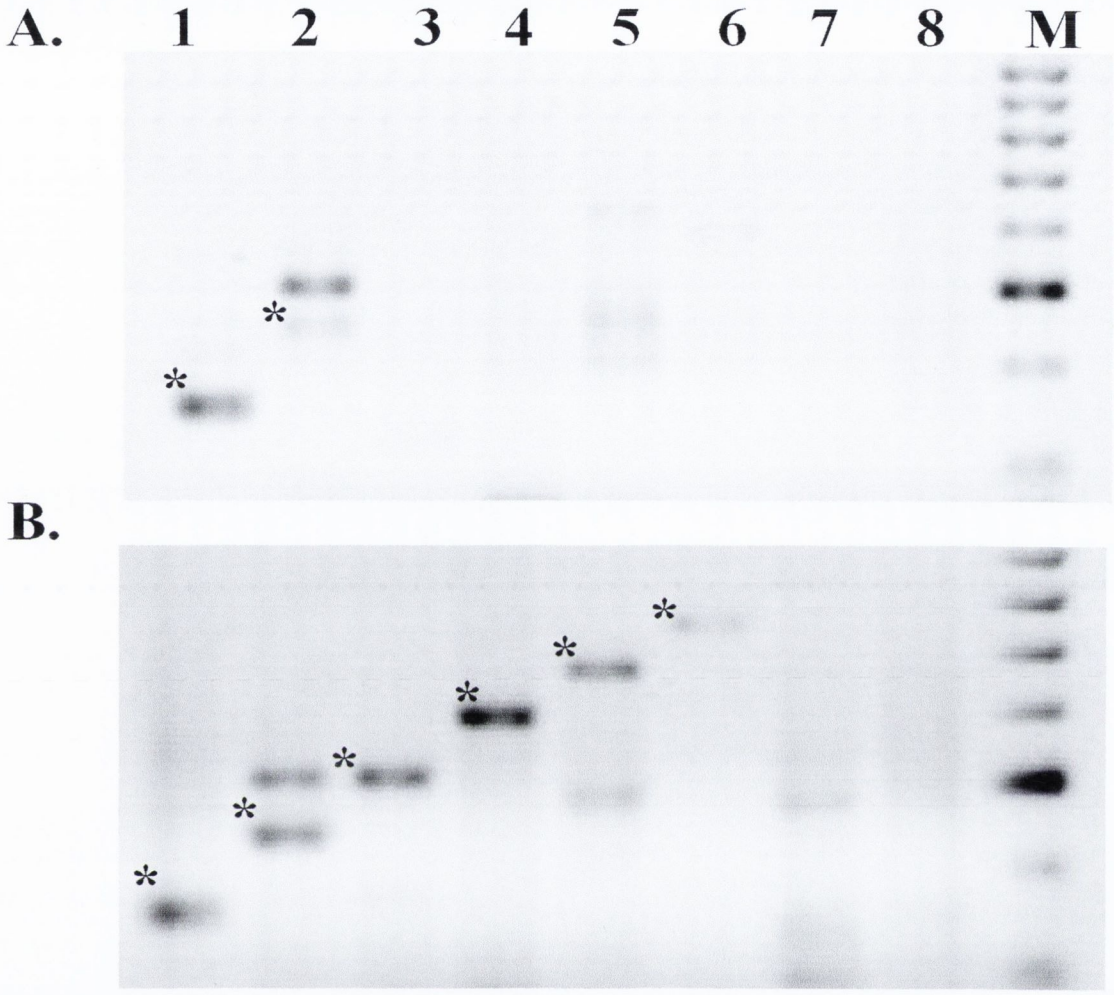

Figure 3.5: Inactivation of *rna14-3/Δrrp6* at 37°C leads to read-through of primary mRNA transcripts. cDNA was prepared from total RNA from *rna14-3/Δrrp6* at 22°C and 37°C using a common forward primer (HTB1 For1) and seven reverse primers spanning the downstream region of *HTB1* (refer to Figure 3.4A). Lane 1; Rev 1 (147nts), lane 2; Rev 2 (231nts), lane 3; Rev 3 (309nts), lane 4; Rev 4 (392nts), lane 5; Rev 5 (468nts), lane 6; Rev 6 (554nts), lane 7; Rev 7 (655nts), lane 8, cDNA from Rev 1 in the absence of Reverse Transcriptase, lane M; 100bp DNA molecular weight marker. The expected sizes of the PCR products (nts) are shown in brackets. **A.** RT-PCR products of *rna14/Δrrp6* at 22 °C. **B.** RT-PCR products of *rna14/Δrrp6* at 37 °C.

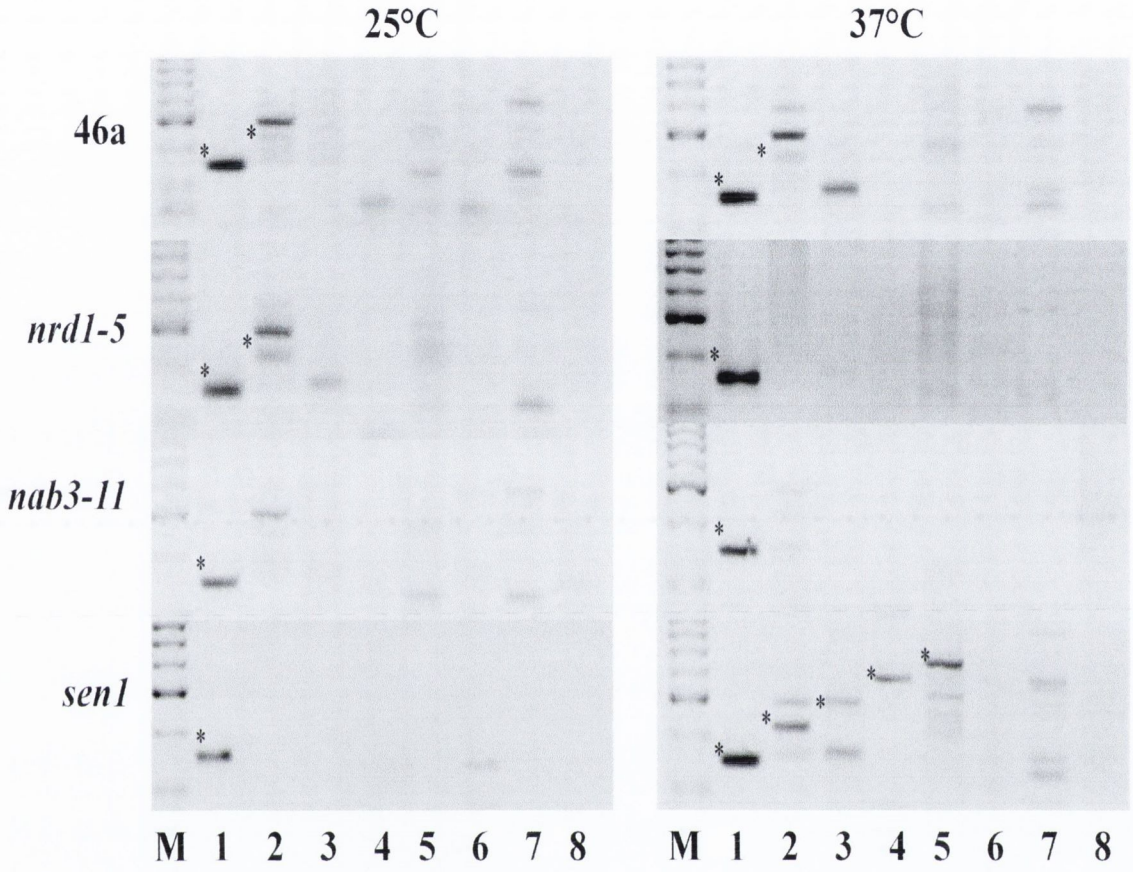

Figure 3.6: Inactivation at the non-permissive temperature leads to read-through *HTB1* primary mRNA transcripts in *sen1*. Total RNA from the individual components of the Nrd1p/Nab3p/Sen1p termination complex was reverse transcribed using primers spanning the downstream region of *HTB1* and amplified using a common forward primer (HTB1 For1). Lane M; molecular weight marker, Lane 1; Rev1 (143nts), Lane 2; Rev2 (231nts), Lane 3; Rev3 (309nts), Lane 4; Rev4 (392nts), Lane 5; Rev5 (468nts), Lane 6; Rev6 (554nts), Lane 7; Rev7 (646nts) and Lane 8; cDNA prepared using Rev1 in the absence of Reverse Transcriptase. * represents *HTB1*-specific PCR products of the expected size and the expected sizes of the PCR products (nts) are shown in brackets. **A.** Wild-type, 46a, at 25°C and 37°C. **B.** *nrd1-5* at 25°C and 37°C. **C.** *nab3-11* at 25°C and 37°C. **D.** *sen1* at 25°C and 37°C.

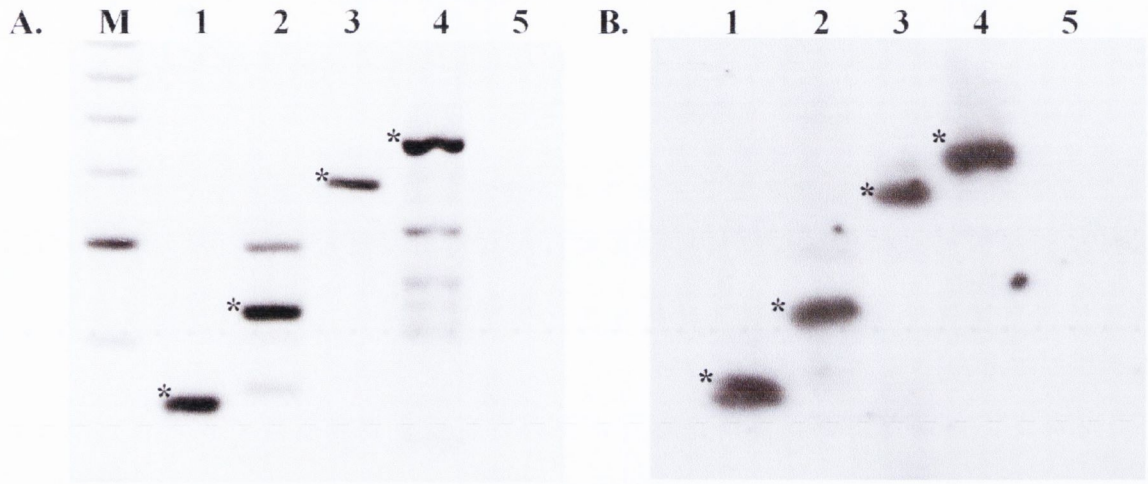

Figure 3.7: Eradication of non-specific bands observed by RT-PCR in *sen1* at the non-permissive temperature. **A.** RT-PCR analysis of *HTB1* mRNA from *sen1* cells grown at 37°C for 2hrs. Lane M; molecular weight marker, Lanes 1-4; cDNAs prepared using reverse primers Rev1, Rev2, Rev4 and Rev5, Lane 5; cDNAs prepared using Rev1 in the absence of Reverse Transcriptase. **B.** Southern blot of gel shown in A. hybridised with a *HTB1*-specific probe. * denote the *HTB1*-specific PCR products of the expected size.

3.2.3 Sen1p disrupts transcription termination in all histone mRNAs

In order to test whether *sen1* has the same effect on transcription termination for all histone genes, the RT-PCR read-through analysis was conducted on four other histone RNAs (*HTA1*, *HHF1*, *HHT1* and *HTB2*). Previously Miura *et al.*, (2006), analysed the open reading frames (ORFs) of *S. cerevisiae* using a large scale cDNA analysis of the budding yeast transcriptome, and from this mapped the length of the 5'UTR, the coding region and the 3'UTR within both total and polyadenylated RNA. Using this data, the location of 3'end cleavage sites for histone RNA were mapped (*Table 3.1).* Oligonucleotides where designed to flank the area of the cleavage sites and the downstream region of the genes, as described above for the *HTB1* gene. Prior to RNA extraction, the wild-type and *sen1* cells were inactivated at the non-permissive temperature (37°C) for 2hrs (Chapter 2, section 2.1). cDNAs were prepared using DNase-treated total RNA (2µg) using primers complementary to sequences downstream of *HTA1*, *HHF1*, *HHT1* and *HTB2* (Chapter 2, section 2.10.2). As described for *HTB1*, the cDNAs were amplified using a common forward primer (*Figure 3.8 -3.12* and Table 2.2).

Gene	Start	End	Length	5' UTR	3' UTR	Coding Region
HTB1	914187	914819	633nts	113nts	124nts	396nts
HTA1	915423	916079	657nts	101nts	157nts	399nts
HHF1	255192	255728	537nts	46nts	179nts	312nts
HHT1	256292	256836	545nts	37nts	97nts	411nts
HTA2	235272	235840	569nts	45nts	125nts	399nts
HTB2	236372	237092	721nts	123nts	202nts	396nts
HHT2	575384	576081	698nts	32nts	255nts	411nts
HHF2	576686	577166	481nts	40nts	129nts	312nts

Table 3.1: Location of the 3' end cleavage sites of the histone RNAs. Through a large scale cDNA analysis of the transcriptome of *S. cerevisiae*, Miura *et al*, (2006) mapped the cleavage sites of the open reading frames within *S. cerevisiae*. From this data, the length of the coding region, the 5'UTR, the 3'UTR was extrapolated for each of the histone RNAs and the locations of 3' end cleavage sites were mapped (Miura et al., 2006).

Histone *HTA1* codes for histone H2A and shares a bidirectional promoter with *HTB1*. In the nucleosome H2A forms a dimer with H2B. Since read-through primary transcripts of *HTB1* were detected in the *sen1* mutant strain at the non-permissive temperature, we tested whether *HTA1* mRNA would be similarly affected in *sen1*. The location of the cleavage site for both *HTA1* and *HTB1* as mapped by Miura *et al.*, (2006) are shown in *Figure 3.8A* while *Figure 3.8B* illustrates the location of the primers used in the RT-PCR. At the permissive temperature, transcription termination of *HTA1* in *sen1* is not significantly affected as only a small amount of read-through primary product was detected with reverse primer 3, which is located approximately 35nts downstream of the 3' end cleavage sites (*Figure 3.8E,* lane 2). At the non-permissive temperature, *sen1* exerted the same effect on *HTA1* as *HTB1*. Read-through past the cleavage sites was detected with reverse primers 3 and 5 (*Figure 3.8D,* lane 2 and 3) which is located 201nts downstream of the cleavage sites. As observed previously, read-through transcripts were detected with *HTB1*-specific primers in *sen1* mutant at the non-permissive temperature (*Figure 3.8C* and *D*).

The genes *HTA2* and *HTB2*, encoding H2A and H2B respectively are also bi-directionally transcribed from a common promoter (Osley and Hereford, 1982). *Figure 3.9A* demonstrates *HTB2* and *HTA2* transcripts as mapped by Miura *et al.*, (2006). The locations of the oligonucleotides used for the *HTB2* RT-PCR reaction are shown *Figure 3.9B*. *HTA2* was not analysed in this study. As previously found for both *HTA1* and *HTB1*, at the permissive temperature, *sen1* exerted no significant effect on transcription termination of *HTB2* with only a small amount of read-through detected for reverse primer 3 which is located approximately 129nts downstream of the known cleavage sites (*Figure 3.9C*, lane 2*)*. At the non-permissive temperature, significant read-through past the known cleavage sites of *HTB2* was detected with PCR products detected with reverse primers 3 to 5 (*Figure 3.9D*, lane 2 and 3*)*.

Figure 3.8: *HTB1* and *HTA1* mRNA RT-PCR results of the temperature-sensitive strain, *sen1*. Total RNA from *sen1* was reverse transcribed using primers spanning the downstream region of *HTB1* and *HTA1* and amplified using the common forward primer. **A.** Map of the boundaries of the *HTB1* and *HTA1* transcripts taken from Miura *et al,* (2006). **B.** Schematic diagram of the *HTB1* and *HTA1* genes. The location of the 3'-end cleavage site (arrows) and the locations of the primers used for cDNA synthesis (Rev1-Rev7) are shown, as are the forward primers (For) used for PCR amplification of the cDNAs. The expected sizes of the RT-PCR products using the common forward primer and specific reverse primers are shown below each reverse primer. The genes located adjacent to *HTB1* and *HTA1* are also shown. **C.** RT-PCR analysis of *HTB1* mRNA from *sen1,* grown at 25°C for 2hrs. Lane M; molecular weight marker, Lanes 1-7; cDNAs prepared using *HTB1* reverse primers Rev1-Rev7 respectively and amplified using the common forward primer For1, Lane 8; cDNA from Rev1 in the absence of Reverse Transcriptase. **D.** RT-PCR analysis of *HTB1* mRNA from *sen1*, grown at 37°C for 2hrs. Lanes are as per C. **E.** RT-PCR analysis of *HTA1* mRNA from *sen1,* grown at 25°C for 2hrs. Lane M; molecular weight marker, Lanes 1-3; cDNAs prepared using *HTA1* reverse primers Rev1, Rev3 and Rev5 respectively and amplified using the common forward primer For, Lane 4; cDNA from Rev1 in the absence of Reverse Transcriptase. **F.** RT-PCR analysis of *HTA1* mRNA from *sen1*, grown at 37°C for 2hrs. Lanes are as per E. * denote the *HTB1*- and *HTA1*-specific PCR products of the expected size.

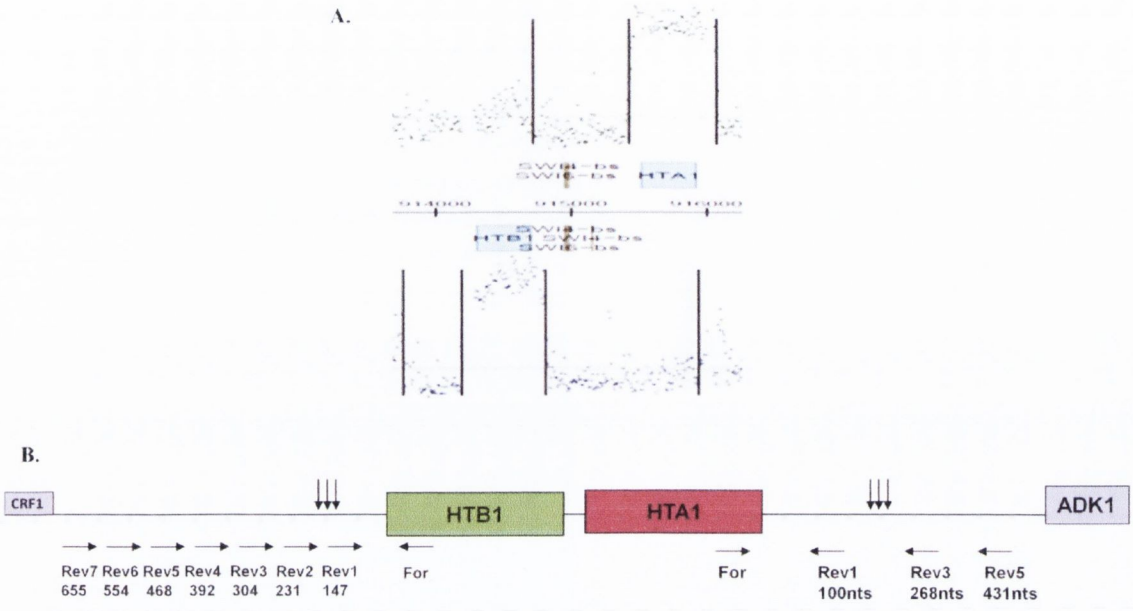
A.
HTA1
B.
CRF1
HTB1
HTA1
ADK1
Rev7 655
Rev6 554
Rev5 468
Rev4 392
Rev3 304
Rev2 231
Rev1 147
For
For
Rev1 100nts
Rev3 268nts
Rev5 431nts

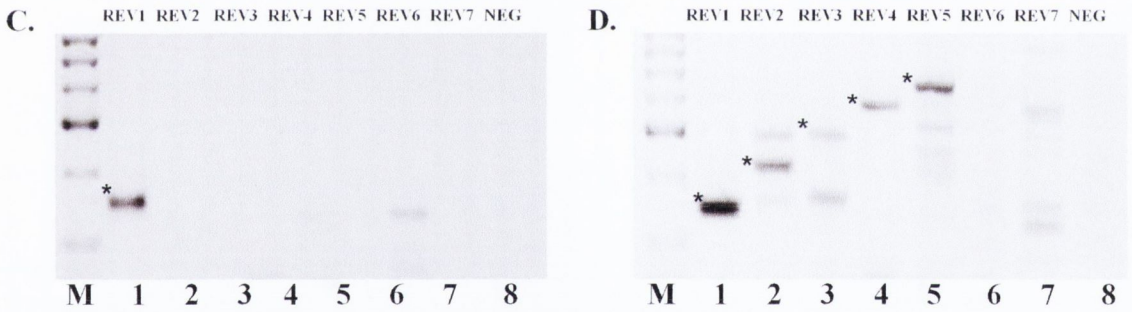
C.
REV1 REV2 REV3 REV4 REV5 REV6 REV7 NEG
M 1 2 3 4 5 6 7 8
D.
REV1 REV2 REV3 REV4 REV5 REV6 REV7 NEG
M 1 2 3 4 5 6 7 8

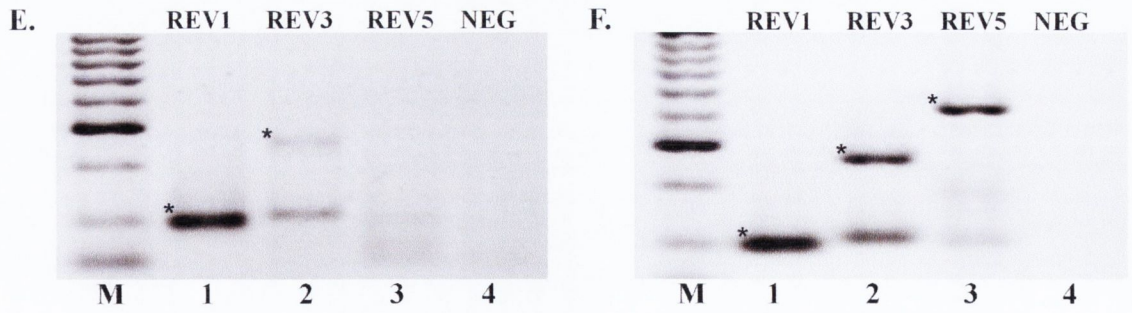
E.
REV1 REV3 REV5 NEG
M 1 2 3 4
F.
REV1 REV3 REV5 NEG
M 1 2 3 4

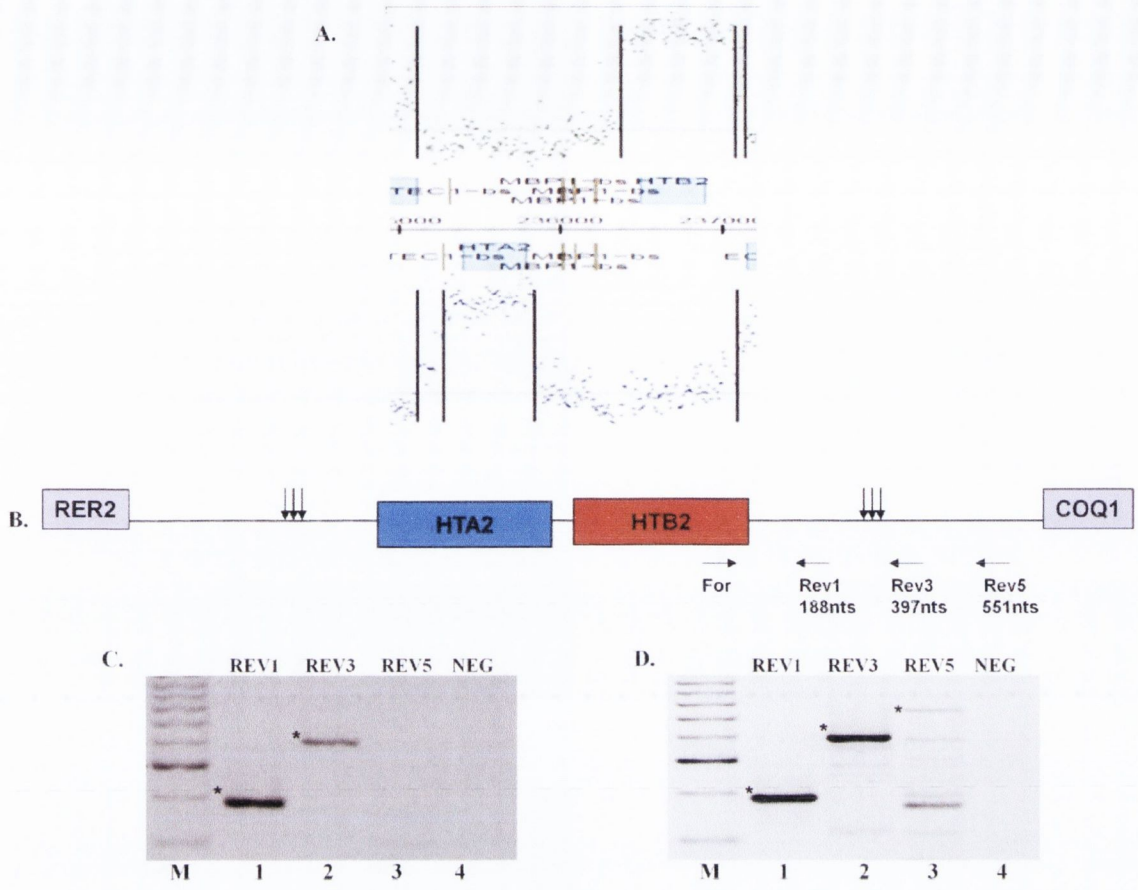

Figure 3.9: *HTB2* mRNA RT-PCR results of the temperature-sensitive strain, *sen1*. Total RNA from *sen1* was reverse transcribed using primers spanning the downstream region of *HTB2* and amplified using the common forward primer. **A.** Map of the boundaries of the *HTB2* and *HTA2* transcripts taken from Miura *et al*, (2006). **B.** Schematic diagram of the *HTB2* gene. The location of the 3'-end cleavage site (arrows) and the location of the primers used for cDNA synthesis (Rev1, Rev3 and Rev5) are shown, as is the forward primer (For) used for PCR amplification of the cDNAs. The expected sizes of the RT-PCR products using the common forward primer and specific reverse primers are shown below each reverse primer. The genes located adjacent to *HTA2* and *HTB2* are also shown. **C.** RT-PCR analysis of *HTB2* mRNA from *sen1*, grown at 25°C for 2hrs. Lane M; molecular weight marker, Lanes 1-3; cDNAs prepared using *HTB2* reverse primers Rev1, Rev3 and Rev5 respectively and amplified using the common forward primer For, Lane 4; cDNA from Rev1 in the absence of Reverse Transcriptase. **D.** RT-PCR analysis of *HTB2* mRNA from *sen1*, grown at 37°C for 2hrs. Lanes are as per C. * denote the *HTB2* -specific PCR products of the expected size.

The histone genes *HHF1* and *HHT1*, encoding for H3 and H4 respectively, share a bi-directional promoter. As with *HTA1*, *HTB1* and *HTB2*, *sen1* had no effect on the transcription termination of *HHF1* or *HHT1* at the permissive temperature, with no read-through primary transcripts detectable beyond reverse primer 1 (*Figure 3.10C* and *E*, lanes 2 and 3). At the non-permissive temperature, read-through primary transcripts were detected for both *HHF1* and *HHT1*. For *HHF1*, read-through was detected by reverse primers 3 and 5 (*Figure 3.10D,* lane 2 and 3). Read-through was also detected up to reverse primer 3 for *HHT1* at the non-permissive temperature in *sen1* (*Figure 3.10F*, lane 2).

To determine if the effect of *sen1* on transcription termination was specific to histone genes, a number of other transcripts were tested for read-through transcription. As with the histone RNAs, data from Miura *et al*, (2006) was used to locate the cleavage sites of the constitutively expressed *TDH3* mRNA (*Figure 3.11A*) and from this, oligonucleotides were designed spanning the downstream region of *TDH3* (*Figure 3.11B*). At the permissive temperature, a small amount of read-through of primary transcript was detected for *TDH3* using reverse primer 2 (*Figure 3.11A*, lane 2). A high level of non-specific bands was visible for reverse primers 2 to 7 which may reflect the high A-T content of the primers (*Figure 3.11C*, lane 2 to 7). At the non-permissive temperature, read-through was detected up to reverse primer 4 which is located 268nts downstream of the known cleavage sites (*Figure 3.11D*, lane 4). A similar result was observed for *ACT1*. At the permissive temperature no read-through of primary transcripts were observed past reverse primer 2 which spans the 3' end cleavage sites (*Figure 3.12C,* lane 1). At the non-permissive temperature, *ACT1* read-through primary transcripts were detected up to reverse primer 4 (*Figure 3.12D,* lanes 1 to 4) indicating that inactivation of Sen1p leads to read-through transcription termination on many mRNA transcripts.

For each of the RT-PCR reactions carried out, non-specific bands were detected at both temperatures tested. These bands reflect the limited quantity of primary transcripts present in the reactions. In order to eliminate these non-specific PCR products Southern blot analysis was conducted using DIG-labelled probes spanning the downstream region of each the genes tested (data not shown).

Figure 3.10: *HHF1* and *HHT1* mRNA RT-PCR results of the temperature-sensitive strain, *sen1*. Total RNA from *sen1* was reverse transcribed using primers spanning the downstream region of *HHF1* and *HHT1* and amplified using the common forward primer. **A.** Map of the boundaries of the *HHF1* and *HHT1* transcripts taken from Miura *et al,* (2006). **B.** Schematic diagram of the *HHF1* and *HHT1* genes. The location of the 3'-end cleavage site (arrows) and the locations of the primers used for cDNA synthesis (Rev1, Rev3 and Rev5) are shown, as are the forward primers (For) used for PCR amplification of the cDNAs. The expected sizes of the RT-PCR products using the common forward primer and specific reverse primers are shown below each reverse primer. The names of the adjacent genes are also shown. **C.** RT-PCR analysis of *HHF1* mRNA from *sen1,* grown at 25°C for 2hrs. Lane M; molecular weight marker, Lanes 1-3; cDNAs prepared using *HHF1* reverse primers Rev1, Rev3 and Rev5 respectively and amplified using the common forward primer For, Lane 4; cDNA from Rev1 in the absence of Reverse Transcriptase. **D.** RT-PCR analysis of *HHF1* mRNA from *sen1*, grown at 37°C for 2hrs. Lanes are as per C. **E.** RT-PCR analysis of *HHT1* mRNA from *sen1,* grown at 25°C for 2hrs. Lane M; molecular weight marker, Lanes 1-3; cDNAs prepared using *HHT1* reverse primers Rev1, Rev3 and Rev5 respectively and amplified using the common forward primer For, Lane 4; cDNA from Rev1 in the absence of Reverse Transcriptase. **F.** RT-PCR analysis of *HHT1* mRNA from *sen1*, grown at 37°C for 2hrs. Lanes are as per E. * denote the *HHF1*- and *HHT1*-specific PCR products of the expected size.

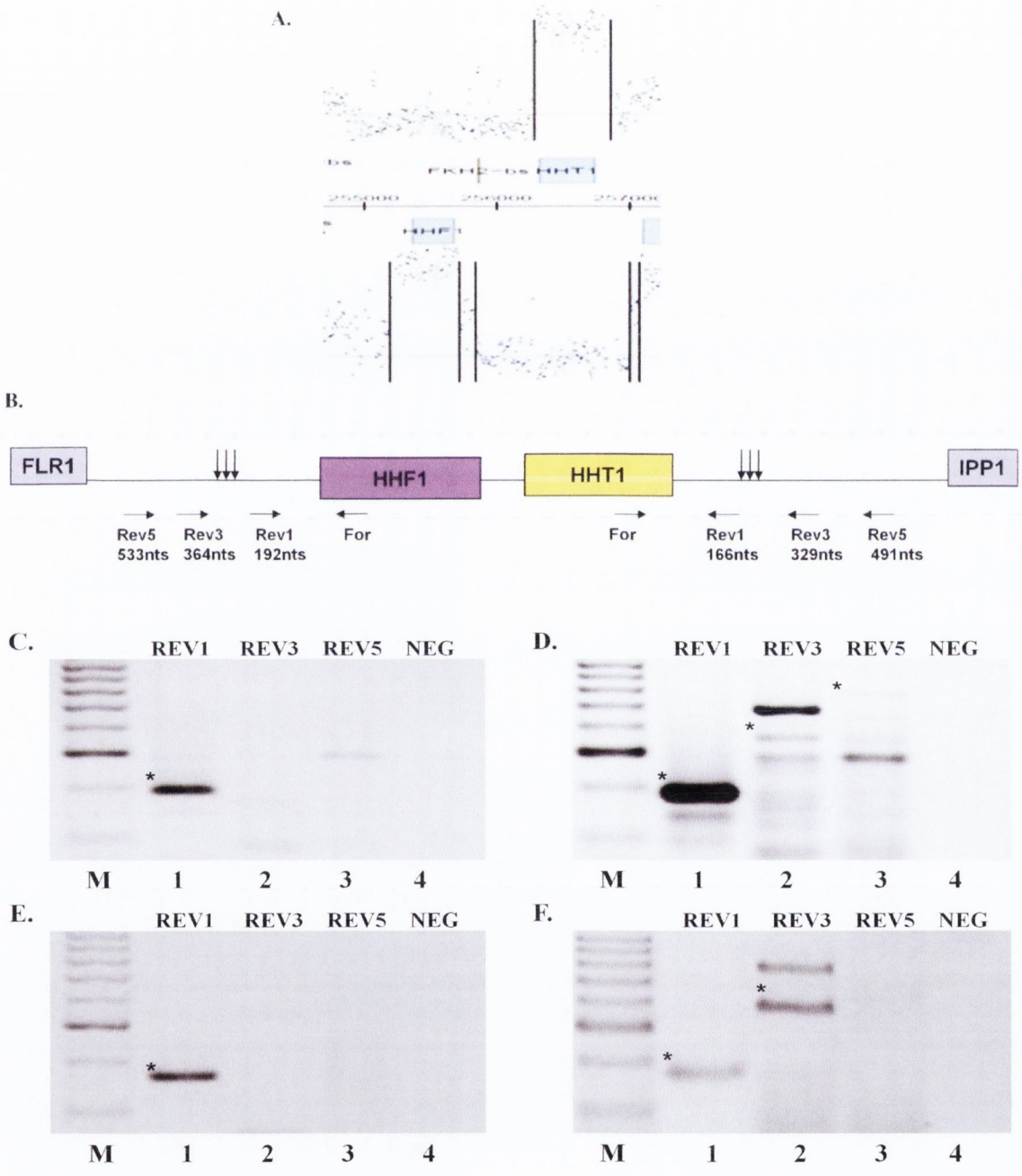
A.
B.
FLR1
HHF1
HHT1
IPP1
Rev5 533nts
Rev3 364nts
Rev1 192nts
For
For
Rev1 166nts
Rev3 329nts
Rev5 491nts
C.
REV1 REV3 REV5 NEG
M 1 2 3 4
D.
REV1 REV3 REV5 NEG
M 1 2 3 4
E.
REV1 REV3 REV5 NEG
M 1 2 3 4
F.
REV1 REV3 REV5 NEG
M 1 2 3 4

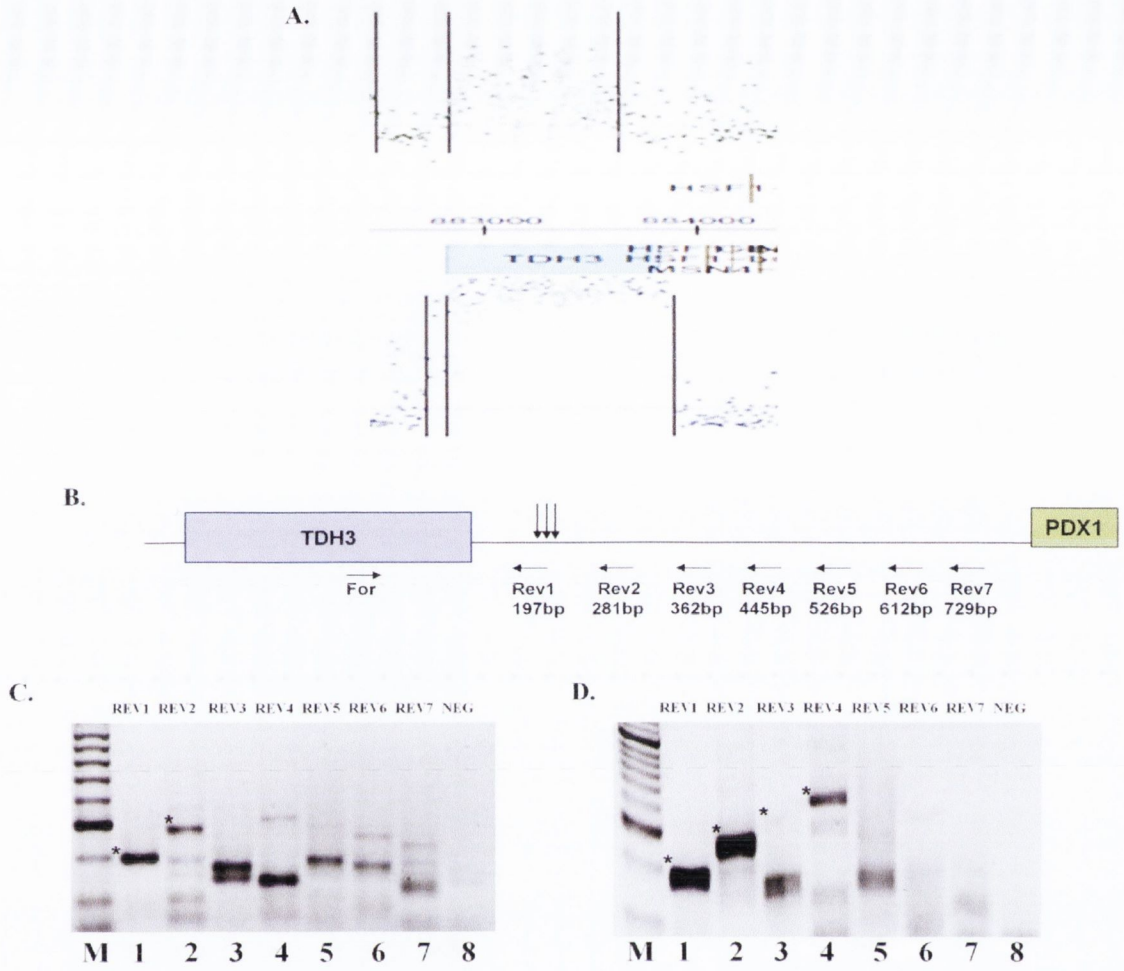

Figure 3.11: *TDH3* mRNA RT-PCR results of the temperature-sensitive strain, *sen1*. Total RNA from *sen1* was reverse transcribed using primers spanning the downstream region of *TDH3* and amplified using the common forward primer. **A.** Map of the boundaries of the *TDH3* transcripts taken from Miura *et al*, (2006). **B.** Schematic diagram of the *TDH3* gene. The location of the 3'-end cleavage site (arrows) and the location of the primers used for cDNA synthesis (Rev1-Rev7) are shown, as is the forward primer (For) used for PCR amplification of the cDNAs. The expected sizes of the RT-PCR products using the common forward primer and specific reverse primers are shown below each reverse primer. The gene *PDX1* which is located downstream of *TDH3* is also shown. **C.** RT-PCR analysis of *TDH3* mRNA from *sen1*, grown at 25°C for 2hrs. Lane M; molecular weight marker, Lanes 1-7; cDNAs prepared using *TDH3* reverse primers Rev1-Rev7 respectively and amplified using the common forward primer For, Lane 8; cDNA from Rev1 in the absence of Reverse Transcriptase. **D.** RT-PCR analysis of *TDH3* mRNA from *sen1*, grown at 37°C for 2hrs. Lanes are as per C. * denote the *TDH3*-specific PCR products of the expected size.

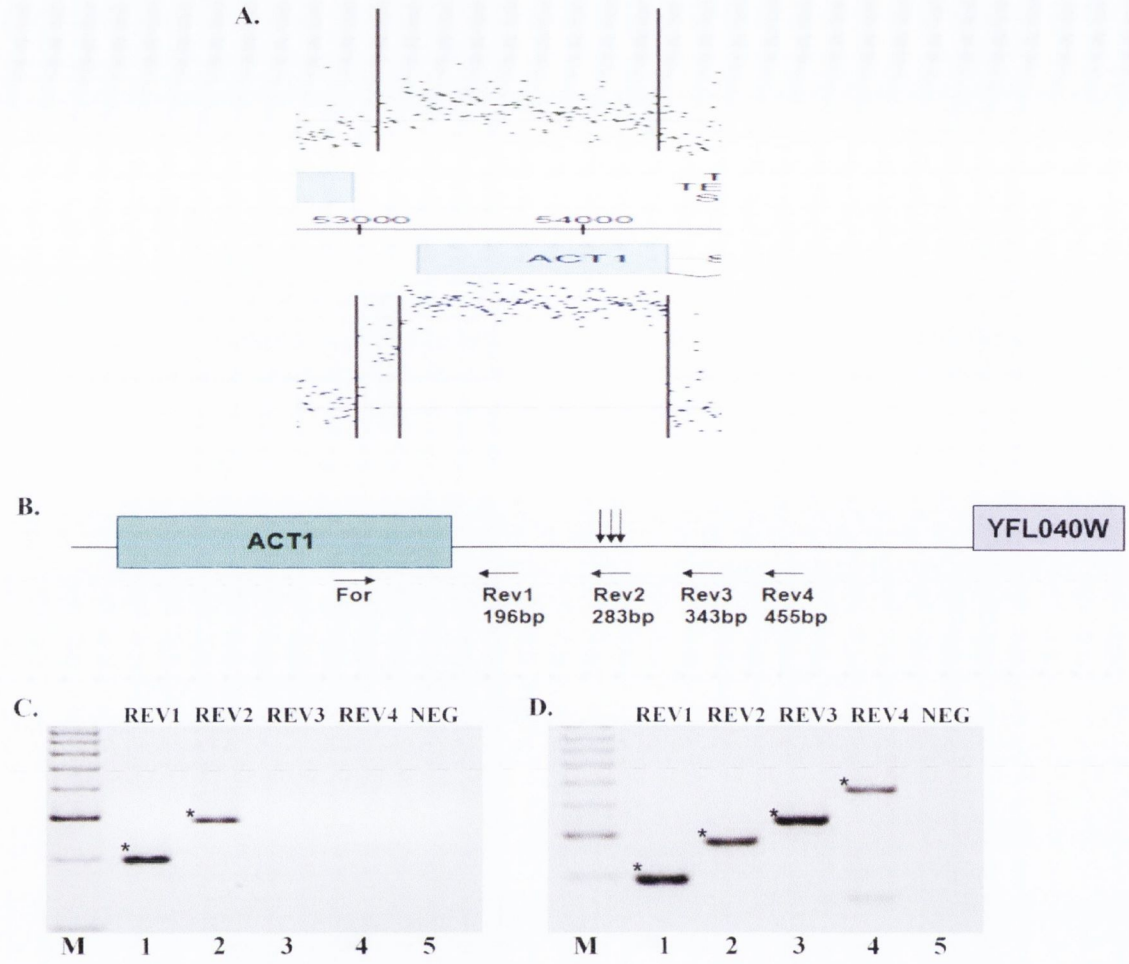

Figure 3.12: *ACT1* mRNA RT-PCR results of the temperature-sensitive strain, *sen1*. Total RNA from *sen1* was reverse transcribed using primers spanning the downstream region of *ACT1* and amplified using the same forward primer. **A.** Map of the boundaries of the *ACT1* transcripts taken from Miura *et al,* (2006). **B.** Schematic diagram of the *ACT1* gene. The location of the 3'-end cleavage site (arrows) and the location of the primers used for cDNA synthesis (Rev1, Rev3 and Rev5) are shown, as is the forward primer (For) used for PCR amplification of the cDNAs. The expected sizes of the RT-PCR products using the common forward primer and specific reverse primers are shown below each reverse primer. The gene *YFL040W*, which is located downstream of *ACT1*, is also shown. **C.** RT-PCR analysis of *ACT1* mRNA from *sen1*, grown at 25°C for 2hrs. Lane M; molecular weight marker, Lanes 1-3; cDNAs prepared using *ACT1* reverse primers Rev1, Rev3 and Rev5 respectively and amplified using the common forward primer For, Lane 4; cDNA from Rev1 in the absence of Reverse Transcriptase. **D.** RT-PCR analysis of *ACT1* mRNA from *sen1*, grown at 37°C for 2hrs. Lanes are as per C. * denote the *ACT1*-specific PCR products of the expected size.

3.3 The role of Hrp1p, Ssu72p and Rpb11p in transcription termination of histone mRNAs

New data presented in this study suggests Sen1p may play a role in transcription termination of polyadenylated mRNAs. A number of Sen1p-interacting proteins have recently been identified by (Kuehner and Brow, 2008) which included Hrp1p, Ssu72p and Rpb11p. These proteins are also components of the 3' end processing pathways of both polyadenylated and non-polyadenylated RNA. Strains containing temperature sensitive mutations in *HRP1-5*, *SSU72* and *RPB11* were tested. As with previous strains, the temperature sensitive strains *hrp1-5*, *ssu72*, *rpb11* and the wild-type strain, 46a, were grown to an OD_{600nm} value of 0.8 ($1x10^7$ cells/ml) at 25 °C and then inactivated for 2hrs at the non-permissive temperature, 37°C (Chapter 2, section 2.1). In addition to treatment at 25°C and 37°C, all strains underwent an inactivation at 16°C for 2hrs as *rpb11* is a cold sensitive strain. Northern blot analysis was performed on the extracted RNA using probes to both *HTB1* and *ACT1* as described in Chapter 2, section 2.9.3.

Figure 3.13 shows the results for Northern blot analysis of RNA extracted from the temperature sensitive mutants of these cleavage and polyadenylation factors and their wild-type counterparts. *HTB1* mRNA levels (*Figure 3.13C)* were compared to levels of *ACT1* mRNA (*Figure 3.13B*). A clear variability in the levels of *HTB1* mRNA was observed for each of the strains at all three temperatures. At 16°C, *HTB1* mRNA levels were consistently higher than the level detected at both 25°C and 37°C, in all strains, with the exception of *hrp1-5* indicating that as temperature increases, histone mRNA levels decrease (*Figure 3.13)*. This decrease in histone mRNA levels at 37°C has previously been observed by (Canavan and Bond, 2007) and is most likely due to the rapid turnover of mRNA.

At the permissive temperature (25°C) and taking into account slight variation in RNA loaded in each lane, the steady state levels of *HTB1* mRNA present in the wild-type strains were similar to the levels detected in the *rpb11* and *ssu72* mutant strains (*Figure 3.13C*, compare lanes 2 and 11 to lanes 5 and 8). However when *hrp1-5* was compared to the wild-type strains at the permissive temperature, the levels of *HTB1* detected for *hrp1-5* were lower than the wild-type strain (*Figure 3.13C*, compare lanes 2 and 11 to lane 14).

As with the components of the Nrd1p/Nab3p/Sen1p termination complex, inactivation at the non-permissive temperature (37°C), caused a reduction in the steady state levels of *HTB1* mRNA in the wild-type and mutant strains (*Figure 3.13C*, lanes 3, 6, 9, 12 and 15). When the levels of *HTB1* mRNA at the non-permissive temperature for each of the mutant strains (*Figure 3.13C*, lanes 6, 9 and 15) were compared to those of the wild-type strains (*Figure 3.13C*, lanes 3 and 12), a similar decline in the steady state levels of *HTB1* mRNA present at the non-permissive temperature were visible for both *rpb11* and *ssu72* indicating that the steady state levels of *HTB1* mRNA were not affected by inactivation at 37°C. Low levels of *HTB1* were detected for *hrp1-5* (*Figure 3.13A*, lanes 13, 14 and 15) and even when loading variance was taken into account, the level of *HTB1* mRNA in *hrp1-5* were constantly lower than those observed in the wild-type strains at both the permissive and non-permissive temperatures.

At 16°C, similar *HTB1* steady state levels were detected for both the wild-type strains and *rpb11* and *ssu72* (*Figure 3.13C*, lanes 1, 4, 7, and 10). As with the other temperatures tested, less HTB1 was detected for *hrp1-5* but this was due to less total RNA extracted (*Figure 3.13C*, lane 13). This result was as expected for the wild-type strains, *hrp1-5* and *ssu72* as they are not cold sensitive strains, unlike *rpb11*. The levels detected for *rpb11* at 16°C indicate that the steady state levels of *HTB1* mRNA were not affected by incubation at 16°C for 2hrs. It should be noted *ACT1* was not the correct gene to use as the control for these strains as the steady state levels of *ACT1* are also affected by the these mutations. For future work alternative controls such as 5.8S rRNA or *SCR1* should be used as they are constitutively expressed.

Overall, the results of the northern blot analysis indicated that the cleavage and polyadenylation factors Ssu72p and Rpb11p do not affect the steady state levels of *HTB1* mRNA. However Northern blot analysis suggests that *hrp1-5* may exert an effect on histone mRNA biogenesis.

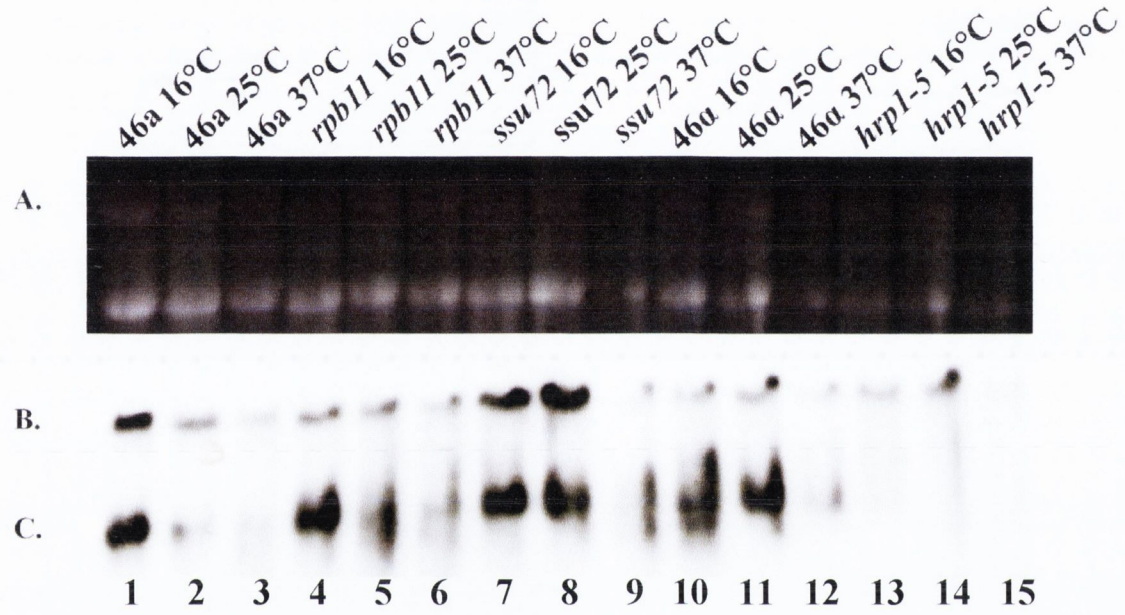

Figure 3.13: Northern blot analysis of *HTB1* mRNA with the temperature-sensitive strains of *rpb11*, *ssu72* and *hrp1-5*. Total RNA, 30μg, was isolated from the following strains, 46a (wild-type); *rpb11*; *ssu72*; 46α (wild-type); and *hrp1-5* upon incubation at 16°C, 25°C and 37°C for 2hrs. **A.** Ethidium bromide stained gel showing the ribosomal RNAs. rRNA was used as a control of equal loading of the gel. **B.** and **C.** The blot was hybridised with the *ACT1* probe (B) and the *HTB1* probe (C).

Transcription termination of *HTB1* transcripts was also assayed in the Hrp1p, Ssu72p and Rpb11p mutants as described above. As previously shown, in the wild-type strain, 46a, no read-through products past reverse primer 2 were detected at either the permissive or non-permissive temperature (*Figure 3.14A*, lane 2) indicating accurate, efficient 3' end cleavage and polyadenylation. In the *hrp1-5* mutant, no read-through primary transcripts were detected past reverse primer 1 at the permissive temperature (*Figure 3.14B*, lanes 2 to 7) or by incubation at the non-permissive temperature, indicating that Hrp1p was not involved in the transcription termination of *HTB1* mRNA (*Figure 3.14B*, lane 1). Similar profiles were obtained following RT-PCR analysis of *ssu72* (*Figure 3.14C*).

As *rpb11* is a cold sensitive strain, RT-PCR was conducted at 16°C, 25°C and 37°C (*Figure 3.14D*) in order to see if *HTB1* mRNA transcription termination is affected. As with the wild-type strain and the other mutant strains tested, no read-through products past reverse primer 1 were detected for *rpb11* at 25°C or 37°C. However at 16°C, a small but detectable amount of read-through primary transcripts were detected for reverse primer 2 suggesting that *rbp11* may contribute to the transcription termination of *HTB1* mRNA (*Figure 3.14D,* lane 2).

The results of the RT-PCR read-through analysis suggest that Hrp1p and Ssu72p do not significantly alter *HTB1* mRNA transcription termination at either the permissive or non-permissive temperature. A transcription termination effect in *rpb11* was observed at 16°C indicating that Rpb11p may play a role in transcription termination of histone mRNAs.

Figure 3.14: *HTB1* mRNA RT-PCR results of the temperature-sensitive strains *hrp1-5, ssu72* and *rpb11*. Total RNA from temperature-sensitive mutants of *HRP1*, *SSU72* and *RPB11* was reverse transcribed using primers spanning the downstream region of *HTB1* and amplified using a common forward primer (For1). Lane M; molecular weight marker, Lane 1; Rev1 (143nts), Lane 2; Rev2 (231nts), Lane 3; Rev3 (309nts), Lane 4; Rev4 (392nts), Lane 5; Rev5 (468nts), Lane 6; Rev6 (554nts), Lane 7; Rev7 (646nts) and Lane 8; cDNA prepared using Rev1 in the absence of Reverse Transcriptase. * represent *HTB1*-specific PCR products of the expected size and the expected sizes of the PCR products (nts) are shown in brackets. **A.** RT-PCR analysis of *HTB1* mRNA from wild-type 46a, grown at 25°C and 37°C for 2hrs. **B.** RT-PCR analysis of *HTB1* mRNA from *hrp1-5*, grown at 25°C and 37°C for 2hrs. **C.** RT-PCR analysis of *HTB1* mRNA from *ssu72,* grown at 25°C and 37°C for 2hrs. **D.** RT-PCR analysis of *HTB1* mRNA from *rpb11*, grown at 25°C, 37°C and 16°C for 2hrs.

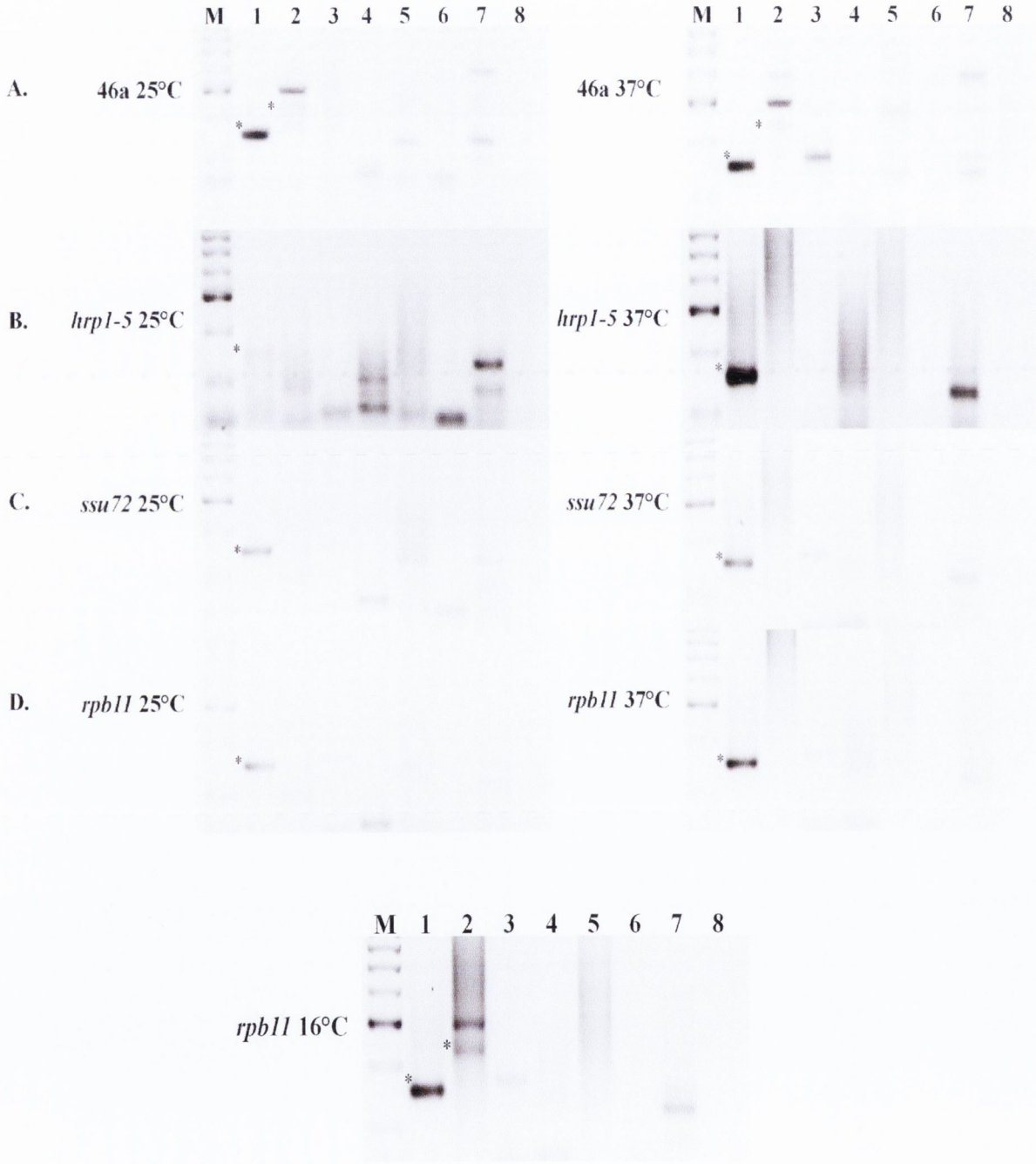
M 1 2 3 4 5 6 7 8
A.
46a 25°C
46a 37°C
B.
hrp1-5 25°C
hrp1-5 37°C
C.
ssu72 25°C
ssu72 37°C
D.
rpb11 25°C
rpb11 37°C
M 1 2 3 4 5 6 7 8
rpb11 16°C

3.4 Discussion

Recently evidence has emerged which implicates the components of the Nrd1p/Nab3p/Sen1p termination complex in the 3' end processing and transcription termination of mRNA (Carroll et al., 2004; Steinmetz et al., 2001; Steinmetz et al., 2006b). As previously discussed, both the mRNA termination pathway and the snRNA/snoRNA termination pathway share many similar features (Carroll et al., 2007). In this study, we sought to discover whether the components of the Nrd1p/Nab3p/Sen1p termination complex are involved in histone mRNA processing. Through both Northern blot analysis and real-time RT-PCR we found that the steady state levels of *HTB1* histone mRNAs were not significantly affected upon inactivation of the temperature-sensitive mutants of the Nrd1p/Nab3p/Sen1p termination complex. However both methods demonstrated that Nrd1p gave a decrease, although not statistically significant, in steady state *HTB1* mRNA levels. Nrd1p is an essential mRNA binding protein with a RNA recognition motif (RRM) located in its carboxyl half which binds RNA in a sequence-specific manner. The N-terminal domain of the protein contains a C-terminal interaction domain (CID) and interacts with RNA Polymerase II (Gudipati et al., 2008; Steinmetz and Brow, 1998; Vasiljeva and Buratowski, 2006; Vasiljeva et al., 2008). Nrd1p was also found to have sequence homology to the CTD-binding domain of Pcf11p, a component of CF IA which is involved in cleavage and polyadenylation of mRNA (Steinmetz et al., 2001). Previously, mass spectrometry identified putative Nrd1-interacting proteins which included components of the nuclear exosome such as Rrp6p, Rrp44p, Rrp4p and Rrp45p, the poly(A) polymerases Trf4p, Air2p and Pab1p and the endonuclease RNase III, Rnt1p (Vasiljeva and Buratowski, 2006). Recent research has provided further evidence of the involvement of the nuclear exosome in both the mRNA termination pathway and the snRNA and snoRNA termination pathway. Canavan and Bond, (2007) found that Rrp6p contributes to the turnover of the endogeneous *HTB1* transcripts in the G2-phase of the cell cycle (Canavan and Bond, 2007). In addition, Reis and Campbell, (2006) found that Rrp6p was recruited by Trf4p of the TRAMP complex in order to initiate degradation of the associated RNA and that there was an increased accumulation of *HHF2* mRNAs during the S-phase in *Δrrp6* cells (Reis and Campbell, 2007). These findings provide further evidence for a role for the exosome in histone mRNA biogenesis and cell cycle regulation.

In this study, Nab3p was also found not to have reduced steady state *HTB1* mRNA levels through both the Northern blot and real-time RT-PCR analysis. Nab3p interacts both genetically and physically with Nrd1p and like Nrd1p, Nab3p has a RRM where it interacts with the nascent RNA (Arigo et al., 2006; Carroll et al., 2007). As Nrd1p and Nab3p are both RNA-binding proteins and have recognition sites that are often found in close proximity on the RNA, it is not surprising that these proteins work in concord and should show similar effects on histone mRNA biogenesis (Carroll et al., 2004).

Sen1p was not found to reduce the steady state levels of *HTB1* mRNA in asynchronous cells. However, inactivation of Sen1p led to read-through transcription beyond the 3' end cleavage sites, indicating a role for this protein in transcription termination of histone mRNAs. This effect was independent of Nrd1p and Nab3p. The differences between the effects of Sen1p on the steady state levels and transcription termination of *HTB1* mRNA may indicate that Sen1p may play a role in a "fail safe mechanism" for transcription termination or may function at a specific stage of the cell cycle, thus any effects would not be evident in asynchronous cells.

Evidence has recently emerged suggesting that Sen1p may have functions that are independent of the Nrd1p and Nab3p (Kawauchi et al., 2008; Steinmetz et al., 2006b; Ursic et al., 2004). Previously Steinmetz *et al*, (2006) performed a global ChIP-on-chip analysis of the genomic occupancy of RNA Polymerase II in a Sen1p temperature-sensitive background. This revealed read-through transcription in genes encoding short transcripts i.e. snRNAs, snoRNAs, CUTs and short mRNAs. No read-through was found for longer genes including long snRNA and snoRNA genes (Steinmetz et al., 2006b). These findings clearly implicated Sen1p as having a role in the 3'end processing of mRNA genes which are less than 600nts in length. These pools of short mRNAs include the histone genes. These results and other findings such as the involvement of factors such as Rrp6p and Trf4p in the regulation of yeast histone mRNA levels suggests that histone mRNAs may be processed through the non-polyadenylated 3' end processing pathway. However, the cleavage and polyadenylation factor CF IA, and specifically Rna14p, Rna15p and Pcf11p, have previously been shown to influence 3' end processing and steady state levels of *HTB1* mRNA. This may indicate that both the general mRNA cleavage machinery and the non-polyadenylated Nrd1p/Nab3p/Sen1p machinery are required for histone mRNA processing or that a sub-set of factors from either pathway may interact to facilitate histone mRNA processing. Coupled with the finding that Nrd1p can mediate

transcription termination of polyadenylated protein encoding genes (Rondon et al., 2009), these findings add to the emerging picture of cross-communication between the 3' end processing/transcription termination machinery of both polyadenylated and non-polyadenylated mRNAs.

Through ChIP-on-chip, Steinmetz et al, (2006) also found that inactivation of Sen1p led to an increase in read-through in both *CYC1* and *PMA1* genes, both of which encode mRNA transcripts (Steinmetz et al., 2006b). Observers of this study suggest that the clear requirement of Sen1p for the termination of *PMA1* termination argues that longer RNA Polymerase II transcribed genes may also require the activity of Sen1p (Kawauchi et al., 2008; Steinmetz et al., 2006b). Evidence to further endorse this argument is the RT-PCR results for *TDH3* and *ACT1* both of which are mRNA encoding genes of > 600nts. It should also be noted that through ChIP-on-chip, Steinmetz *et al*, 2006 also detected read-through for *TDH3* in a sen1 mutant background (Steinmetz et al., 2006b).

Previously it has been shown that Sen1p physically interacts with the CTD of Rpb1p, a component of RNA Polymerase II and an internal segment of Rad2p, a single stranded DNA endonuclease (Ursic et al., 2004). Sen1p has also been found to co-purify with Rnt1p, an endoribonuclease III protein which is required not only to generate initial 3'end cleavage of pre-rRNA and but also for efficient RNA Polymerase I termination (Kawauchi et al., 2008; Lykke-Andersen and Jensen, 2007; Ursic et al., 2004). In addition to these findings, Kawauchi *et al.*, (2008) found that Sen1p cooperates with the 5'-3' exonuclease Rat1p to mediate efficient termination of both RNA Polymerase I and II transcripts (Kawauchi et al., 2008). It has been proposed that the helicase activity of Sen1p may act directly with Rat1p to expose the nascent transcript following Rnt1p cleavage or poly(A) site cleavage and so promotes efficient Rat1p exonucleolytic degradation (Kawauchi et al., 2008; Ursic et al., 2004). Rondon *et al.*, (2009) demonstrated that in the event of incorrect or inefficient 3' end processing, Sen1p, with Nrd1p and Nab3p, provides a "fail safe" mechanism for transcription termination for a number of RNA Polymerase II mRNA transcripts (Rondon et al., 2009). Here Sen1p interacts with Rnt1p to mediate the degradation of read-through transcripts by the nuclear exosome (Rondon et al., 2009).

The results of the read-through RT-PCR analysis conducted in this study indicated Sen1p may work independently to Nrd1p and Nab3p. The finding that Sen1p interacts with components of both the RNA Polymerase I and II termination pathways (Kawauchi et al., 2008) and coupled with the new data presented in this study, this

provides further support for an independent role for Sen1p. This appears especially likely as Nrd1p and Nab3p are known to interact with the CTD of RNA Polymerase II which is absent from RNA Polymerase I (Kawauchi et al., 2008).

The role of Hrp1p, Ssu72p and Rpb11p, cleavage and polyadenylation factors which are known to be involved in 3' end processing of both polyadenylated RNA and non-polyadenylated RNA was also investigated (Carroll et al., 2004; Ursic et al., 2004). Previously it has been shown that mutations in *HRP1* cause read-through in both *NRD1* and *HRP1* regulatory sequences and Kuehner and Brow, (2008), have hypothesised that Hrp1p acts directly as a Sen1-dependent termination factor by binding elements in the nascent transcript (Kuehner and Brow, 2008). It has also been suggested that *HRP1* mRNA uses the Nrd1p/Nab3p/Sen1p termination pathway to auto-regulate its expression (Steinmetz et al., 2006b). Our data indicates Hrp1p was not required for *HTB1* mRNA transcription termination in a *HRP1* mutant background but is involved in histone mRNA biogenesis as the steady state levels were reduced at three different temperatures. Previous co-immunoprecipitation experiments have also shown that Hrp1p localizes to some snoRNA genes (Kuehner and Brow, 2008).

In this research Ssu72p was also found to have no effect on the transcription termination of histone mRNAs. Steinmetz and Brow, (2003) demonstrated that Ssu72p is a general component of the Nrd1p/Nab3p/Sen1p termination pathway and that *SSU72* mutants are deficient in poly(A) termination but competent for cleavage and polyadenylation (Steinmetz and Brow, 2003). These findings act to verify the new data presented in this study which found histone mRNA 3' end processing and transcription termination was not affected by inactivation of Ssu72p.

Steinmetz *et al.*, (2006) proposed that Sen1p and other cleavage and polyadenylation factors interact with the *RPB3/11* heterodimer to promote termination as the heterodimer may act as a contact point for factors that transmit termination signal to RNA Polymerase II (Steinmetz et al., 2006a). Our data indicates that incubation of the *rpb11* temperature sensitive mutant at 16°C for 2hrs leads to a small amount of read-through of histone *HTB1* mRNA. This suggests that Rpb11p may play a role in histone mRNA transcription termination.

The new data presented in this research indicates that Sen1p is necessary to promote termination of RNA Polymerase II transcripts and that it has functions which are independent to that of Nrd1p and Nab3p.

Chapter 4

Cleavage site usage and Poly(A) tail length of histone *HTB1* mRNAs in asynchronous and cell cycle regulated cells

4.1 Introduction

Histone mRNAs in *S. cerevisiae* have been described as being polyadenylated (Fahrner et al., 1980), although recent data indicates that yeast histone RNAs belong to a class of mRNAs bearing short poly(A) tails along with a number of other cell cycle regulated transcripts (Beilharz and Preiss, 2007). Components of CF IA (Rna14p, Rna15p and Pcf11p) have previously been shown to be required for yeast histone mRNA biogenesis (Canavan and Bond, 2007). Data presented in this study (Chapter 3) also suggests that Hrp1p, the only component of CF IB, may also be required for histone mRNA biogenesis. Components of CF IA and CF IB, specifically Rna14p, Rna15p, Pcf11p and Hrp1p are recruited to genes encoding both polyadenylated (general mRNAs) and non-polyadenylated RNAs (snRNAs) (Kim et al., 2006a), suggesting substantial cross-communication between the 3' end processing machineries.

Components of the nuclear exosome (Rrp6p) and the TRAMP complex (Trf4p/Trf5p), which play a substantial role in the 3' end processing of non-polyadenylated snRNAs have also been implicated in histone mRNA biogenesis (Canavan and Bond, 2007; Reis and Campbell, 2007). Deletion of either *RRP6* or *TRF4* affects the cell cycle regulation of histone mRNAs and consequently alters cell cycle progression. Deletion of *RRP6* resulted in delayed exit of cell S-phase into G2-phase (Canavan and Bond, 2007), suggesting that levels of histone mRNA may be sensed by cells as a checkpoint to cell cycle progression.

New data presented in this study (Chapter 3), demonstrated that inactivation of Sen1p, a component of the Nrd1p/Nab3p/Sen1p transcription termination complex and Rpb11p, a component of RNA Polymerase II, led to read-through transcription beyond the 3' end cleavage sites of primary histone mRNAs, suggesting that both Sen1p and Rpb11p are involved in transcription termination of histone mRNAs. The link between transcription termination and 3' end processing was first discovered in *S. cerevisiae* in 1998 (Birse et al., 1998). Using transcription run-on analysis in temperature sensitive mutants of *RNA14*, *RNA15* and *PCF11*, Birse *et al.*, (1998) found that inhibition of 3' end cleavage led to a lack of transcription termination and the accumulation of read-through transcripts.

The findings that factors involved in the processing of non-coding, non-polyadenylated RNAs are required for histone mRNA biogenesis prompted us to re-evaluate the polyadenylated status of these mRNAs. Recently, Miura *et al.*, (2006) carried out a genome-wide analysis of the 3' ends of mRNAs in *S. cerevisiae* which yielded ambiguous results regarding their poly(A) status (Miura et al., 2006). In mammals, histone mRNAs are non-polyadenylated but it is interesting to note that Mullen and Marzluff, (2008) recently found a short oligo(U) tail at the 3' end of mammalian histones that is added during the degradation of these transcripts (Mullen and Marzluff, 2008). These findings and the new data presented in Chapter 3 prompted us to examine the role of Sen1p in the cleavage and polyadenylation of histone mRNAs.

4.2 Results

4.2.1 Cleavage site usage in asynchronous cells

Data presented in the previous chapter and (Canavan and Bond, 2007) linked Sen1p, Rna14p and Rrp6p to histone mRNA biogenesis. The effect of mutants in these genes on the cleavage and polyadenylation of histone mRNAs was therefore examined. In order to determine the length of the poly(A) tail and to map the cleavage sites used within cells, a hybrid selection procedure (Chapter 2, section 2.13.1) was carried out to purify *HTB1* transcripts. Previously histone mRNAs have been shown to be poorly retained on oligo dT columns compared to other mRNAs such as *ACT1* and are therefore difficult to enrich for (S. Campbell and U. Bond, unpublished results).

Briefly, asynchronous cells from the wild-type strain 46a and the mutant strains *sen1*, *rna14/Δrrp6* and *Δrrp6* were grown in YEPD media to an optical density (OD_{600nm}) value of 0.8 (approximately $1x10^7$ cells/ml) at 25°C or 30°C. The cell cultures were divided in two and resuspended in YEPD pre-warmed to 25°C or 37°C. Both cultures were re-incubated at their respective temperatures for a further 2hrs (Chapter 2, section 2.1). Total RNA was isolated and *HTB1* transcripts were selected using an antisense biotinylated *HTB1* oligonucleotide (Chapter 2, section 2.13.1 and Table 4.2). After lyophilisation, the selected hybrid RNA was G-tailed using Poly(A) Polymerase (Chapter 2, section 2.13). Poly(G) polymerase works in the same manner as Poly(A) polymerase. It catalyzes the addition of guanine residues to the 3' end of the RNA in a sequence independent manner. In addition to Poly(G) polymerase, Terminal Transferase or RNA Ligase could be used but as both of these enzymes add on a vast amount of A/G residues, sequencing would be difficult. Following G-tailing, cDNAs were synthesised using an oligo C and *HTB1* specific primer (HTB1 For^{1-22}, Table 2.2). As the expected length of the *HTB1* cDNAs spanning the coding and downstream region (including the poly(A) tail) was 521nts (*Figure 4.1A*), RT-PCR products over 500nts were deemed to be *HTB1* specific products (*Figure 4.1B, lane 2).* As an internal control and to further ensure that the G-tailed cDNA were *HTB1* specific products, the G-tailed cDNAs were amplified using internal *HTB1* specific primers (HTB1 For^{1-22} and HTB1 $Rev^{252-270}$, Table 2.2) with an expected size of 270nts (*Figure 4.1B*, lane 3). A faint but larger band of approximately 550nts was also observed in lane 3 which was a result of the amplification from the residual oligo C primer from the original cDNA

synthesis. A negative control of the cDNA prepared with HTB1 $Rev^{252-270}$ in the absence of Reverse Transcriptase and subsequently amplified using HTB1 For^{1-22} was included for each sample (*Figure 4.1B*, lane 4).

Prior to cloning of the cDNA PCR products, the purity of the *HTB1* hybrid selected RNA was examined. To do this, 2µg of total RNA, 8% of the lyophilised selected RNA and 0.6% of the unbound RNA from the hybrid selection process was reverse transcribed using *HTB1* specific and *ACT1* primers (*Figure 4.1C*). If the hybrid selection process for the *HTB1* RNA has occurred correctly, then little or no *ACT1* RNA should be detected in the selected *HTB1* RNA sample. The ratio of *HTB1:ACT1* mRNA was higher in the hybrid selected sample than in the unbound sample and much higher than in the total RNA pool indicating that the hybrid selection with an antisense *HTB1* oligo was successful (*Figure 4.1C*, lanes 2, 3, 5, 6, 8, 9). The presence of a strong band for *HTB1* in the unbound fraction suggests that not all of the *HTB1* transcripts bound to the streptavidin-paramagnetic beads. As a further check of the purity of the selected RNA, cDNA was synthesised using an oligo C primer and a *TDH3* forward primer (Chapter 2, section 2.10.2). However no products were observed for the reaction upon electrophoresis (data not shown). This further acts to confirm the specificity of the *HTB1* hybrid selection process.

As a final internal control, the oligo C RT-PCR products were re-amplified using both *HTB1* specific internal primers and the oligo C and *HTB1* specific primer in order to ensure that the same size PCR products were visible upon re-amplification (data not shown).

Figure 4.1: Amplification of *HTB1* transcripts from the wild-type strain, 46a, at the permissive temperature. A. Schematic diagram of the location primers used in hybrid selection procedure. The *HTB1* open reading frame 1-397 is designated by a black rectangle and the location of the primers used in the cDNA synthesis (HTB1 $Rev^{252-270}$ and oligo C) are shown as is the forward primer (HTB1 For^{1-22}) used for PCR amplification of the cDNAs. The expected sizes of the RT-PCR products are also shown. **B.** G-tailed selected RNA was reverse transcribed using oligo C and amplified using HTB1 For^{1-22} (lane 2) or HTB1 For^{1-22} and $Rev^{252-270}$ (lane 3). A negative control of the cDNA prepared with HTB1 $Rev^{252-270}$ in the absence of Reverse Transcriptase (lane 4). A molecular weight marker is shown in lane 1 with the 200bp, 300bp, 400bp and 500bp bands indicated. **C.** The efficiency of the hybrid selection was investigated through synthesis of cDNAs from Total, Selected and Unbound RNA using both *HTB1* (HTB1 For^{1-22} and $Rev^{252-270}$) and *ACT1* (ACT1 For(2) and Rev(2)) primers (Table 2.2). A negative control was included for each RNA sample using HTB1 For^{1-22} and $Rev^{252-270}$ (lanes 4, 7 and 10). Lane M; molecular weight marker, Lanes 2 and 3; Total RNA with *HTB1* and *ACT1* samples respectively, Lanes 5 and 6; Selected RNA with *HTB1* and *ACT1* samples respectively, Lanes 8 and 9; Unbound RNA with *HTB1* and *ACT1* samples respectively.

A.

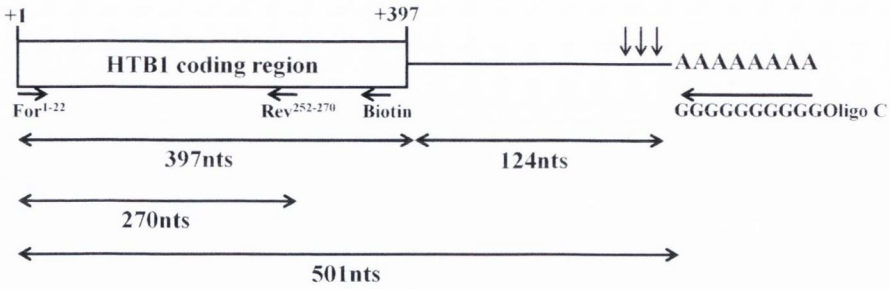
+1
+397
HTB1 coding region
AAAAAAAA
For1-22
Rev252-270
Biotin
GGGGGGGGGOligo C
397nts
124nts
270nts
501nts

B.

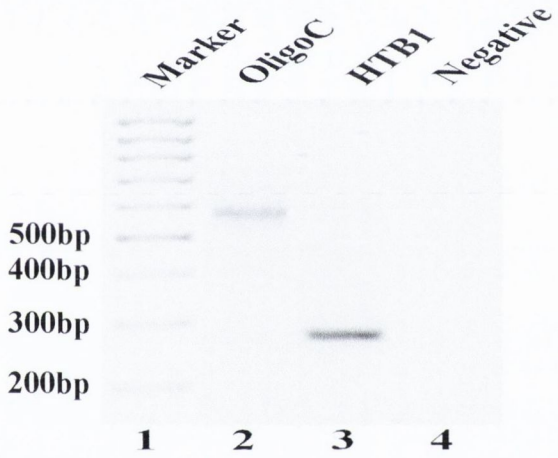
Marker
OligoC
HTB1
Negative
500bp
400bp
300bp
200bp
1
2
3
4

C.

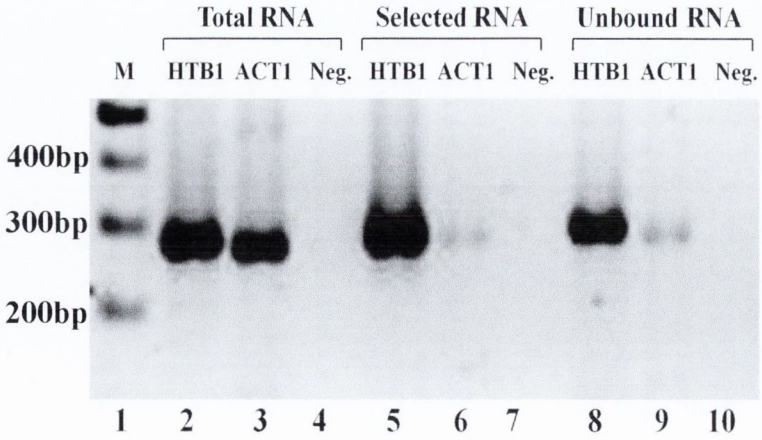
Total RNA
Selected RNA
Unbound RNA
M
HTB1
ACT1
Neg.
HTB1
ACT1
Neg.
HTB1
ACT1
Neg.
400bp
300bp
200bp
1
2
3
4
5
6
7
8
9
10

PCR products amplified using the oligo C and HTB1 For[1-22] primers were cloned into TOPO TA (*Figure 2.1*) as described in Chapter 2, section 2.13.2. The colonies were screened by direct colony PCR using M13 forward and reverse primers which flank the cloning site (Chapter 2, section 2.10.5, Table 2.2). *Figure 4.2A* demonstrates the variability of insert size retrieved by colony PCR. Amplification of the colonies using *E. coli* 16S ribosomal primers (Table 2.2) was also carried out to ensure the direct colony PCR had worked correctly (*Figure 4.2A,* lane ii of colonies 1 to 20). Plasmid DNA was prepared from colonies 3, 8, 10, 15 and 16 (*Figure 4.2A,* lanes 3i, 8i, 10i, 15i and 16i) as well as a number of lower sized bands (*Figure 4.2A,* lanes 5i, 12i, 13i, 14i and 19i). PCR was carried out on the plasmid DNA using M13 forward and reverse primers and *HTB1* specific primers in order to confirm the size and *HTB1* specificity of the clone (*Figure 4.2B*). In all cases, inserts of ~750nts were shown to be *HTB1* specific. DNA sequencing of both small and large sized inserts confirmed the identity of *HTB1* inserts and indicated that that small sized inserts were identical to *RPP2B* or *AHP1* (*Table 4.1*). On average, 45% of the clones for each strain were found to contain a *HTB1* specific insert.

Figure 4.2: Identification of *HTB1* specific inserts. **A.** Direct colony PCR was carried out on colonies 1 to 20 using M13 forward and reverse primers which flank the insert site (Table 2.1). Lane M; molecular weight marker, the 300bp, 400bp, 500bp, 600bp and 700bp bands are indicated, Lanes 1 -20; colonies 1 to 20 respectively of wild-type clones at the permissive temperature selected RNA. (i) denotes DNA amplified with M13 forward and reverse primers to check the insert size while (ii) denotes DNA amplified with *E. coli* 16S rRNA primers to confirm the amplification had worked correctly. **B.** Insert size and *HTB1* specificity of extracted DNA from clones showing inserts >550nts. Plasmid DNA from colonies showing inserts >550nts was amplified using M13 forward and reverse primers and HTB1 For$^{1-22}$ and Rev$^{252-270}$ primers (Table 2.1). Lane M; molecular weight marker, the 200bp, 300bp, 400bp, 500bp and 800bp bands are indicated, Lanes 1 -5; colonies 1 to 5 respectively of *sen1* at the permissive temperature selected RNA. (i) denotes DNA amplified with M13 forward and reverse primers to confirm the insert size while (ii) denotes DNA amplified with HTB1 For$^{1-22}$ and Rev$^{252-270}$ primers to confirm the insert was specific to *HTB1*.

A.

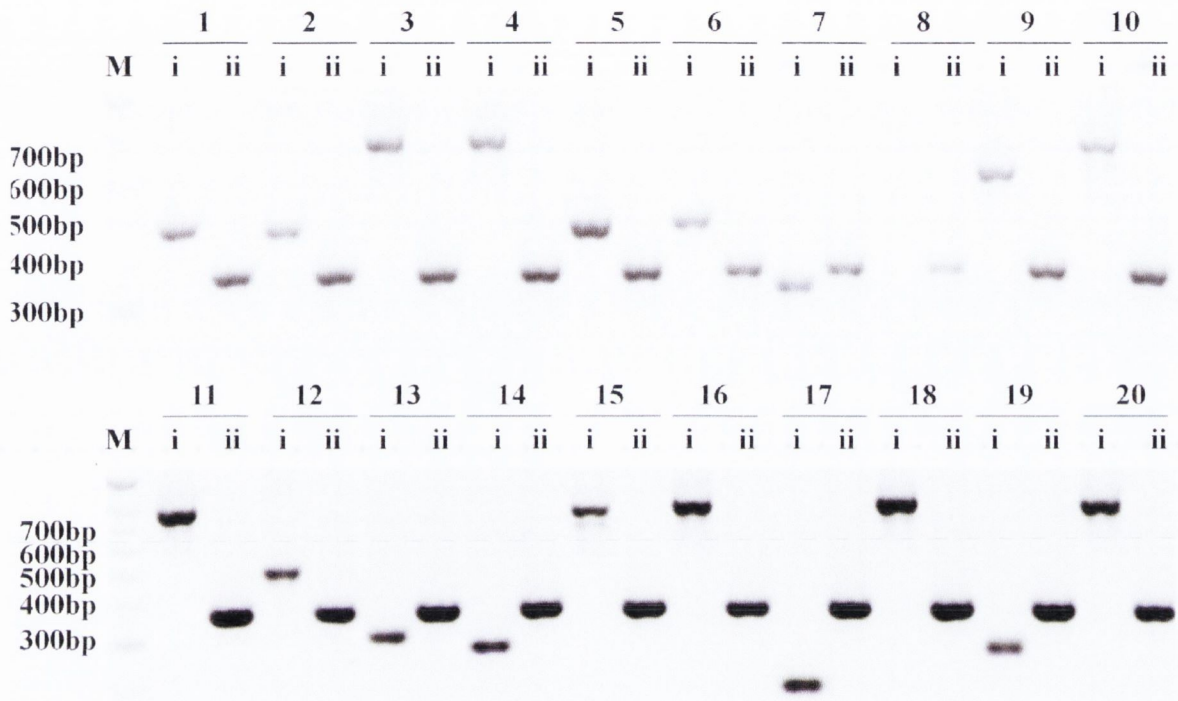
1 2 3 4 5 6 7 8 9 10
M i ii i ii i ii i ii i ii i ii i ii i ii i ii i ii
700bp
600bp
500bp
400bp
300bp
11 12 13 14 15 16 17 18 19 20
M i ii i ii i ii i ii i ii i ii i ii i ii i ii i ii
700bp
600bp
500bp
400bp
300bp

B.

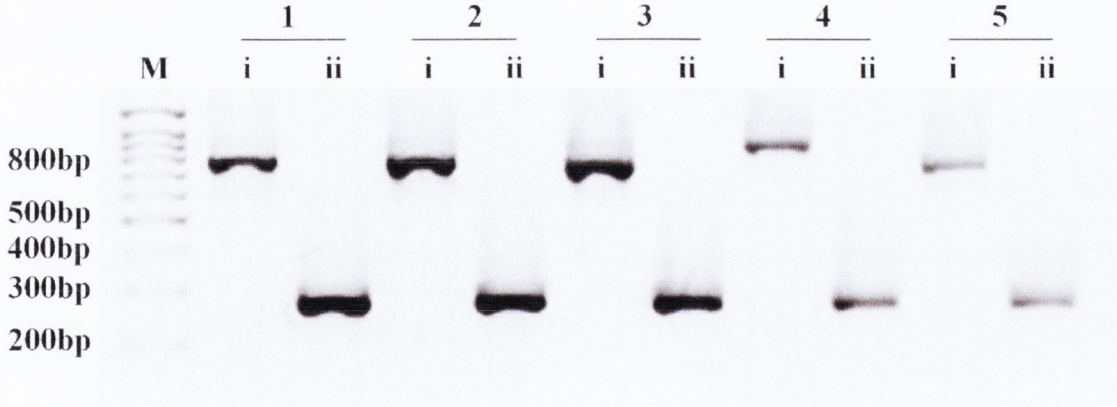
1 2 3 4 5
M i ii i ii i ii i ii i ii
800bp
500bp
400bp
300bp
200bp

Colony Number	Band Size	Identity
3	750nts	*HTB1*
5	500nts	*RPP2B*
8	722nts	*HTB1*
10	722nts	*HTB1*
12	550nts	*RPP2B*
13	300nts	Cloning vector pHC04
14	300nts	Cloning vector pHC04
15	722nts	*HTB1*
16	800nts	*HTB1*
19	350nts	*AHP1*

Table 4.1: Sequencing results of the various sized bands shown in *Figure 4.2A*.

DNA sequence analysis of the cloned G-tailed cDNAs allowed for the precise location of the 3' ends of the transcripts. As *HTB1* is a relatively small gene (<600nts), a high quality Reverse Transcriptase enzyme was used to ensure the mRNA was transcribed accurately. For larger genes, a high quality polymerase enzyme should also be used to amplify the transcript to ensure few errors are incorporated into the transcribed sequence. However to fully ensure accurate DNA sequence analysis of the pool of mRNA, alternative sequencing tools such as Illumina sequencing should be utilised. The 3' ends were compared to the previously identified sites by (Campbell et al., 2002; Miura et al., 2006). In an asynchronous wild-type population, four major cleavage sites were identified (*Figure 4.3*, Table 4.2). Of the four major cleavage sites identified, site 4 was the most frequently used. Three of the four cleavage sites (indicated by a * in *Figure 4.3*) have previously been identified by S1 mapping and/or cDNA cloning of *HTB1* mRNAs (Campbell et al., 2002; Miura et al., 2006). However their relative site usage had not been identified. For comparison with the temperature sensitive strains, the pattern of cleavage in the wild-type strain after incubation for 2hrs at 37°C was also examined. At this temperature, site 4 was almost exclusively used and there was also one additional site (site 1) identified (*Figure 4.3,* site 1, Table 4.2 and Appendix 1). This indicates that incubation at a higher temperature does not significantly affect 3'end processing of the *HTB1* transcripts. In the *sen1* mutant, site 4 was exclusively used at the permissive temperature while sites 1 to 4 were used at the non-permissive temperature (Table 4.2 and Appendix 1). Data presented in Chapter 3 demonstrated that read-through primary transcripts were observed in *sen1* at the non-permissive temperature. Despite this, only 6% of cDNAs were cleaved downstream at site B (*Figure 4.3* and Appendix 1) for *sen1* at the non-permissive temperature and no read-through transcripts were detected in the steady state pool of *HTB1* mRNAs suggesting that *sen1* may be exerting an effect on transcription termination rather than on 3' end cleavage site selection.

Cleavage site usage was also examined in the deletion strain Δ*rrp6* and in a *rna14/Δrrp6* mutant background as both of this mutants have been previously shown to have an effect on histone biogenesis (Canavan and Bond, 2007). For *Δrrp6* at 30°C, sites 1 and 2 were used but site 4 remained the most dominant with 60% usage (Table 4.2 and Appendix 1). However another cleavage site did emerge for Δ*rrp6* which is upstream of the cleavage sites mapped from the wild-type cells (site A, *Figure 4.3*).

For *rna14/Δrrp6* at 37°C, sites 1, 3 and 4 were used with site 4 remaining the most dominant site (Table 4.2 and Appendix 1).

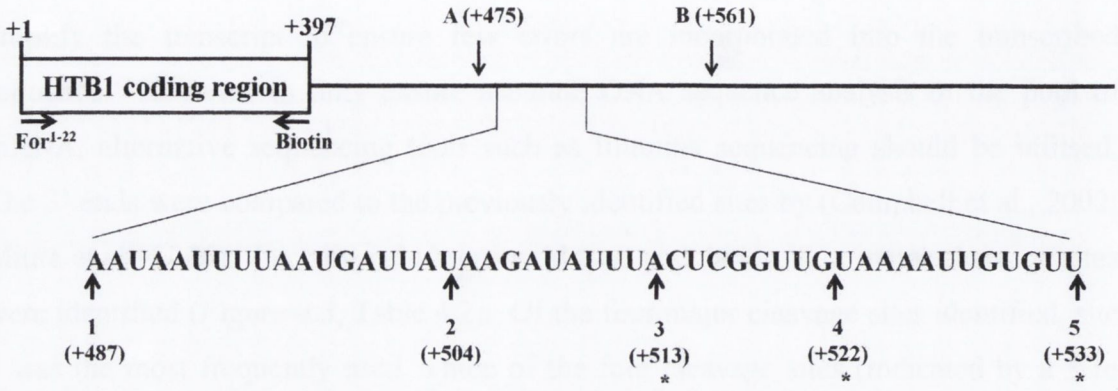

*Campbell *et al*, 2002; Miura *et al*, 2006

Figure 4.3: Schematic diagram of the 3'-end of *HTB1*. The locations of the cleavage sites and their nucleotide position are shown (arrows) with the previously mapped cleavage sites denoted by *. Their nucleotide positions of the primers are shown in Table 2.2.

Cleavage site	WT 30°C	WT 37°C	*sen1* 25°C	*sen1* 37°C	*rna14/Δrrp6* 37°C	*Δrrp6* 30°C
1 (+487)		10		62.5	10	10
2 (+504)	25	10		12.5		20
3 (+513)	12.5	10		37.5	40	
4 (+522)	37.5	70	100	37.5	50	60
5 (+533)	25					
A (+475)						10
B (+561)				6.25		

Table 4.2: Percentage cleavage site usage in asynchronous population.

4.2.2 Poly(A) tail length in asynchronous cells

In addition to mapping the cleavage sites used in asynchronous cells, sequence analysis of the cDNA clones identified two distinct populations of RNAs based on the poly(A) tail length. In wild-type cells, the majority of *HTB1* mRNAs contain poly(A) tails of between 25-50nts while a small proportion (10%) have tails < 25nts (*Figure 4.4* and Appendix 1). Incubation of the wild-type cells at 37°C for 2hrs did not drastically alter the poly(A) tails length distribution however a small population of clones had a poly(A) tails of > 50nts. The distribution of poly(A) tail length was significantly altered in the *sen1* mutant. At the permissive temperature, an increase in the percentage of RNAs with tails of < 25nts was observed while at the non-permissive temperature, this pool significantly increased (*Figure 4.4* and Appendix 1). For *sen1* at both the permissive and non-permissive temperature, a small proportion of RNA also had poly(A) tails of > 50nts. Similarly, the pool of transcripts bearing tails < 25nts was significantly higher in cells lacking *RRP6* or both the *RRP6* and the 3' end processing factor *RNA14* (Appendix 1). Inactivation of Rna14p in a *Δrrp6* background did not significantly increase the percentage of transcripts with short poly(A) tails although some transcripts bearing tails of 5-6 As were identified. This is consistent with exosome-mediated degradation of transcripts in *rna14* mutants due to a lack of 3' end processing. A small percentage of poly(A) tail length of > 50nts was also observed in Δ*rrp6* mutant cells but the two main populations of poly(A) tails were < 25nts and 25-50nts (Appendix 1). This was the case for all strains tested thus indicating that *HTB1* transcripts appear to have much shorter tails then the general pool of mRNAs, which have poly(A) tails of approximately 70-100nts (Beilharz and Preiss, 2007).

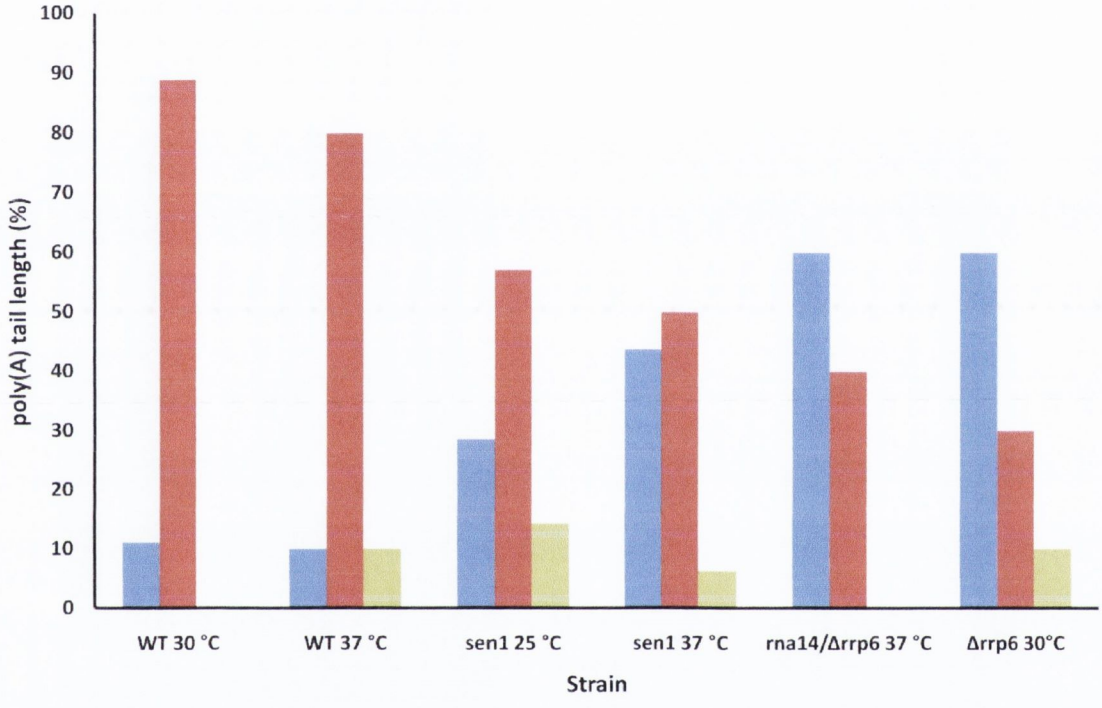

Figure 4.4: Poly(A) tail length of *HTB1* mRNAs in asynchronous cells. Analysis of the poly(A) tail length of G-tailed cloned cDNA from WT, *sen1*, *Δrrp6* and *Δrrp6/rna14* cells. Cells were grown at the permissive (25-30°C) or non-permissive temperatures (37°C) prior to RNA extraction. Percentage of clones with poly(A) tails of 25-50nts; red columns, <25nts; blue columns, >50nts; green columns.

4.2.3 Cleavage site usage during the cell cycle

The identification of two distinct populations and one smaller population of poly(A) tail lengths in *HTB1* transcripts, specifically in the *sen1* and *rrp6* mutants, prompted us to examine the poly(A) tail length of *HTB1* transcripts at different stages of the cell cycles. Wild-type yeast cells were synchronised at the G1 checkpoint by incubation with α-factor. The cells were deemed synchronised when > 90% of the cells displayed signs of schmooing. The α-factor was removed and RNA was isolated from samples which were taken every 15 min (Chapter 2, section 2.11). Cell cycle progression was monitored by propidium iodide staining of the cells and subsequent FACs analysis. From the FACs analysis, it can be seen that the cells began to enter S-phase at 30 min and began to exit into G2-phase at 75min (*Figure 4.5*). The levels of *HTB1* mRNAs and *ACT1* mRNAs at each stage of the cell cycle were determined by semi-quantitative RT-PCR as described in Chapter 2, section 2.10.2 (*Figure 4.6*). Increased levels of *HTB1* were detected by the RT-PCR at 30, 45 and 60 min, coinciding with DNA synthesis (*Figure 4.5*) and thereafter decrease, as cells enter into G2-phase (*Figure 4.6*). The *ACT1* mRNA levels were constant throughout the cell cycle (*Figure 4.6*).

The cleavage site usage and poly(A) tail length of *HTB1* transcripts within the synchronised cell population was also determined. The cells captured in G1-phase (0 min) appeared to be extremely homogenous as they exclusively used cleavage site 4 (*Figure 4.7A*, purple bars and Appendix 2). As the cells entered S-phase, an increase in the diversity of 3' end cleavage site usage was observed, with a decrease in the use of cleavage site 4 (purple bars) and a dramatic increase in the use of cleavage site 3 (green bars) at 60 min (*Figure 4.7A* and Appendix 2). In *Figure 4.4*, a decrease in *HTB1* mRNA levels was observed at 60 and 75 min. This coincides with a significant increase in RNAs with non-canonical 3' ends (sites other than 1-5) being observed at theses time-points. By 75 min, almost 50% of the cDNAs were cleaved at the non-canonical 3' ends (*Figure 4.7A*, orange bars and Appendix 2) but this trend decreased at 90 min. Here the use of cleavage site 4 increased with it becoming almost exclusively used by 120 min where mitosis had occurred and the cells had begun a new round of replication (*Figure 4.7B* and Appendix 2). Non-canonical 3' ends were also detected at 15, 30 and 60 mins but they were not as detected frequently as at 75 mins (*Figure 4.7A* and Appendix 2).

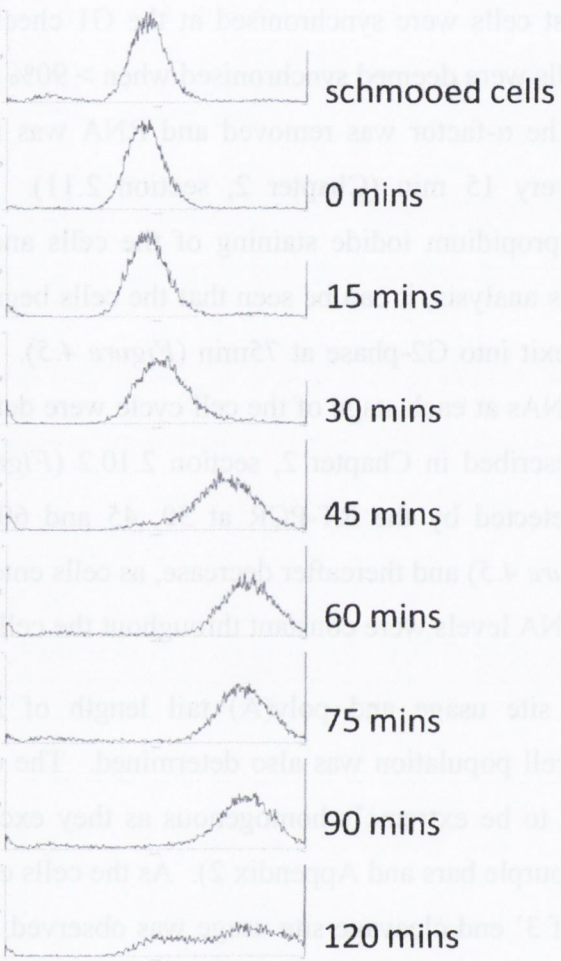

Figure 4.5: Flow cytometry analysis of synchronized 46a cells. Cells were synchronized as described in the Materials and Methods section. Samples were taken at 15 min intervals following removal of α-factor. The cells were stained with propidium iodide and sorted as described in Materials and Methods.

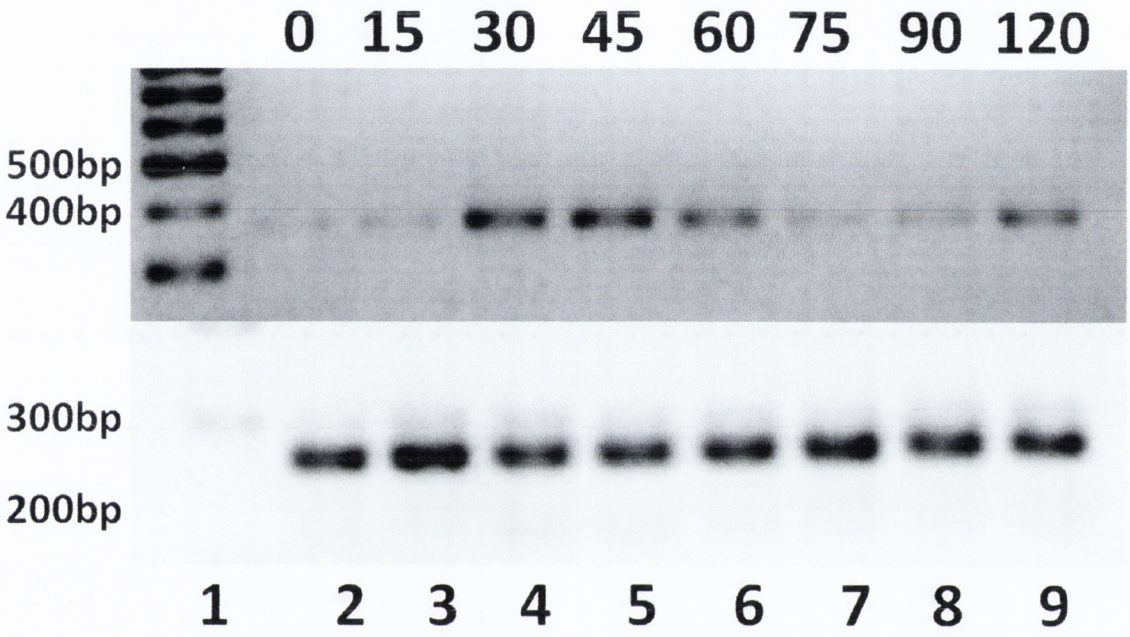

Figure 4.6: Cell cycle analysis of *HTB1* mRNA expression. RNA was extracted from each sample and *HTB1* mRNA levels were determined by semi-quantitative RT-PCR (top panel). As an internal control, the levels of *ACT1* mRNA were also analysed (bottom panel). Lane 1; molecular weight marker, the 200bp, 300bp, 400bp and 500bp bands are indicated, Lanes 2-9; RT-PCR products from RNA extracted at the time intervals (mins) shown above the panels using the primers HTB1 For$^{16\text{-}32}$ and Rev$^{368\text{-}388}$ and ACT1 For1 and Rev1 (Table 2.2).

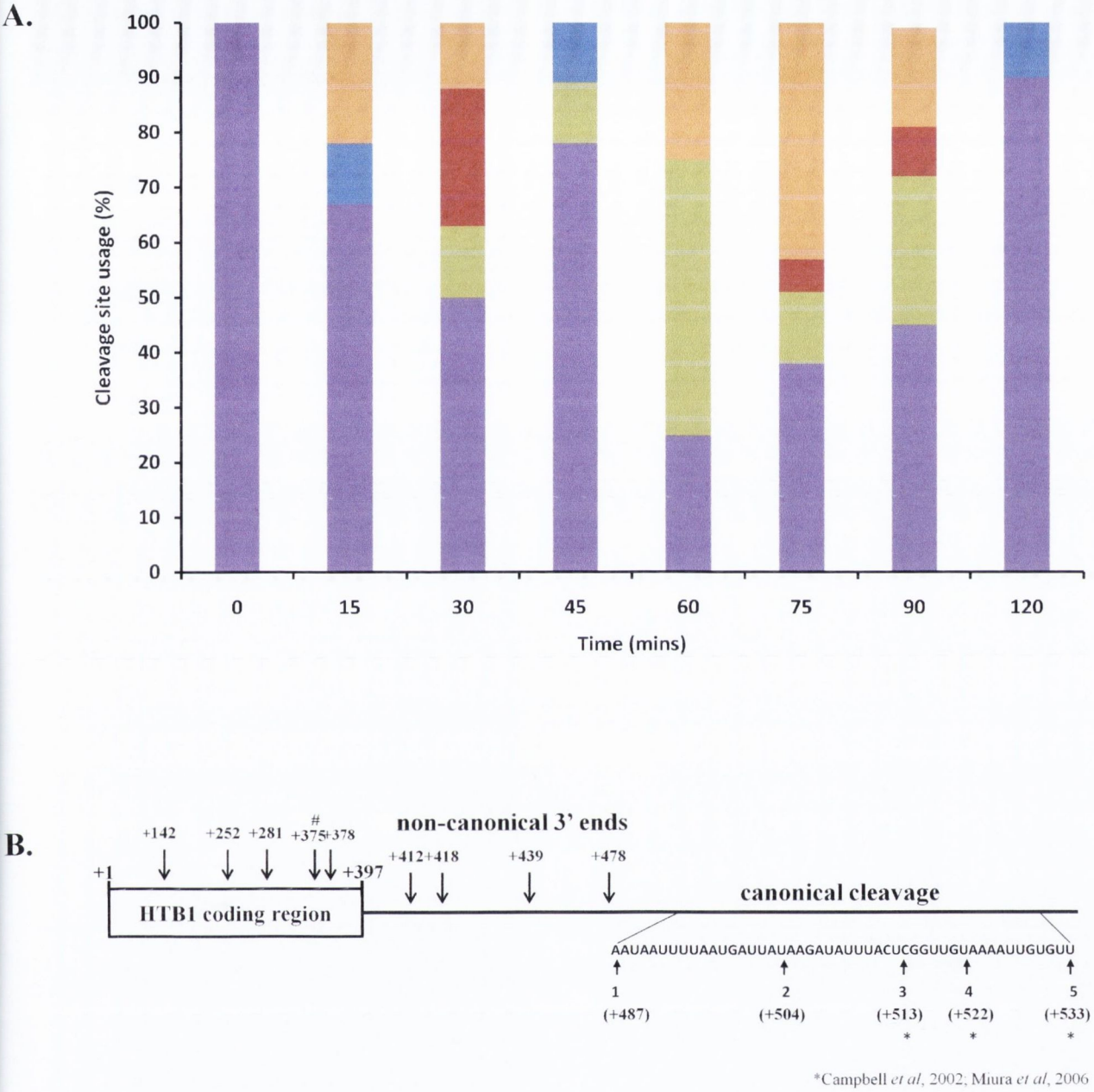

Figure 4.7: 3' end cleavage site usage of *HTB1* mRNAs during the cell cycle. A. Percentage (%) usage of the canonical and non-canonical 3' end cleavage sites at intervals (mins) following release from α-factor. Blue columns; cleavage site 1, Red columns; cleavage site 2, Green columns; cleavage site 3, Purple columns; cleavage site 4, Orange columns; non-canonical 3'ends. **B.** Schematic diagram of *HTB1* mRNA showing the major canonical sites and non-canonical 3' ends detected during the cell cycle. # denotes the 3' end of a cDNA containing two additional non-encoded A residues.

4.2.4 Fluctuations in poly(A) tail length during the cell cycle

The length of the poly(A) tail during the cell cycle was also examined. In G1 (0 min), *HTB1* mRNAs were found to have poly(A) tails with an average tail length of 46nts (*Figure 4.8A*). In asynchronous cells, only a small proportion (<10%) of transcripts were found to have poly(A) tails of > 50nts (*Figure 4.4* and Appendix 1) while in synchronised cells, over 60% of RNAs had tails of > 50nts in G1-phase (*Figure 4.8B*, green columns). The average length of the poly(A) tail decreased as cells progressed through the cell cycle (*Figure 4.8A* and Appendix 2). The percentage of RNAs containing poly(A) tails < 25nts increased significantly from 15-90 min and thereafter decreased (*Figure 4.8B*, blue columns and Appendix 2). As previously mentioned, a large percentage of RNAs at 60, 75 and 90 min have non-canonical 3' ends, all of which lie upstream of the cleavage sites mapped in wild-type asynchronous cells (*Figure 4.7B* and Appendix 2). The vast majority of these were found not to contain poly(A) tails: of the nine clones examined from the 60, 75 and 90 min time points, 8 did not contain a poly(A) tail while the ninth clone contained two additional non-encoded A residues (denoted by #, *Figure 4.7B* and Appendix 2). These clones may represent intermediate mRNA degradation products resulting from rapid 3' to 5' degradation of *HTB1* mRNA as cells enter G2-phase demonstrating that the reduced levels of histone mRNAs in G2 involves the active mRNA degradation in a 3'-5' direction.

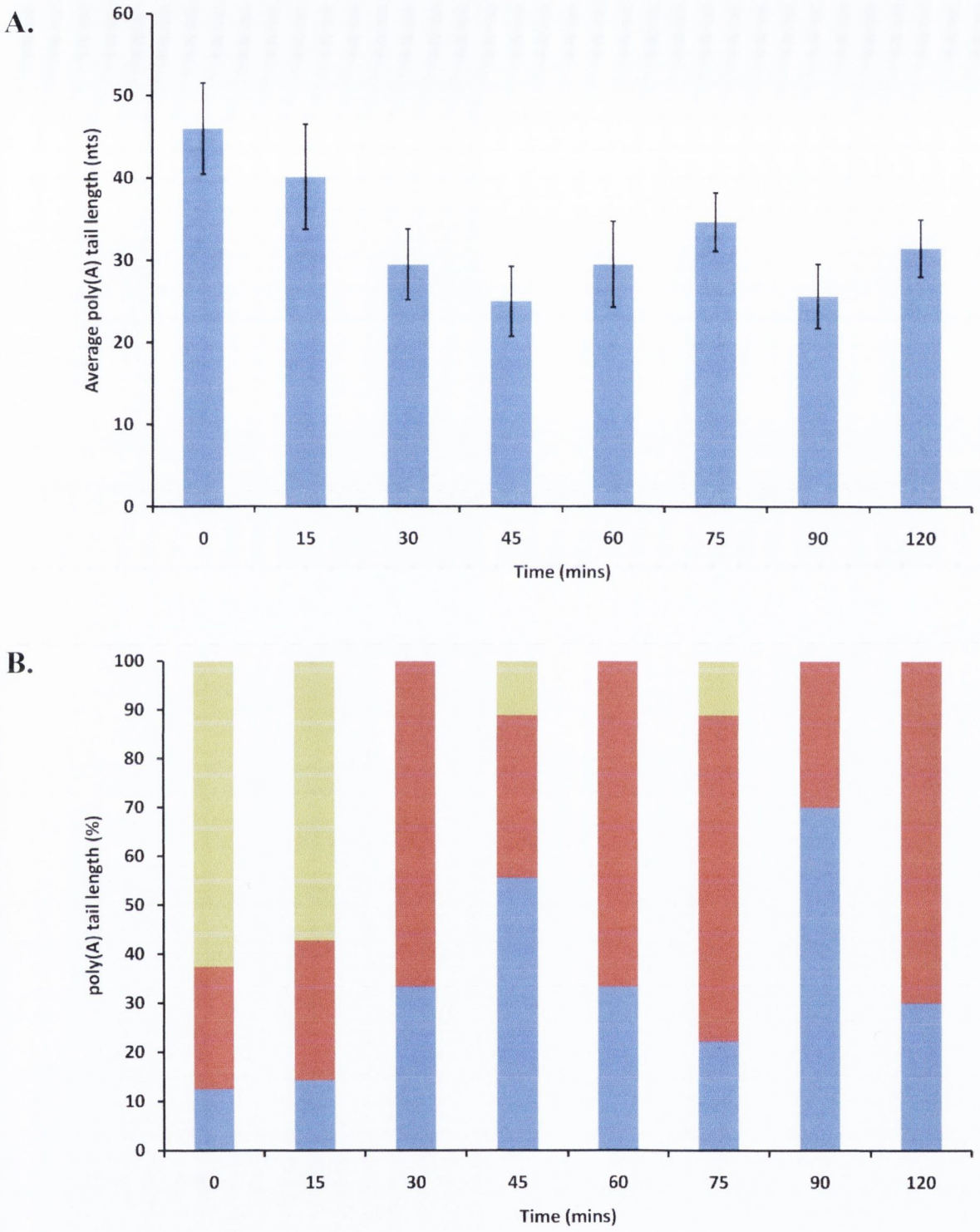

Figure 4.8: The poly(A) tail length of *HTB1* mRNA varies during the cell cycle. A. Average poly(A) tail length (nts) of cDNAs isolated from RNA extracted at intervals (mins) following release from α-factor. **B.** Percentage of *HTB1* mRNAs with poly(A) tails <25nts (blue columns), 25-50nts (red columns) and >50nts (green columns) at time intervals after α-factor release.

4.2.5 Sen1p acts at G1-phase of the cell cycle

Since poly(A) tail length varied during the cell cycle and was influenced by Sen1p and Rrp6p, it is possible that Sen1p may contribute to cell cycle poly(A) tail length regulation. Rrp6p also influenced poly(A) tail length and has previously been shown to influence cell cycle regulation (Canavan and Bond, 2007). Data accumulated from sequencing of *HTB1* transcripts isolated from wild-type cells indicated that poly(A) tail lengths of *HTB1* mRNAs varied at different stages of the cell cycle – long tails at G1-phase, short tails in S-phase and no tails during G2-phase. In addition to this, isolation of the poly(A) tail in asynchronous cells demonstrated that inactivation of Sen1p led to a clear increase in the presence of short poly(A) tails. To determine if mutations in Sen1p may be affecting cell cycle progression flow cytometry analysis was carried out. Briefly, asynchronous wild-type and *sen1* mutant cells were grown to an OD_{600nm} value of 0.8 (approximately $1x10^7$ cells) in YEPD media at 25°C. As described in Chapter 2, section 2.1, the cultures were split in half and underwent re-incubation in fresh YEPD media at 25°C or 37°C for 2hrs. Following ethanol fixation, the cells were stained with propidium iodide and passed through the flow cytometer for analysis (Chapter 2, section 2.12).

The proportion of actively replicating cells was compared in wild-type and Sen1p cells at the permissive and non-permissive temperatures. In the asynchronous wild-type cells, two peaks were observed corresponding to 1n and 2n cells (*Figure 4.9A*). The larger peak observed corresponded to 2n cells suggesting that the majority of the cell population were actively replicating (S-phase). Upon inactivation at 37°C, the percentage of wild-type 2n cells decreases, suggesting a decrease in replication at the higher temperature (*Figure 4.9B*). For *sen1* at the permissive temperature, the flow cytometry analysis appeared to be very similar to those observed for the wild-type cells at the same temperature (*Figure 4.9C*) indicating that the majority of the cells were in S-phase. However, upon inactivation at the non-permissive temperature, the majority of the cells for *sen1* showed 1n distribution (*Figure 4.9D*). This was in direct contrast to the flow analysis for the wild-type strain at the non-permissive temperature where two peaks corresponding to 1n and 2n were observed (*Figure 4.9B*).

In order to quantitatively compare the flow cytometry analysis, gating of the total sorted cells was carried out. This revealed that at the permissive temperature, 80-85% of cells

for both wild-type and *sen1* were 2n (*Figure 4.9E*). At the non-permissive temperature, the percentage of wild-type cells in 2n was reduced to 60%. This analysis was conducted using four independent samples. For Sen1p the percentage of 2n cells at the permissive and non-permissive temperatures was 80% and 40% respectively (*Figure 4.9E*). These results indicate that upon inactivation, the rate of replication in a *SEN1* mutant is decreased suggestive of a cell cycle defect.

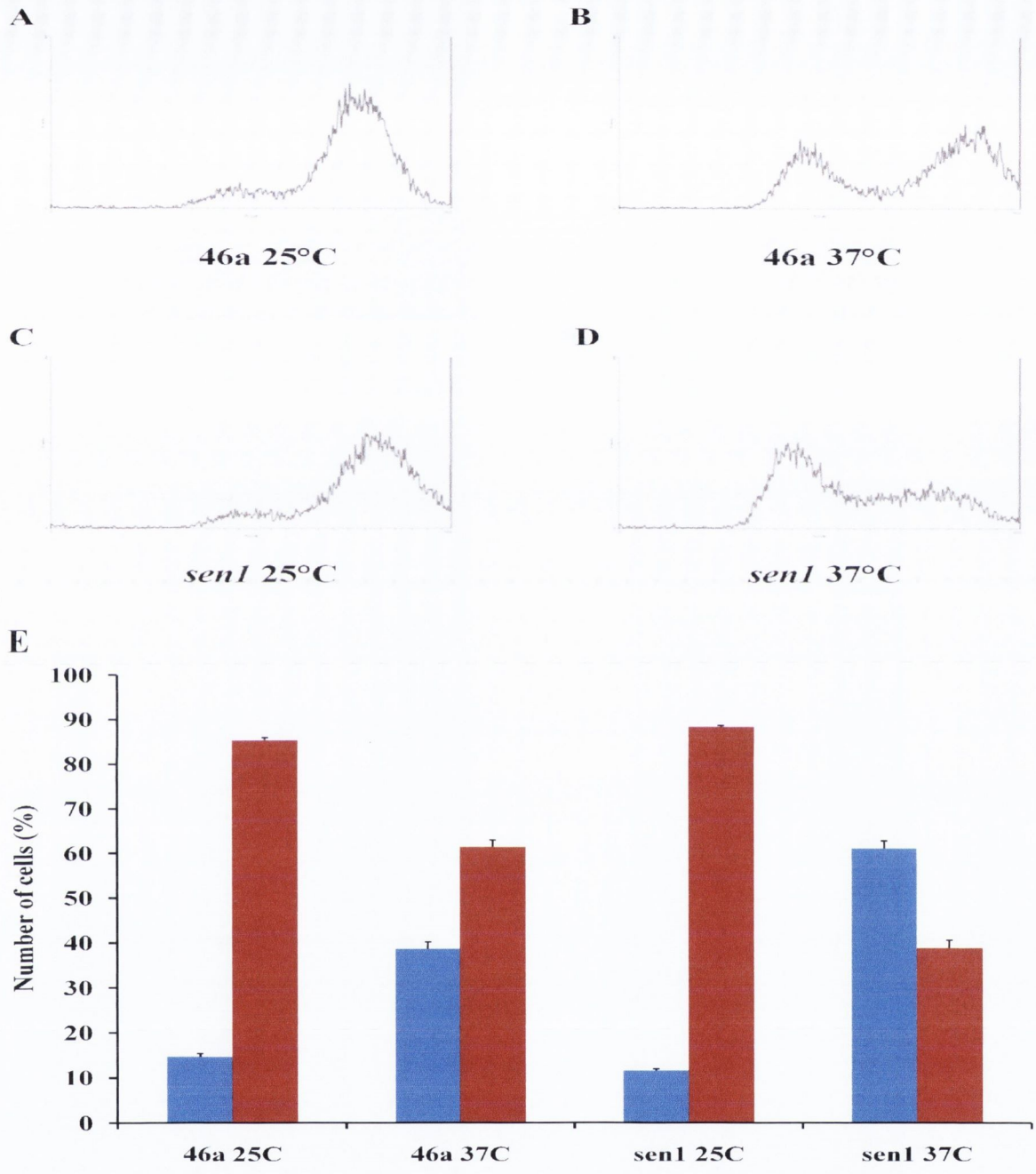

Figure 4.9: Flow cytometry analysis of asynchronous cultures of *sen1*. Wild-type (46a) (panels A and B) or *sen1* cells (panels C and D) were grown at the permissive (25°C; A and C) and non-permissive temperature (37°C; B and D) and stained with propidium iodide as described in the Materials and Methods section. The cells were passed through a flow cytometer. The pattern of cell sorting is indicated for each of the strains. **E.** The flow-sorted cells were gated to distinguish 1n from 2n cells. Blue columns; 1n, Red columns; 2n. The results represent the averages of four independent experiments and the standard error for each sample is shown.

4.3 Discussion

The data presented in this study re-examines the polyadenylation status of *HTB1* mRNA in both asynchronous and synchronised populations of yeast cells. Previous studies have indicated that histone mRNAs in yeast were polyadenylated but the length of the poly(A) tail remained unknown (Fahrner et al., 1980; Miura et al., 2006; Osley and Hereford, 1981). In this study, the average length of the poly(A) tail in *HTB1* mRNAs was found to be 33nts which is much shorter than the general pool of mRNA which have previously been reported to have tails of 70-100nts (Beilharz and Preiss, 2007; Libri, 2010). This shorter poly(A) tail found in *HTB1* mRNA was consistent with data obtained from Beilharz and Preiss, (2007) who conducted a genome-wide study of poly(A) tail length in *S. cerevisiae*. Through a combination of the ligation-mediated poly(A) test (LM-PAT) and polyadenylation state array (PASTA) analysis, they observed an enrichment of transcripts encoding cell cycle related functions in a pool of RNAs with short poly(A) tails (Beilharz and Preiss, 2007). In addition to the shorter poly(A) tailed transcripts found in the histone mRNAs, we also found three distinct pools of poly(A) tail length in *HTB1* transcripts of asynchronous cells- those that are <25nts, 25-50nts and >50nts.

When the length poly(A) tail was investigated in asynchronous Sen1p and Rrp6p cells, a trend towards a short poly(A) tail was observed. As both of these proteins are found in the nucleus, this suggests that nuclear events may contribute to histone mRNA regulation. The data indicates that inactivation of Sen1p led to inefficient transcription termination. Sequencing of the captured read-through *HTB1* transcripts in *sen1* did not lead to a significant accumulation of transcripts with cleavage sites downstream of the normal cleavage sites suggesting that the read-through transcripts were unstable. Previously Canavan and Bond, (2007) demonstrated that deletion of *RRP6* led to increased stability of *HTB1* and a delay in exit from S-phase into G2-phase leading to the hypothesis that the turnover of histone mRNAs at the S/G2 boundary may act as a checkpoint for cell cycle progression (Canavan and Bond, 2007). Northern blot analysis conducted in Chapter 3 found that inactivation of Sen1p did not affect the steady state levels of *HTB1* mRNA in an asynchronous population. Flow cytometry analysis revealed a cell cycle defect in *sen1* cells at the non-permissive temperature. The decrease in 2n cells at the non-permissive temperature in *sen1* may result from a

delay in exit from G1-phase or an inability to exit from G2-phase to M-phase. Taken together, the role for Sen1p in transcription termination of histone mRNAs and its influence on poly(A) tail length suggests that Sen1p plays an important role in the cell cycle regulation of histone mRNAs. While the cell cycle defect observed in *sen1* cells may result from its role in snRNA transcription termination, it is intriguing to speculate that this defect results directly from its role in histone mRNA biogenesis. Sen1p has been shown to play a "fail-safe" role in transcription termination of polyadenylated gene transcripts, thus, it is possible that Sen1p may exert differential effects on histone mRNA biogenesis at different stages of the cell cycle via this fail-safe mechanism. A recent paper by Mischo *et al.*, (2011) has shown that Sen1p is required to release R-loops which are known to be required for transcription termination. They found that loss of Sen1p leads to a delay in exit from G1-phase of the cell cycle and that *sen1* leads to increased read-through in associated Sen1p genes and an increase in the accumulation of R-loops which in turn leads to DNA damage (Mischo et al., 2011).

When the length of the poly(A) tail during the cell cycle was examined, we found that the tail length of *HTB1* transcripts varies as cells progress through the cell cycle. Three distinct pools of tails were identified and although long-tailed transcripts (> 50nts) were found throughout the cell cycle, other pools of poly(A) tail length appear at distinct stages of the cell cycle. In G1-phase, the average length of the poly(A) tail on the *HTB1* transcript was found to be 46nts. As the cells proceeded into S-phase, the average length of the poly(A) tail decreased to 22nts and finally as the cells approached G2-phase, *HTB1* transcripts with two types of transcripts were observed- transcripts with no poly(A) tails and those with long poly(A) tails. As previously discussed, histone mRNAs accumulate during the S-phase of the cell cycle and are then rapidly degraded upon entry into G2-phase (Campbell et al., 2002; Hereford et al., 1981; Marzluff et al., 2008; Mullen and Marzluff, 2008). During S-phase the majority of transcripts produced had short poly(A) tails suggesting that during the S-phase when *HTB1* steady state mRNA levels are at their highest and therefore most stable, short poly(A) tails are present on the transcripts which is contrary to convention. However during G1-phase when *HTB1* steady state levels were at their lowest and most unstable, longer tailed transcripts were found. Coupled with the discovery of a small amount of long tailed transcripts during S-phase and G2-phase, the finding of long-tailed transcripts in G1-phase indicates that long-tailed transcripts are produced continuously

during the cell cycle but may be unstable. This contradicts the belief that addition of poly(A) tails lead to stability of the transcript through the binding of poly(A) binding proteins (Pab1p) which is known to assist in nuclear export of mRNAs (Vanacova et al., 2005; Yamanaka et al., 2010; Yao et al., 2007). Viphakone *et al*, (2008) found that Nab2p, a poly(A) binding protein, not only collaborates with Pab1p to regulate polyadenylation but is also involved in mRNA export and has the ability to inhibit re-adenylation (Viphakone et al., 2008). It has also been suggested that Nab2p helps Pab1p to load onto the poly(A) tail (Dunn et al., 2005). However new evidence is emerging which suggests that poly(A) binding proteins may also play a role in degrading and processing of transcripts in the nucleus (Libri, 2010; Yamanaka et al., 2010). In fission yeast, deletion of *PAB2*, a poly(A) binding protein which has no known homologue in *S. cerevisiae*, results in hyperadenylation of traditionally non-polyadenylated snoRNAs by an unknown mechanism (Lemay et al., 2010). Pab2p has also been shown to play a role in the degradation of meiosis-specific transcripts during mitotic growth, through an interaction with Rrp6p and Dis3p of the nuclear exosome and Mmi1p (Harigaya et al., 2006; Lemay et al., 2010; Yamanaka et al., 2010). Mmi1p is RNA-binding protein found in fission yeast which directs destruction of meiosis-specific mRNAs (Yamanaka et al., 2010). The meiosis-specific mRNAs contain a determinant of selective removal (DSR) region which serves as a marker for mRNA degradation. Mmi1p binds to the DSR region which in turn serves to recruit Pab2p to the poly(A) tail. The exosome is then recruited for degradation of the transcript (Yamanaka et al., 2010). Harigaya *et al*, (2006) found that elimination of unnecessary meiosis-specific messages by Mmi1p is physiologically indispensible as growth was severely impaired when expression of Mmi1p was lost (Harigaya et al., 2006). Taken together, the data suggests that the presence of a poly(A) tail on certain transcripts can invoke nuclear degradation similarly to the way that Trf4p of the TRAMP complex uses the poly(A) tail to mark CUTs for degradation by the exosome in *S. cerevisiae* (Lemay et al., 2010; Wilusz and Wilusz, 2008).

The data presented in this study identified *HTB1* mRNA transcripts with non-canonical 3' ends, at time-points corresponding to the shift from S- to G2-phase. This indicates that active degradation of histone mRNAs takes place during the cell cycle. As all of the transcripts with the exception of one, were found to have no poly(A) tails, cytoplasmic degradation of the mRNA is most likely to have taken place. The CCR4-

Not1 complex is a global regulator of transcription. The complex consists Caf1p/Pop2p, Ccr4p and five Not proteins. While both Caf1p and Ccr4p are involved in mRNA deadenylation, Ccr4p is the catalytic component of the complex and regulates poly(A) tail length, mRNA degradation and translation (Maillet and Collart, 2002; Woolstencroft et al., 2006). Caf1p and Ccr4p are associated with Not1p, the only known component of the complex to be essential for yeast viability (Maillet and Collart, 2002). Recent studies have identified histone mRNAs as a category of transcripts particularly sensitive to mutations in *CCR4* and a role for *CCR4* in cell cycle progression has also been identified (Beilharz and Preiss, 2007; Maillet and Collart, 2002; Westmoreland et al., 2004).

The transcripts detected with non-canonical 3'ends may be the result of forms of degradation by the exosome which are not associated with the addition of a poly(A) tail to the 3' end of the mRNA. The exosome is involved in the nonsense-mediated decay pathway and the non-stop decay pathway which are activated by the presence of a premature termination codon and ribosomes stalled at the end of mRNA respectively (Houseley et al., 2006).

Here a model is proposed to explain how the poly(A) tail length may contribute to the regulation of the steady state levels of histone mRNAs during the cell cycle based on the findings of this study (*Figure 4.10*). Histone mRNAs, resulting from an increase in transcription in S-phase contain short poly(A) tails suggesting that only shorter tailed transcripts can be exported from the nucleus into the cytoplasm for translation. At G2-phase, the degradation of these cytoplasmic histone mRNAs occurs triggered by a signal. Based on the position of oligonucleotides used in this study, we suggest that this degradation takes place in a 3'-5' direction by the exosome and possibly the CCR4-NOT1 complex. Our model suggests that only shorter-tailed transcripts present in the cytoplasm are targets for degradation in G2-phase as even though longer-tailed transcripts were present in small quantities throughout the cell cycle, they appeared to be accumulated after the initial degradation of transcripts at the S/G2-phase border. As longer-tailed transcripts are inversely correlated with stable mRNA transcripts, we propose that these transcripts are retained in the nucleus and are targeted for degradation by the nuclear exosome. Based on the findings of Canavan and Bond, (2007), we propose that this degradation is carried out specifically by Rrp6p as they demonstrated that deletion of *RRP6* of the nuclear exosome lead to accumulation of

HTB1 transcripts and delay in exit from S-phase (Canavan and Bond, 2007). Data presented in Chapter 3 demonstrated that inactivation of Sen1p led to read-through of not only of histone mRNAs but also of *ACT1* and *TDH3* mRNAs indicating that Sen1p may be involved in transcription termination of RNA Polymerase II transcripts. Here we also found that inactivation of Sen1p led to an accumulation of shorter-tailed transcripts and a cell cycle defect. As components of the nuclear exosome and Nrd1p/Nab3p/Sen1p complex are known to interact in the nucleus, we predict that the nuclear degradation of longer-tailed transcripts is linked to transcription termination (Rasmussen and Culbertson, 1998). Thus, longer-tailed transcripts are degraded in the nucleus in G1-phase and shorter-tailed transcripts are degraded in the cytoplasm in G2-phase. This two-phase degradation in G1 and G2 ensures that histone mRNAs only accumulate in S-phase.

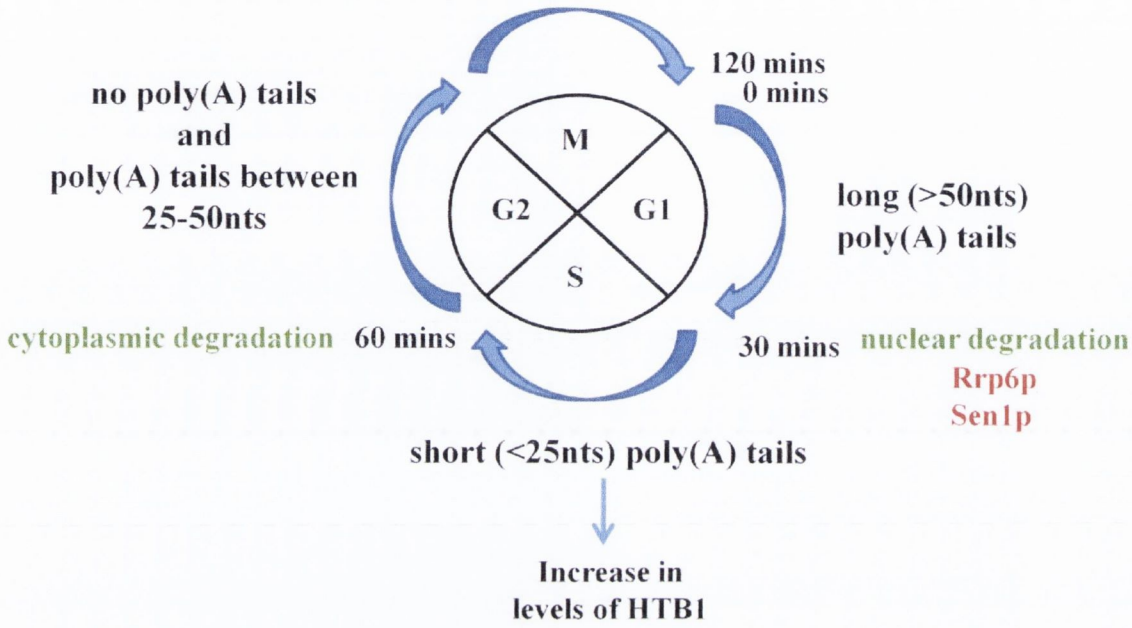

Figure 4.10: Model of the contribution of poly(A) tail length to the regulation of the steady state levels of histone mRNAs during the cell cycle. Long-tailed transcripts were observed throughout the cell cycle but particularly in G1-phase were the majority of the transcripts synthesised were long-tailed. In S-phase the majority of the transcripts were short-tailed, while two distinct pools of transcripts were observed at the G2-/M-phase border – transcripts with no poly(A) tail and transcripts with poly(A) tails of 25-50nts. The model proposes that nuclear degradation of the long-tailed transcripts takes place at G1-/S-phase while cytoplasmic degradation takes place at S-/G2-phase leading to transcripts with no poly(A) tails and non-canonical 3' ends. Transcripts with poly(A) tails of 25-50nts are retained in the nucleus for the next replication cycle.

Pirngruber and Johnson, (2010) observed polyadenylation of canonical histone mRNAs in mammalian cells arrested in G1-phase (Pirngruber and Johnsen, 2010). Polyadenylation of these transcripts was found to be dependent on a decrease in the levels of Nuclear Protein Ataxia-Telangiectasia (NPAT) which is required for recruitment of specific 3' end processing factors to replication dependent histones (Gao et al., 2003; Pirngruber and Johnsen, 2010; Pirngruber et al., 2009). NPAT was also found to stimulate the transcription of all replication-dependent histone genes during S-phase in a phosphorylation-dependent manner (Pirngruber and Johnsen, 2010). The finding that polyadenylation of canonical histone mRNAs in mammalian cells can regulate histone mRNA levels supports the model proposed whereby longer polyadenylated histone mRNAs are targeted for degradation in G1-phase.

Interestingly, deletions and mutations in *NPAT* and Senataxin, the homologue of yeast Sen1p, have been implicated in the development of a number of neurological disorders. NPAT is encoded in the Ataxia-Telangiectasia (AT) Locus on chromosome 11 (11q22-q23) (Finkel et al., 2010; Suraweera et al., 2007). Mutations in the AT locus are associated with the autosomal recessive disease AOA1 which leads to cerebellar ataxia and oculocutaneous telangiectasian in humans (Moreira et al., 2004). Senataxin is defective in Ataxia-ocular apraxia 2 (AOA2) and is encoded by *SETX* (Finkel et al., 2010; Moreira et al., 2004; Suraweera et al., 2007). Mutations in *SETX* are associated with an autosomal dominant, juvenile onset form of amyotrophic lateral sclerosis (Suraweera et al., 2007). AOA1 and AOA2 share several clinical features which can be distinguished by age of onset. AOA1 affects children between the ages of 2 and 15 years while AOA2 affects adolescents between the ages of 10 and 22 years (Suraweera et al., 2007). The observation that both *NPAT* and Sen1p play important roles in regulating histone mRNA polyadenylation may suggest an important role for histone mRNA regulation in the development of Ataxia-related diseases.

Chapter 5

The role of members of the SCF (Skp1p/Cul1p/F-box protein) complex in 3'-end processing and transcription termination of histone mRNAs

5.1 Introduction

The data presented thus far indicates that histone mRNAs form a distinct class of mRNAs with shorter than average poly(A) tails that vary in length during the cell cycle. Furthermore, 3' end processing and transcription termination requires factors of both the polyadenylated and non-polyadenylated RNA 3' end processing pathways.

Previous work by Campbell *et al.*, (2002) defined a cis-acting element called the Distal Downstream Element (DDE) which lies approximately 100nts downstream of the 3' end cleavage site that is required for transcription termination and also contributes to the cell cycle regulation of the upstream mRNA. Mutation in the DDE led to a delay in the accumulation of histone mRNAs in S-phase (Campbell et al., 2002). A three-hybrid analysis was carried out and a number of putative DDE –binding proteins were identified including YJL171c, Arf1p, Pop4p, Ttr1p, Pet20p and Skp1p (Beglan and Bond, unpublished data). The most abundant protein identified in the screen was YJL171c, a protein of unknown function that shares sequence homology with Tos1p (YBR162c), a cell wall protein (Yin et al., 2005). Pop4p, a component of the MRP and RNase P endoribonuclease complexes, functions in the processing of pre-tRNAs and pre-rRNAs and has also been shown to function in the degradation of *CLB2* mRNA, a cell cycle regulated cyclin (Houser-Scott et al., 2002; Xiao et al., 2006). Arf1p is an ADP ribosylation factor which is involved in signal transduction. Arf1p has also been found to have small monomeric GTPase activity and evidence suggests that Arf1p may act in the nucleus (Stearns et al., 1990; Trautwein et al., 2004). Pet20p is required for respiratory growth while Ttr1p is a glutathione peroxidise with transferase activity (Polevoda et al., 2006). *SKP1* or Suppressor of Kinetochore Protein 1 encodes an evolutionarily conserved kinetochore protein which has homologues in humans, *Caenorhabditis elegans* and *Arabidopsis thaliana* (Bai et al., 1996; Connelly and Hieter, 1996). Skp1p has been found to be essential for both the G1/S and G2/M phase transitions of the cell cycle in *Saccharomyces cerevisiae* and is also a component of the SCF complex (Bai et al., 1996; Connelly and Hieter, 1996). The SCF complex is required for the ubiquitin-mediated proteolysis of cell cycle regulators at the G1/S phase transition of the cell cycle (Willems et al., 2004). The SCF complex contains a least four subunits: Skp1p, a Cullin, a RING finger protein (Hrt1p in yeast, Rbx1p in mammals) and an F-box protein (*Figure 5.1*) (Ho et al., 2006; Kipreos and Pagano,

2000). Within the complex, the F-box protein is required for substrate recruitment through protein-protein interaction while Cullin functions as the scaffold in assembling the different subunits of the SCF complex. At its carboxy-terminal domain, Cullin interacts with the RING domain protein, Hrt1p, to form a catalytic domain. Cullin also interacts with Skp1p through its amino-terminal end (Hermand, 2006). Skp1p binds to the F-box protein through the F-box motif and in doing so provides a link for the F-box protein and its bound substrate to the rest of the complex (*Figure 5.1*) (Hermand, 2006; Kipreos and Pagano, 2000; Yoshida, 2007). However Skp1p can also have functions which are independent of the SCF complex (Hermand, 2006). Skp1p associates with Sgt1p and Hsp90p to form part of the centromere binding factor (CBF3) complex which binds centromeric DNA for proper kinetochore function (Kim et al., 2006b). Skp1p has also been found in the regulator of the (H^+)-ATPase of the vacuolar and endosomal membrane (RAVE) complex which regulates the assembly of the V-ATPase for endocytosis intracellular lysosomal targeting and protein processing (Kim et al., 2006b).

F-box proteins contain a 50 amino acid motif and are named for their similarity to the mammalian cyclin F protein. F-box proteins are evolutionarily conserved with 17 known examples in *S. cerevisiae* (*Table 5.1*), 33 identified in *Drosophila*, 326 in *Caenorhabditis elegans*, at least 38 in humans and nearly 700 predicted in *Arabidopsis thaliana*. However there are no known examples of F-box protein motifs in prokaryotes (Hermand, 2006; Kipreos and Pagano, 2000). The cell cycle regulatory role of F-box proteins is provided in the context of the SCF complex with the F-box proteins Cdc4, Dia2 and Grr1 previously shown to be involved in the regulation the cell cycle (Goh and Surana, 1999; Koepp et al., 2006; Li and Johnston, 1997).

Based on the finding that Skp1p has been identified as a DDE-interacting proteins and evidence that they play a role in cell cycle regulation, we investigated the role of Skp1p and F-box proteins in the 3' end formation of histone *HTB1* mRNA.

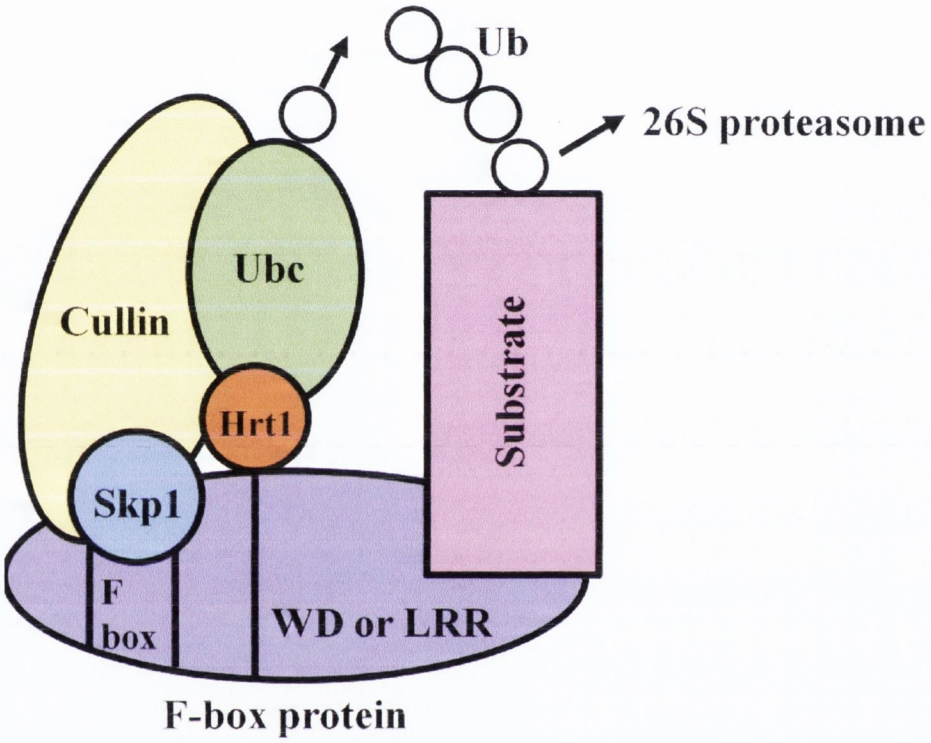

Figure 5.1: Schematic diagram of the Skp1p-Cullin-F-box protein (SCF) complex. The SCF complex is composed of Skp1p, Cullin, Ubc, Hrt1p and an F-box protein. The F-box protein is linked to the SCF complex via interaction between the F-box and Skp1. An ubiquitin-conjugating enzyme (Ubc) binds to the SCF complex and transfers ubiquitin (Ub) onto substrates bound by the F-box protein. When the substrate becomes poly-ubiquitinated, it is degraded by the 26S proteasome. Figure adapted from (Kipreos and Pagano, 2000).

Table 5.1: Mutant F-box protein strains and their functions.

Strain	F-box protein	Function
YOR080w	Dia2	Role in DNA replication
YNL311c	Skp2	Predicted involvement in ubiquitin-dependent protein catabolism
YNL230c	Ela1	Forms a heterodimer with Elc1p and participates in transcription elongation
YML088c	Ufo1	Binds to phosphorylated HO endonuclease
YMR258c	Unknown function	Physically interacts with Skp1p
YJR090c	Grr1	Required for Cln1p and Cln2p degradation. Involved in carbon catabolite repression
YLR368w	Mdm30	Physically interacts with mitochondria
YLR352w	Unknown function	Interacts with Skp1p and Cdc53p
YLR224w		Involved in ubiquitin-dependent protein catabolism
YLR097c	Hrt3	Putative nuclear ubiquitin ligase which associates with Cdc53p, Skp1p and Ubi4p
YIL046w	Met30	Interacts with and regulates Met4p
YJL149w	Unknown function	Interacts physically with both Cdc53p and Skp1p and genetically with CDC34
YJL204c	Rcy1	Involved in recycling plasma membrane proteins internalised by endocytosis
YFL009w	Cdc4	Required for G1/S and G2/M transition.
YDR131c		Substrate-specific adaptor subunit that recruits substrates to a core ubiquitination complex
YBR280c	Saf1	Involved in proteasome-dependent degradation of Aah1p during entry of cells into quiescence
YDR219c	Mfb1	Involved in maintenance of normal mitochondrial morphology

5.2 Results

5.2.1 Skp1p is not involved in transcription termination of *HTB1* mRNA

As Skp1p was identified as a putative DDE-interacting protein and is involved in cell cycle regulation, we tested the role of Skp1p in 3' end formation of histone *HTB1* mRNA. To determine if *SKP1* contributes to transcription termination of histone mRNA, the temperature sensitive *skp1* mutants were incubated at 22°C and 37°C for 3hrs and 6hrs and the total RNA was isolated (Chapter 2, section 2.1). To capture any unprocessed primary transcripts that have not been cleaved and polyadenylated at the correct 3'-end of the mRNA, RT-PCR was carried out using reverse primers spanning the region downstream of the correct 3'-end cleavage site of the *HTB1* mRNA (*Figure.5.2A*) as described in Chapter 3.

Figure 5.2B-D demonstrates the results observed for the RT-PCR reaction carried out on the wild-type strain, W303, at 22°C, 30°C and 37°C after 3hrs. As with previous wild-type strains tested, a PCR product was obtained with reverse primer 1 (*Figure 5.2B,* lane 1) for all three temperatures. No *HTB1* specific bands were observed past reverse primer 1 for any of the temperatures indicating that at the three hour time-point, the *HTB1* transcripts were correctly cleaved and polyadenylated at all three temperatures. A similar pattern of results was observed at all three temperatures for both *skp1-3* (*Figure 5.2C*) and *skp1-4* (*Figure 5.2D*) at the 3hr time-point. The read-through assay was also carried out for each of the *skp1* mutants and the wild-type strain for all three temperatures after the six hour incubation and a similar pattern of results was observed for the wild-type and *skp1* mutants (data not shown). These results indicate that Skp1p is not required for the transcription termination of histone *HTB1* mRNAs.

Figure 5.2: *HTB1* mRNA RT-PCR results of the temperature-sensitive strains *skp1-3* and *skp1-4*. Total RNA from temperature-sensitive mutants, *skp1-3* and *skp1-4*, and the wild-type strain W303 was reverse transcribed using primers spanning the downstream region of *HTB1* and amplified using a common forward primer (For1). The expected size of the *HTB1* specific products are shown in brackets. Lane M; molecular weight marker, the 200bp, 300bp and 400bp bands are indicated, Lane 1; Rev1 (143nts), Lane 2; Rev2 (231nts), Lane 3; Rev3 (309nts), Lane 4; Rev4 (392nts), Lane 5; Rev5 (468nts), Lane 6; Rev6 (554nts), Lane 7; Rev7 (646nts) and Lane 8; cDNA prepared using Rev1 in the absence of Reverse Transcriptase. * represent *HTB1*-specific PCR products of the expected size. **A.** Location of the *HTB1* primers used in the cDNA synthesis. **B.** RT-PCR analysis of *HTB1* mRNA from wild-type W303, grown at 22°C, 30°C and 37°C for 3hrs. **C.** RT-PCR analysis of *HTB1* mRNA from *skp1-3*, grown at 22°C, 30°C and 37°C for 3hrs. **D.** RT-PCR analysis of *HTB1* mRNA from *skp1-4*, grown at 22°C, 30°C and 37°C for 3hrs.

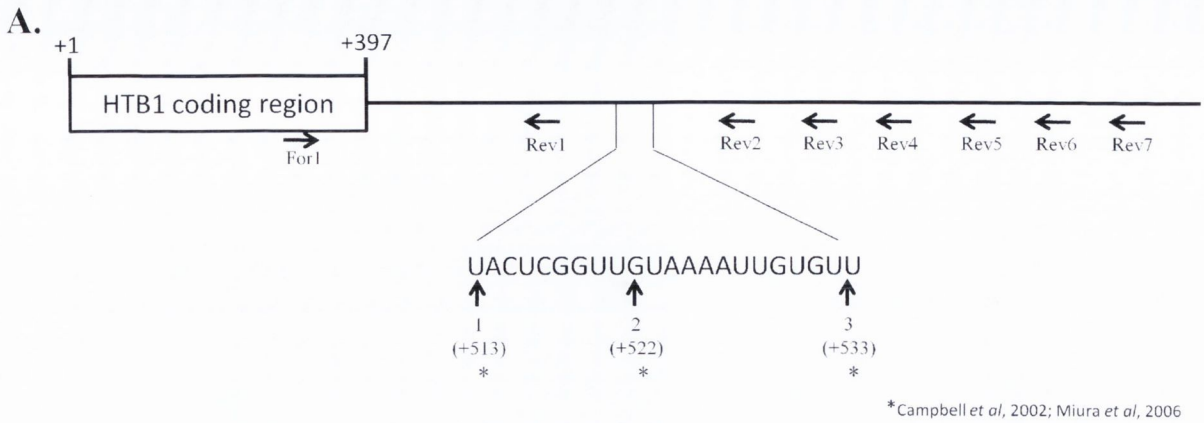
A.
+1
+397
HTB1 coding region
For1
Rev1
Rev2
Rev3
Rev4
Rev5
Rev6
Rev7
UACUCGGUUGUAAAAUUGUGUU
1
(+513)
2
(+522)
3
(+533)
*Campbell et al, 2002; Miura et al, 2006

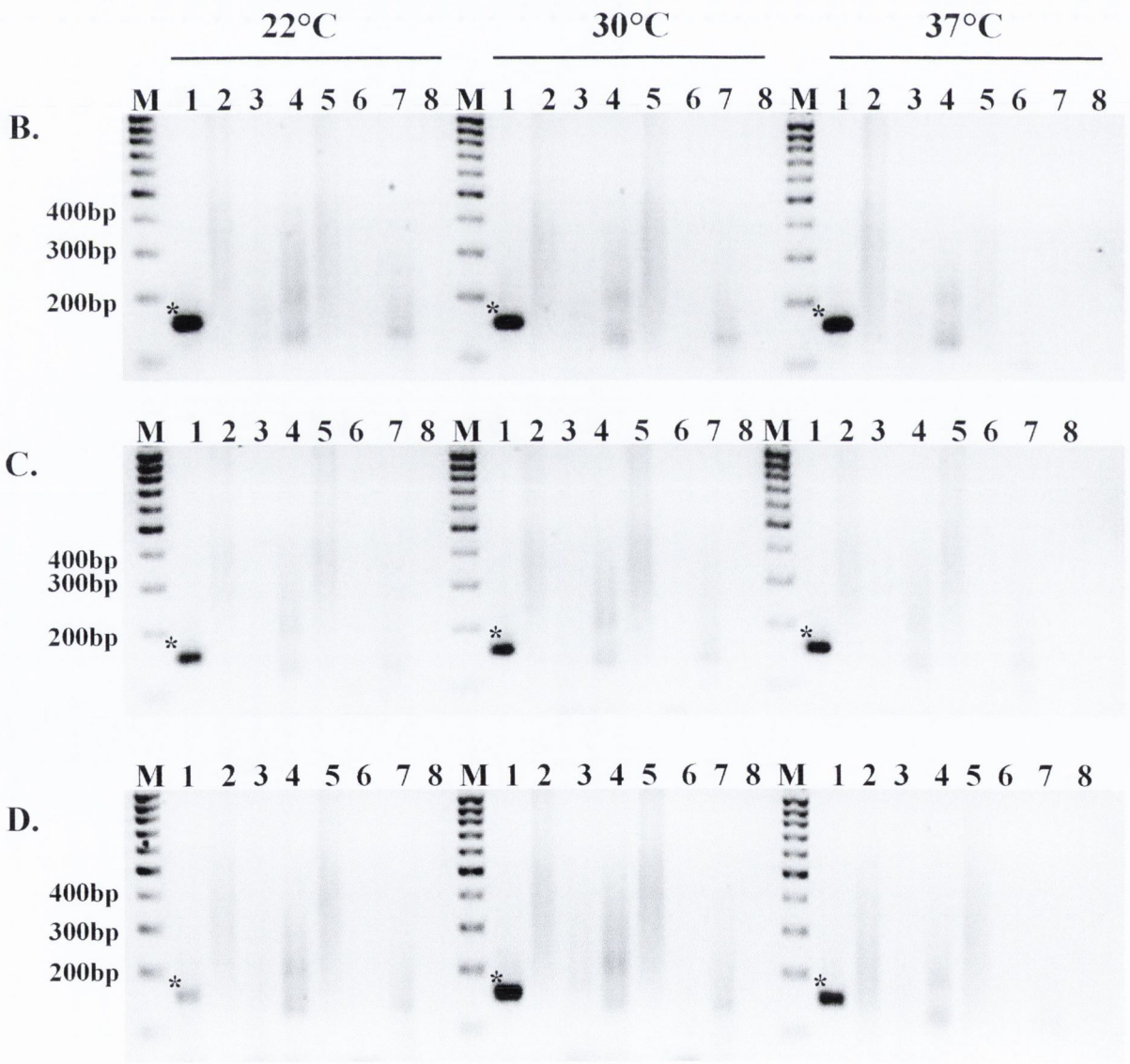
22°C
30°C
37°C
M 1 2 3 4 5 6 7 8 M 1 2 3 4 5 6 7 8 M 1 2 3 4 5 6 7 8
B.
400bp
300bp
200bp
C.
400bp
300bp
200bp
D.
400bp
300bp
200bp

5.2.2 Some F-box proteins affect the steady state levels of *HTB1* mRNA

Since F-box proteins, via their interaction with Skp1p, may be putative DDE-interacting proteins we tested whether these proteins affect the steady state levels of *HTB1* mRNA. To do this Northern blot analysis and real-time RT-PCR were carried out in deletion mutant strains of each of the F-box proteins (*Table 2.1*). Briefly, the individual mutant F-box protein strains and their parental wild-type strains, BY4741 and BY4742 (*Table 2.1*), were grown to an optical density (OD_{600nm}) value of 0.8 (approximately 1 x 10^7 cells/ml) at 30°C. Total RNA was extracted and Northern blot analysis was carried out using DIG-labelled probes to both *HTB1* and *ACT1*. The steady state levels of *HTB1* mRNA were compared to the *ACT1* mRNA levels in each strain tested (*Figure 5.3B* and *C* and *E* and *F*). The expression levels within the mutant strains were then compared to those within the wild-type strains. It should be noted that the levels of *ACT1* mRNA detected differed for each strain indicating that this was not the correct gene to use as a control. For future experiments, alternative genes such as 5.8S rRNA or *SCR1* should be used as these are both constitutively expressed. However, the Northern blot analysis revealed some qualitative and quantitative variability between the mutant strains. In mutants *YDR131c*, *YLR352w*, *YIL046w* and *YLR224w*, the band representing the *HTB1* transcript was broader and more smeared than the equivalent band in either the wild-type or other mutants suggestive of some degradation (*Figure 5.3C*). The degradation appears specific to the *HTB1* transcript as the *ACT1* mRNA appears intact (*Figure 5.3B*). *HTB1* levels appeared reduced in mutants *YDR219c* and particularly in *YLR368w* (*Figure 5.3F*).

To quantify the steady state levels of *HTB1* mRNA in the mutant strains, real-time RT-PCR was carried out on the individual F-box protein mutants using the *HTB1* endogenous primers. To control for variations in total RNA pools, the levels of 5.8S rRNA was also measured (Chapter 2, section 2.10.4, Table 2.2). To ensure that the RNA used was not contaminated with DNA, a negative control was set up for each reaction without the Reverse Transcriptase using the HTB1 endogenous forward and reverse primers (Table 2.2). Each reaction was carried out in triplicate and a melt curve was included in each experiment (data not shown). Using the calculations described in Chapter 2, section 2.10.4, the average Ct values were calculated for each primer set and the levels of *HTB1* expression in the mutant strains compared to those detected in the wild-type strains. The relative expression level of *HTB1* (*HTB1*:5.8S rRNA) was set at

1.0 for the wild-type strain, BY4741, and all the mutant strains were compared to this. The values represent the average levels of expression of triplicate samples of a single sample of each strain (*Figure 5.3G*).

While levels of *HTB1* varied between experiments (average error ±25%), the real-time RT-PCR analysis revealed some significant reductions in *HTB1* in a number of the mutant strains (*YDR131c*, *YLR352w*, *YLR224w* and *YLR368w*) (*Figure 5.3G*). Interestingly the reduced levels in *YDR131c*, *YLR352w* and *YLR224w* correlated with the increased degradation of *HTB1* as observed in the Northern blot. Likewise the level of *HTB1* in *YLR368w* in real-time RT-PCR analysis was significantly lower in the Northern blot. While the reduced levels of *HTB1* were observed in *YDR219c* on the Northern blot, this was not borne out by real-time RT-PCR analysis (*Figure 5.3F* and *G*). Taken together the data suggests that *HTB1* levels may be influenced by mutations in some F-box proteins.

Figure 5.3: Northern blot and real-time RT-PCR analysis of the steady state levels of *HTB1* mRNA within mutant F-box protein strains. Total RNA, 30μg was electrophoresised on a 1% TAE agar and subsequently blotted onto a nylon membrane via capillary action. The membrane was then probed using DIG-labelled *HTB1* and *ACT1* probes. **A.** Ethidium bromide stained gel showing the ribosomal RNAs of the strains shown above each lane. rRNA was used as a control of equal loading of the gel. **B.** The blot was hybridised with the *ACT1* probe. **C.** The blot was hybridised with the *HTB1* probe. **D.** Ethidium bromide stained gel showing the ribosomal RNAs containing the strains shown above each lane. **E.** The blot was hybridised with the *ACT1* probe. **F.** The blot was hybridised with the *HTB1* probe. **G.** Comparison of the ratio of *HTB1* mRNA in mutant F-box protein strains. Error bars represent the standard deviation of three replicates from an individual data set.

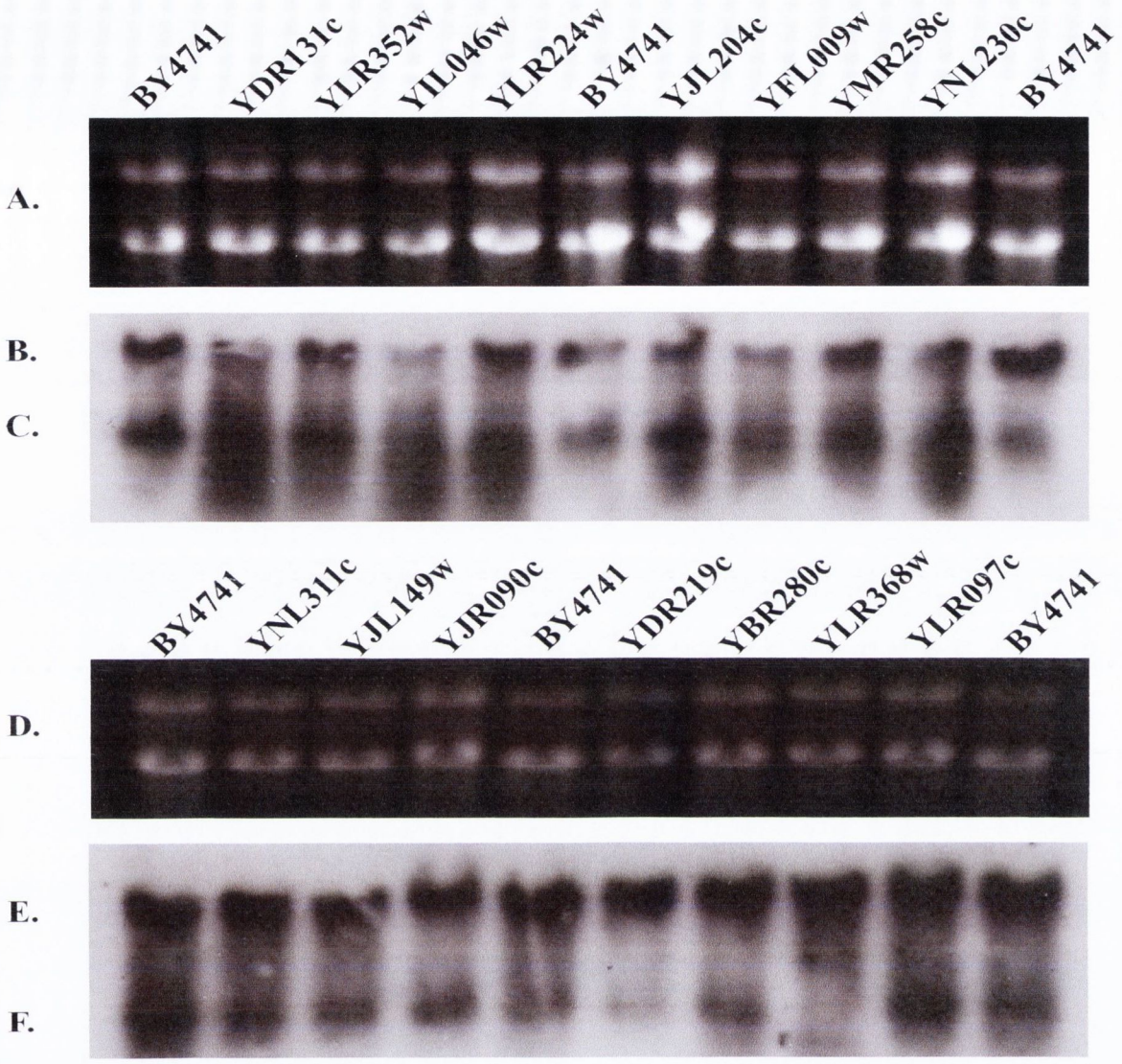
BY4741
YDR131c
YLR352w
YIL046w
YLR224w
BY4741
YJL204c
YFL009w
YMR258c
YNL230c
BY4741
A.
B.
C.
BY4741
YNL311c
YJL149w
YJR090c
BY4741
YDR219c
YBR280c
YLR368w
YLR097c
BY4741
D.
E.
F.

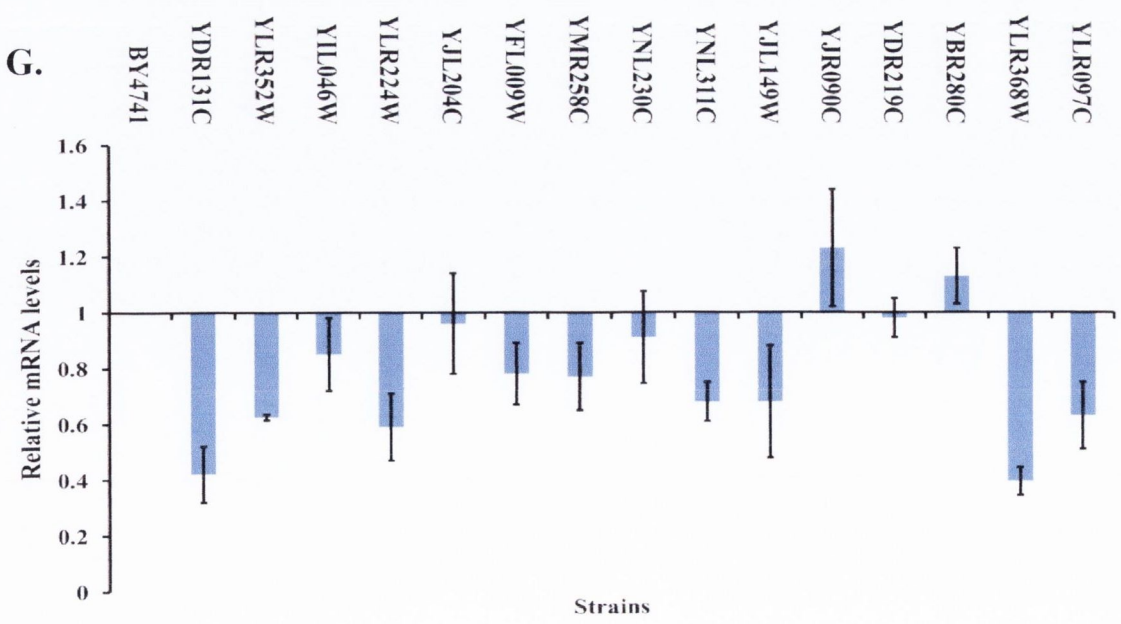
G.
BY4741
YDR131C
YLR352W
YIL046W
YLR224W
YJL204C
YFL009W
YMR258C
YNL230C
YNL311C
YJL149W
YJR090C
YDR219C
YBR280C
YLR368W
YLR097C
Relative mRNA levels
1.6
1.4
1.2
1
0.8
0.6
0.4
0.2
0
Strains

5.2.3 F-box proteins do not effect 3' end processing and transcription termination of histone mRNAs

Since some of the F-box proteins appeared to affect the steady state levels of histone mRNA, we next tested whether these proteins are required for transcription termination of histone *HTB1* mRNA. Using the same read-through assay described in Chapter 3, total RNA from the wild-type strains, BY4741 and BY4742, and the individual mutant F-box protein strains were analysed.

Figure 5.4A and *B* demonstrates the results observed for the RT-PCR reaction carried out on the wild-type strains, BY4741 and BY4742, at 30°C. PCR products were obtained with reverse primer 1 (*Figure 5.4A* and *B*, lane 1) transcript indicating that the majority of *HTB1* transcripts are correctly cleaved and polyadenylated at 30°C. No read-through products were detected with any of the downstream primers (lanes 2-8). The strong band of 304nts observed in lane 2 was identified through sequencing to be 99% identical to yeast *HKA* gene and 98% identical to the *NIN1* gene, a subunit of the 19S regulatory particle of the 26S proteasome lid.

As with the wild-type strains, correctly processed RNA was detected with reverse primer 1 for each of the mutant strains (*Figure 5.4C-H*, lane 1). A small amount of read-through transcripts (231nts) was observed with reverse primer 2 in *YLR352w* and *YIL046w* (*Figure 5.4D* and *E*, lane 2 respectively). The 304nts artefactual band was also evident with this primer. When the remaining eleven mutant F-box protein strains (*Table 5.1*) were analysed, no read-through was detected past reverse primer 1 (data not shown). These results indicate that deletion of these F-box protein strains does not affect transcription termination histone mRNA.

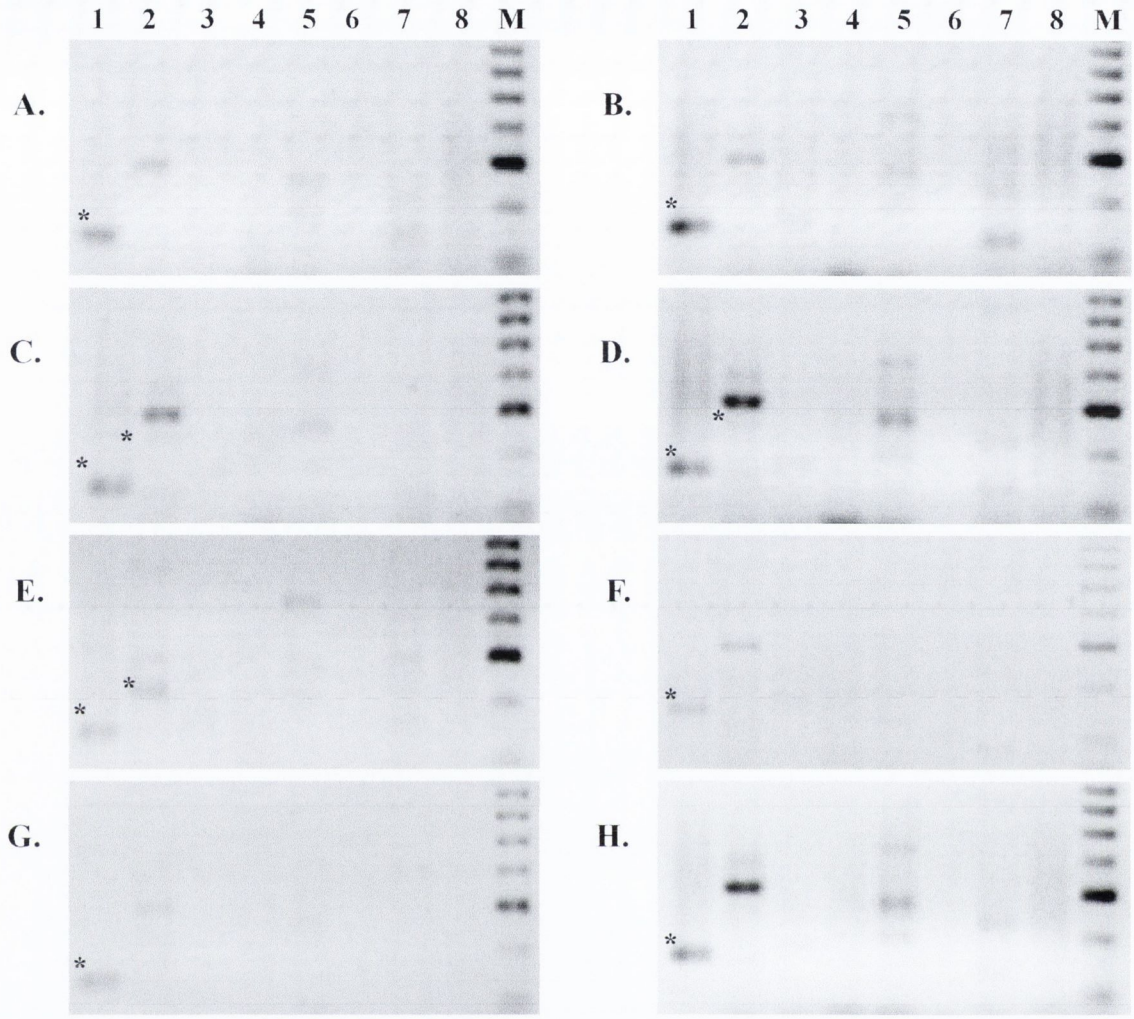

Figure 5.4: *HTB1* mRNA RT-PCR results of the F-box protein deletion strains. Total RNA from wild-type and F-box protein deletion strains was reverse transcribed using primers spanning the downstream region of *HTB1* and amplified using a common forward primer (For1). Lane 1; Rev1 (143nts), Lane 2; Rev2 (231nts), Lane 3; Rev3 (309nts), Lane 4; Rev4 (392nts), Lane 5; Rev5 (468nts), Lane 6; Rev6 (554nts), Lane 7; Rev7 (646nts), Lane 8; cDNA prepared using Rev1 in the absence of Reverse Transcriptase and Lane M; molecular weight marker. * represent *HTB1*-specific PCR products of the expected size. **A and B.** RT-PCR analysis of *HTB1* mRNA from wild-type strains, BY4741 and BY4742, respectively. **C-H.** RT-PCR analysis of *HTB1* mRNA from F-box protein deletion strains *YDR131c*, *YLR352w*, *YIL046w*, *YLR224w*, *YJL204c* and *YFL009w* respectively.

5.3 Discussion

Previous research carried out identified the DDE, a purine rich sequence which lies ~100nts nucleotides downstream of the 3' end cleavage sites of *HTB1*. Using a cell cycle regulated chimera gene, *neo-HTB1*, it was shown that mutations in the DDE appeared to prevent the cell cycle-dependent degradation of *neo-HTB1*, leading to its accumulation in G2-phase of the cell cycle (Campbell et al., 2002). Using a three-hybrid screen, a number of proteins that interact with the DDE at the 3' end of the histone mRNAs were identified. One such protein was Skp1p, a component of the SCF complex, which plays a role in cell cycle progression through the action of ubiquitin ligases (Bai et al., 1996; Kim et al., 2006b). Proteins targeted for degradation by the SCF complex are recognized by specific F-box proteins, which are responsible for substrate recruitment. Since Skp1p appears to interact with histone mRNAs, it was hypothesized that F-box proteins may also play a role in regulating histone mRNA levels though its interaction with Skp1p. Using deletion strains of F-box proteins and temperature sensitive *skp1* mutant strains, the efficiency of transcription termination of the histone *HTB1* mRNA was examined. Data presented in this study indicates that none of the mutants analysed effect transcription termination.

The effect of mutation of *SKP1* and deletion of individual F-box proteins on the steady state levels of *HTB1* mRNA was also examined in this study. However due the instability of *HTB1* mRNA at 37°C, analysis of the temperature sensitive *skp1* mutants by Northern blotting was difficult. In order to analyse *SKP1* in the future, experiments utilizing degron plasmids could be carried out. By using this approach, expression of the *SKP1* gene would be under the control of an inducible promoter and therefore the problem of unstable RNA in temperature sensitive mutants would be avoided. Previous research has demonstrated that the human homologue of Skp1p was present in a protein complex with cyclin A-CDK2 and Skp2p, a protein essential for G1/S phase cell cycle progression indicating that Skp1p had a role in cell cycle regulation (Li and Johnston, 1997). Skp1p was also found to be associated with Sgt1p and Hsp90p to modulate assembly and turnover of the centromere binding factor 3 (CBF3) complex for proper kinetochore function (Kim et al., 2006b). Many other SCF complexes, such as SCF^{Dia2} and SCF^{Cdc4} have been found to be involved in the degradation of cell cycle regulatory proteins and as Skp1p is also a component of the SCF complex, this strongly suggests a

role for Skp1p in histone mRNA biogenesis although further research is required to confirm this (Goh and Surana, 1999; Koepp et al., 2006).

Northern blot analysis and real-time RT-PCR analysis of the individual mutant F-box proteins indicates that *HTB1* mRNA levels are reduced in the mutant strains *YDR131c*, *YLR352w*, *YLR224w* and *YLR368w*. Many of the other strains tested also appeared to alter *HTB1* mRNA expression but as the Northern blot and real-time RT-PCR analysis gave conflicting results for these F-box proteins, we believe that the differences detected through the two methods may be a more qualitative difference than a quantitative difference. Although the F-box proteins *YDR131c*, *YLR352w* and *YLR224w* are known to be components of the SCF complex, little else is known about their functions. Therefore further research is required in order to understand their true function in histone mRNA biogenesis. The mutant *YLR368w*, which has a mutated Mdm30 protein, was found to have the greatest affect on the *HTB1* mRNA levels through both types of analysis. Fitz *et al.*, (2003) found that Mdm30p regulates mitochondrial fusion by directly or indirectly stimulating degradation of Fzo1, a GTPase and a key component of the mitochondrial fusion machinery (Fritz et al., 2003). Further research revealed that a small portion of Mdm30p was associated with the mitochondria *in vivo* that the function of Mdm30p in mitochondrial regulation was independent of SCF^{Mdm30} (Durr et al., 2006). The data presented here suggests that the F-box proteins *YDR131c*, *YLR352w*, *YLR224w* and *YLR368w* are involved in histone mRNA biogenesis but it is not known if there is redundancy within these proteins. In order to examine if deletion of an individual F-box protein causes another F-box protein to takes over its function, studies involving multiple F-box protein deletions should be carried out. One such investigation was carried out by Durr *et al.*, (2006). In this study, the authors mutated the two mitochondria-associated F-box proteins, Mdm30p and Mfb1p. Through deletion of Mdm30p and over expression of Mfb1p, they found that loss of Mdm30p cannot be compensated by over expression Mfb1p. This suggests that there is no redundancy between the F-box proteins. However in order to confirm this, multiple mutations of other F-box proteins should be carried out.

Chapter 6

Conclusion

6.1 General Discussion

In eukaryotes, pre-mRNAs must undergo a number of tightly controlled processes in order to become functional mature mRNAs. These processes include transcription termination, cleavage and polyadenylation of the newly formed 3' end and nuclear export (Marzluff et al., 2008).

In yeast, RNA Polymerase II transcribes two types of RNAs; polyadenylated mRNAs and non-polyadenylated non-coding RNAs (Rondon et al., 2009). Two types of processing machinery are involved in creating the 3' ends of these different types of RNAs, although emerging evidence suggests that they may share a number of common components (Dheur et al., 2003; Sheldon et al., 2005; Steinmetz and Brow, 2003). Thus, a common theme of cross-communication between both pathways has emerged over the past few years.

Although recent research has shown that mammalian histone mRNAs possess a fail-safe cleavage and polyadenylation site downstream of the stem-loop, mammalian histone mRNAs are usually not polyadenylated (Narita et al., 2007). Unlike their mammalian counterparts, histone mRNAs in yeast are described as being polyadenylated (Fahrner et al., 1980). The reasons for the structural dichotomy of histone mRNAs in higher and lower eukaryotes and the evolution in higher eukaryotes of unique factors such as SLBP and the U7 snRNP, which are required for histone mRNA 3' end processing, remains unclear. Despite the structural divergence, cell cycle regulation of histone mRNAs is conserved in lower and higher eukaryotes.

The mechanism of 3' end processing of histone mRNAs in yeast has not been fully elucidated, however recent findings indicate that components of both the polyadenylated and non-polyadenylated 3' end processing pathways are required for the biogenesis of yeast histone mRNAs (Canavan and Bond, 2007; Reis and Campbell, 2007). These findings may suggest that histone mRNAs belong to an intermediary class of RNA Polymerase II transcripts requiring components of both pathways for efficient 3' end processing. Alternatively, it has been suggested that some RNA Polymerase II transcripts may contain cis-acting sequences to direct 3' end formation by both pathways in order to provide a failsafe mechanism to ensure proper transcription termination and to prevent read-through into the downstream region.

This thesis sets out to explore further the role of factors involved in 3' end processing of both polyadenylated and non-polyadenylated RNAs in yeast histone mRNA biogenesis and to elucidate in more detail the mechanism of 3' end formation of these mRNAs. Such a study may provide insight into the evolutionary mechanisms that have led to the production of histone mRNAs in higher eukaryotes by an almost exclusively non-polyadenylated pathway.

Sen1p affects transcription termination and poly(A) tail length of histone mRNAs.

The role of the snoRNA/snRNA 3' end processing and transcription termination complex Nrd1p/Nab3p/Sen1p was first examined as this complex is known to interact with the nuclear exosome, which has been shown to play a role in the cell cycle regulation of yeast histone mRNAs. Analysis of the effect of Sen1p on the transcription termination of histone *HTB1* mRNA revealed that inactivation of Sen1p leads to the detection of read-through primary transcripts downstream of the known cleavage sites. Observations from both Northern blot and real-time RT-PCR analysis revealed that inactivation of Sen1p did not significantly affect the steady state levels of *HTB1* mRNA, suggesting that this may not be the dominant transcription termination mechanism. Surprisingly the effect of Sen1p on transcription termination of *HTB1* mRNAs was independent of Nrd1p and Nab3p as read-through transcripts were not detected upon inactivation of these components. A slight decrease in the steady state levels of *HTB1* mRNA, however, was detected for *nrd1-5* cells incubated at 37°C by both Northern blot analysis and real-time RT-PCR. Recent studies have demonstrated that in the event of incorrect or inefficient 3' end processing, Sen1p, via Nrd1p/Nab3p, can provide a "failsafe" mechanism for transcription termination of a number of RNA Polymerase II mRNA transcripts (Rondon et al., 2009). In the case of histone mRNAs, the effect of Sen1p on transcription termination was independent of Nrd1p and Nab3p and was evident in asynchronous cells when 3' end processing is operating efficiently. Thus, the role of Sen1p in histone mRNA transcription termination may differ from the failsafe mechanism observed when 3' end processing by the polyadenylated pathway is inefficient.

The transcription termination analysis was carried out in an asynchronous population of cells. In this population, cell cycle specific effects of *sen1* on *HTB1* mRNA levels would not be evident. In order to investigate whether Sen1p has an effect on a specific

stage of the cell cycle, transcription read-through assays and Northern Blotting could be carried out in a synchronised population of cells in a *SEN1* mutant background. However since *HTB1* mRNA levels are highly unstable in both *WT* and *sen1* cells incubated at 37°C and since *Δsen1* cells are inviable, this type of analysis may prove to be difficult. An alternative approach might be to use DEGRON-mediated protein degradation to reduce Sen1p levels. DEGRONs are small stretches of amino acids that when placed at the N- or C-terminus of a protein can mediate protein degradation via the ubiquitin pathway. The recently described auxin-mediated DEGRON system (Nishimura et al., 2009) may be useful in this case as protein inactivation does not depend on an incubation at high temperatures. Additionally, an analysis of the effects of Sen1p on transcription termination of histone mRNAs during the cell cycle could be carried out in strains over expressing *SEN1* from an inducible promoter such as GAL1. It would also be interesting to examine if Nrd1p and Nab3p may also be exerting cell cycle specific effects on histone mRNA.

In addition to affecting transcription termination, G-tailed cDNA analysis revealed a trend towards a shorter poly(A) tail on histone mRNAs in *sen1* cells. This affect was more pronounced upon inactivation at 37°C. This trend towards a shorter poly(A) tail was also observed in a *RRP6* mutant background. Flow cytometry analysis revealed that *sen1* had a higher percentage of 1n cells than 2n cells when compared to the wild-type strain at 37°C, indicative of a cell cycle defect in *sen1*. Since Sen1p has pleiotropic effects on the transcription termination of many genes including snoRNAs, snRNAs, CUTs and now many mRNAs, the cell cycle defect observed in *sen1* cells may not be directly linked to its role in histone mRNA biogenesis. However, given the secondary effect of Sen1p on poly(A) tail length of histone mRNAs, it is intriguing to speculate that these two effects are linked.

Analysis of the 3' end of *HTB1* mRNA in *NRD1* and *NAB3* mutant backgrounds using the G-tailing method would also be interesting in order to see if polyadenylation was affected by Nrd1p and Nab3p in a manner similar to Sen1p.

The poly(A) tail length of histone mRNAs varies during the cell cycle.

Analysis of the length of the poly(A) tail during the cell cycle revealed the presence of three distinct poly(A) tails lengths present at different stages of the cell cycle. During

G1-phase, *HTB1* transcripts with longer poly(A) tails were visible while during the S-phase, transcripts with shorter poly(A) tails were observed. During G2-phase, two types of poly(A) tail lengths were observed- those with poly(A) tails of 25-50 nts and those with no poly(A) tails. It is interesting to note that Beilharz and Preiss, (2007) also observed a trend towards a shorter poly(A) tail in cell cycle regulated transcripts.

Although the 3' end cleavage and polyadenylation pathway is thought to be the main mechanism of cell cycle regulation of histone mRNAs, it is possible that the different poly(A) tail lengths visible during the cell cycle are a result of the differential use of the polyadenylation and non-polyadenylation pathways at different stages of the cell cycle. By doing this, the polyadenylation pathway for example, may be more active during the S-phase were histone mRNA levels are up-regulated. The non-polyadenylation pathway could then be more active during G2-phase were histone mRNAs are rapidly degraded. The detection of two different poly(A) tail lengths during G2-phase also suggests that this may be the case. During G2-phase, the transcripts with no poly(A) tail may be the result of regulation of histone mRNA levels by the components of the polyadenylation pathway upon exit from S-phase. The presence of poly(A) tails of 25-50nts on transcripts in G2-phase may be a result of a failsafe mechanism by the non-polyadenylation pathway to ensure a low level of histone *HTB1* mRNAs are present for the next round of replication.

Other factors required for histone mRNA biogenesis.

Previous studies have shown that the 3' end processing machinery of polyadenylated mRNA and non-polyadenylated non-coding RNA share a number of components, which include Hrp1p, Ssu72p and Rpb11p (Dheur et al., 2003; Sheldon et al., 2005; Steinmetz and Brow, 2003). Therefore we sought to understand the role of these proteins in histone mRNA biogenesis. Hrp1p, the only component of CF IB, is required for correct cleavage *in vivo* and acts as a RNA-binding protein that shuttles between the nucleus and the cytoplasm (Kessler et al., 1997; Steinmetz et al., 2006a). Hrp1p has also been found to influence the binding of non-polyadenylation termination machinery in the presence of additional RNA-binding proteins (Carroll et al., 2004). The phosphatase Ssu72p connects the 3' end processing to transcription by providing a bridge for transcription factor II B (TFIIB) and members of the CPF (Proudfoot, 2004). Ganem *et al.*, (2003) demonstrated that mutations in Ssu72p alter transcription

termination of the *NRD1* gene with read-through primary mRNA transcripts observed at the non-permissive temperature (Ganem et al., 2003). It has also been shown that mutations in Ssu72p not only alter the 3' end processing of snoRNAs but also some specific pre-mRNAs. This suggests that Ssu72p may play a specific role in the transcription termination of snoRNAs and some specific mRNAs (Carroll et al., 2004; Ganem et al., 2003; Steinmetz and Brow, 2003).

The *RPB11* gene encodes for the second smallest subunit of RNA Polymerase II which forms a heterodimer with *RPB3*, the third largest subunit of RNA Polymerase II (Steinmetz et al., 2006a). Steinmetz *et al.*, (2006) found that substitution in *RPB11* affected the recognition of both a snoRNA and an mRNA. It has been proposed that *sen1* interacts with the Rpb3/11p heterodimer and it has been previously shown through two-hybrid analysis and co-immunoprecipitation that *sen1* interacts with *RPB1* of RNA Polymerase II (Ursic et al., 2004).

The data presented in this research indicates that inactivation of Hrp1-5p alters the steady state levels of histone mRNA, while inactivation of Rpb11p led to a small but significant amount of read-through *HTB1* transcripts. Ssu72p was not found to exert an effect on transcription termination or steady state levels of *HTB1* mRNA. As each of these proteins may also exert a cell cycle specific effect on cleavage and polyadenylation of histone mRNAs, it would be interesting to examine their effect on cleavage and polyadenylation using the G-tailing method. Another protein of interest is Nab2p as it is involved in the binding of Pab1p onto the transcripts and is also involved in controlling the length of the poly(A) tail (Libri, 2010; Yamanaka et al., 2010). The protein Ccr4p may also warrant further analysis as mutations in a *CCR4* background have recently been shown to effect histone mRNAs (Azzouz et al., 2009b) and it has also been found to play a role in cell cycle progression (Westmoreland et al., 2004). Additionally, the CCR4-NOT complex has recently been shown to physically interact with both TRAMP and the exosome, indicating that it may play a role in nuclear mRNA degradation (Azzouz et al., 2009a).

Finally, we sought to uncover new factors required for histone mRNA biogenesis. Analysis of the DDE-interacting protein, Skp1p and the putative DDE-interacting F-box proteins revealed that mutations of these proteins had no effect on transcription termination of histone mRNA. Additionally, Northern blot and real-time RT-PCR

analysis of the mutants revealed that mutation of *SKP1* had no significant effect on the steady state levels of *HTB1* mRNA, while deletion of the F-box proteins *YDR131c*, *YLR352w*, *YLR224w* and *YLR368w* resulted in a decrease in the steady state levels of *HTB1* mRNA. Qualitative differences in histone mRNAs were also apparent in some of these mutants. In order to further understand the role of these F-box proteins and Skp1p in the 3' end processing of histone mRNA, it would be interesting to analyse their 3' ends via the G-tailing method. Skp1p may also be exerting cell cycle specific effects on the *HTB1* mRNA so analysis of a synchronised population in a *SKP1* mutant background should be carried out although an approach using the DEGRON plasmids may be necessary as mentioned above.

The observations presented in this study have uncovered many questions. The findings of this study suggest that regulation of poly(A) tail length contributes to the regulation of histone *HTB1* mRNA and that both Sen1p and Rrp6p may be contributing to this regulation. These findings also lead to the development of a model where both Sen1p and Rrp6p are active at the G1-/S-phase checkpoint of the cell cycle. In order to prove this hypothesis future work should include the analysis of poly(A) tail length during a cell cycle in a *sen1/Δrrp6* mutant. This would allow for the determination of whether mutation of both proteins has a significant effect on poly(A) tail length, particularly at the G1-/S-phase checkpoint of the cell cycle.

The model presented in this study also hypothesised that following S-phase of the cell cycle, active degradation of the *HTB1* mRNA occurs in a 3'-5' manner in the cytoplasm. This allows for the rapid reduction in levels of *HTB1* mRNA present in the cell upon entry into G2-phase. It was also hypothesised that a small number of transcripts with poly(A) tails of 25-50nts remain in the nucleus of the cell so a steady state level of *HTB1* mRNA is present in the nucleus throughout the cell cycle while shorter tailed (<25nts) transcripts are exported into the cytoplasm. In order to verify this hypothesis, fractionation of synchronised wild type cells and subsequent analysis of poly(A) tail length within each of the fractions should be carried out at different time-points of the cell cycle. This would allow for the distribution of the different classes of poly(A) tail length within the nuclear and the cytoplasmic fractions during G1- and G2-phase to be determined. To verify the fractionation of the samples was successful, RT-PCR on mRNA from both fractions could be carried out using *ACT1* primers which span the intron.

Furthermore, analysis of the effect of mutation of known degradation factors such as *CCR4* or *RRP6* on poly(A) tail length during the cell cycle would reveal more information about what degradation pathway is responsible for the production of transcripts with non-canonical 3' ends and whether this is a nuclear or cytoplasmic event.

As this study concentrated on *HTB1* mRNA it would be wise to apply the hybrid selection assay to the other histone genes. This would allow for the determination of whether *HTB1* is contributing to the regulation of poly(A) tail length independently of the other histone genes. This analysis should be carried out in both an asynchronous and synchronised population of wild type cells and also in the mutant strains mentioned in this study. In addition to investigating the length of the poly(A) tail in the other histone genes, analysis of poly(A) tail length within non-histone genes such as *ACT1* should also be conducted. A question of particular interest is whether poly(A) tail length during a cell cycle fluctuates in non-histone genes in a manner similar to *HTB1*?

The findings of this research also identified *HTB1* mRNA as having short (<25nts) poly(A) tails during S-phase of the cell cycle. However it is unknown whether this short poly(A) tail is added by Trf4p or Pap1p. In order to determine which poly(A) polymerase is responsible, analysis of poly(A) tail length during S-phase of the cell cycle should be carried out using both single and double mutants of these poly(A) polymerases. However this analysis may prove difficult as research has previously shown that Trf5p compensates for loss of Trf4p in a Δ*trf4* mutant (Reis and Campbell, 2007). This research suggests that a double Δ*trf4/Δtrf5* mutant and a triple Δ*trf4/Δtrf5/Δpap1* mutant would be necessary. The establishment of which poly(A) polymerase and therefore which 3' end processing pathway is active during S-phase of the cell cycle would add further information as to the role of the 3' end non-polyadenylated processing pathway in the regulation of histone mRNAs and whether it is truly a fail-safe mechanism or if it has a more active role in histone mRNA expression. If Trf4p was identified as the poly(A) polymerase responsible for the addition of short poly(A) tails to histone mRNA during S-phase of the cell cycle, it would be interesting to identify whether this was also the case for non-histone genes.

In conclusion, the data presented in this thesis confirms the previous findings of a role for non-polyadenylated processing factors in the biogenesis of histone mRNAs and

extends this analysis by showing that such factors can also influence poly(A) tail length. Furthermore, it was discovered that poly(A) tail length of histone mRNAs varies during the cell cycle. These data indicate for the first time that 3'end processing of histone mRNAs varies during the cell cycle correlation of these transcripts.

Chapter 7

References

Akhtar, M.S., Heidemann, M., Tietjen, J.R., Zhang, D.W., Chapman, R.D., Eick, D., and Ansari, A.Z. (2009). TFIIH kinase places bivalent marks on the carboxy-terminal domain of RNA polymerase II. Mol Cell *34*, 387-393.

Amrani, N., Minet, M., Wyers, F., Dufour, M.E., Aggerbeck, L.P., and Lacroute, F. (1997). PCF11 encodes a third protein component of yeast cleavage and polyadenylation factor I. Mol Cell Biol *17*, 1102-1109.

Arigo, J.T., Eyler, D.E., Carroll, K.L., and Corden, J.L. (2006). Termination of cryptic unstable transcripts is directed by yeast RNA-binding proteins Nrd1 and Nab3. Mol Cell *23*, 841-851.

Azzouz, N., Panasenko, O.O., Colau, G., and Collart, M.A. (2009a). The CCR4-NOT complex physically and functionally interacts with TRAMP and the nuclear exosome. PLoS One *4*, e6760.

Azzouz, N., Panasenko, O.O., Deluen, C., Hsieh, J., Theiler, G., and Collart, M.A. (2009b). Specific roles for the Ccr4-Not complex subunits in expression of the genome. RNA *15*, 377-383.

Bai, C., Sen, P., Hofmann, K., Ma, L., Goebl, M., Harper, J.W., and Elledge, S.J. (1996). SKP1 connects cell cycle regulators to the ubiquitin proteolysis machinery through a novel motif, the F-box. Cell *86*, 263-274.

Baxevanis, A.D., and Landsman, D. (1997). Histone and histone fold sequences and structures: a database. Nucleic Acids Res *25*, 272-273.

Baxevanis, A.D., and Landsman, D. (1998). Histone Sequence Database: new histone fold family members. Nucleic Acids Res *26*, 372-375.

Beilharz, T.H., and Preiss, T. (2007). Widespread use of poly(A) tail length control to accentuate expression of the yeast transcriptome. RNA *13*, 982-997.

Birnstiel, M., ed. (1988). Structure and function of minor snRNPs. (New York: Springer-Verlang).

Birse, C.E., Minvielle-Sebastia, L., Lee, B.A., Keller, W., and Proudfoot, N.J. (1998). Coupling termination of transcription to messenger RNA maturation in yeast. Science *280*, 298-301.

Bond, U., and Yario, T.A. (1994). The steady state levels and structure of the U7 snRNP are constant during the human cell cycle: lack of cell cycle regulation of histone mRNA 3' end formation. Cell Mol Biol Res *40*, 27-34.

Bond, U.M., Yario, T.A., and Steitz, J.A. (1991). Multiple processing-defective mutations in a mammalian histone pre-mRNA are suppressed by compensatory changes in U7 RNA both in vivo and in vitro. Genes and Development *5*, 1709-1722.

Buratowski, S. (2005). Connections between mRNA 3' end processing and transcription termination. Curr Opin Cell Biol *17*, 257-261.

Buratowski, S. (2009). Progression through the RNA polymerase II CTD cycle. Mol Cell *36*, 541-546.

Callahan, K.P., and Butler, J.S. (2010). TRAMP complex enhances RNA degradation by the nuclear exosome component Rrp6. J Biol Chem *285*, 3540-3547.

Campbell, S.G., Li Del Olmo, M., Beglan, P., and Bond, U. (2002). A sequence element downstream of the yeast HTB1 gene contributes to mRNA 3' processing and cell cycle regulation. Mol Cell Biol *22*, 8415-8425.

Canavan, R., and Bond, U. (2007). Deletion of the nuclear exosome component RRP6 leads to continued accumulation of the histone mRNA HTB1 in S-phase of the cell cycle in Saccharomyces cerevisiae. Nucleic Acids Res *35*, 6268-6279.

Carroll, K.L., Ghirlando, R., Ames, J.M., and Corden, J.L. (2007). Interaction of yeast RNA-binding proteins Nrd1 and Nab3 with RNA polymerase II terminator elements. RNA *13*, 361-373.

Carroll, K.L., Pradhan, D.A., Granek, J.A., Clarke, N.D., and Corden, J.L. (2004). Identification of cis elements directing termination of yeast nonpolyadenylated snoRNA transcripts. Mol Cell Biol *24*, 6241-6252.

Cho, D.C., Scharl, E.C., and Steitz, J.A. (1995). Decreasing the distance between the two conserved sequence elements of histone pre-messenger RNA interferes with 3' processing in vitro. RNA *1*, 905-914.

Chowdhury, A., Mukhopadhyay, J., and Tharun, S. (2007). The decapping activator Lsm1p-7p-Pat1p complex has the intrinsic ability to distinguish between oligoadenylated and polyadenylated RNAs. RNA *13*, 998-1016.

Ciais, D., Bohnsack, M.T., and Tollervey, D. (2008). The mRNA encoding the yeast ARE-binding protein Cth2 is generated by a novel 3' processing pathway. Nucleic Acids Res *36*, 3075-3084.

Connelly, C., and Hieter, P. (1996). Budding yeast SKP1 encodes an evolutionarily conserved kinetochore protein required for cell cycle progression. Cell *86*, 275-285.

Davila Lopez, M., and Samuelsson, T. (2008). Early evolution of histone mRNA 3' end processing. RNA *14*, 1-10.

Dheur, S., Nykamp, K.R., Viphakone, N., Swanson, M.S., and Minvielle-Sebastia, L. (2005). Yeast mRNA Poly(A) tail length control can be reconstituted in vitro in the absence of Pab1p-dependent Poly(A) nuclease activity. J Biol Chem *280*, 24532-24538.

Dheur, S., Vo le, T.A., Voisinet-Hakil, F., Minet, M., Schmitter, J.M., Lacroute, F., Wyers, F., and Minvielle-Sebastia, L. (2003). Pti1p and Ref2p found in association with the mRNA 3' end formation complex direct snoRNA maturation. EMBO J *22*, 2831-2840.

Dichtl, B., Blank, D., Sadowski, M., Hubner, W., Weiser, S., and Keller, W. (2002). Yhh1p/Cft1p directly links poly(A) site recognition and RNA polymerase II transcription termination. EMBO J *21*, 4125-4135.

Dichtl, B., and Keller, W. (2001). Recognition of polyadenylation sites in yeast pre-mRNAs by cleavage and polyadenylation factor. EMBO J *20*, 3197-3209.

Dominski, Z., and Marzluff, W.F. (1999). Formation of the 3' end of histone mRNA. Gene *239*, 1-14.

Dominski, Z., and Marzluff, W.F. (2007). Formation of the 3' end of histone mRNA: getting closer to the end. Gene *396*, 373-390.

Dunn, E.F., Hammell, C.M., Hodge, C.A., and Cole, C.N. (2005). Yeast poly(A)-binding protein, Pab1, and PAN, a poly(A) nuclease complex recruited by Pab1, connect mRNA biogenesis to export. Genes Dev *19*, 90-103.

Durr, M., Escobar-Henriques, M., Merz, S., Geimer, S., Langer, T., and Westermann, B. (2006). Nonredundant roles of mitochondria-associated F-box proteins Mfb1 and Mdm30 in maintenance of mitochondrial morphology in yeast. Mol Biol Cell *17*, 3745-3755.

Dye, M.J., and Proudfoot, N.J. (1999). Terminal exon definition occurs cotranscriptionally and promotes termination of RNA polymerase II. Mol Cell *3*, 371-378.

Egloff, S., O'Reilly, D., Chapman, R.D., Taylor, A., Tanzhaus, K., Pitts, L., Eick, D., and Murphy, S. (2007). Serine-7 of the RNA polymerase II CTD is specifically required for snRNA gene expression. Science *318*, 1777-1779.

Eriksson, P.R., Mendiratta, G., McLaughlin, N.B., Wolfsberg, T.G., Marino-Ramirez, L., Pompa, T.A., Jainerin, M., Landsman, D., Shen, C.H., and Clark, D.J. (2005). Global regulation by the yeast Spt10 protein is mediated through chromatin structure and the histone upstream activating sequence elements. Mol Cell Biol *25*, 9127-9137.

Fahrner, K., Yarger, J., and Hereford, L. (1980). Yeast histone mRNA is polyadenylated. Nucleic Acids Res *8*, 5725-5737.

Finkel, J.S., Chinchilla, K., Ursic, D., and Culbertson, M.R. (2010). Sen1p performs two genetically separable functions in transcription and processing of U5 small nuclear RNA in Saccharomyces cerevisiae. Genetics *184*, 107-118.

Fritz, S., Weinbach, N., and Westermann, B. (2003). Mdm30 is an F-box protein required for maintenance of fusion-competent mitochondria in yeast. Mol Biol Cell *14*, 2303-2313.

Ganem, C., Devaux, F., Torchet, C., Jacq, C., Quevillon-Cheruel, S., Labesse, G., Facca, C., and Faye, G. (2003). Ssu72 is a phosphatase essential for transcription termination of snoRNAs and specific mRNAs in yeast. EMBO J *22*, 1588-1598.

Gao, G., Bracken, A.P., Burkard, K., Pasini, D., Classon, M., Attwooll, C., Sagara, M., Imai, T., Helin, K., and Zhao, J. (2003). NPAT expression is regulated by E2F and is essential for cell cycle progression. Mol Cell Biol *23*, 2821-2833.

Gavin, A.C., Bosche, M., Krause, R., Grandi, P., Marzioch, M., Bauer, A., Schultz, J., Rick, J.M., Michon, A.M., Cruciat, C.M., *et al.* (2002). Functional organization of the yeast proteome by systematic analysis of protein complexes. Nature *415*, 141-147.

Ghazal, G., Gagnon, J., Jacques, P.E., Landry, J.R., Robert, F., and Elela, S.A. (2009). Yeast RNase III triggers polyadenylation-independent transcription termination. Mol Cell *36*, 99-109.

Glover-Cutter, K., Larochelle, S., Erickson, B., Zhang, C., Shokat, K., Fisher, R.P., and Bentley, D.L. (2009). TFIIH-associated Cdk7 kinase functions in phosphorylation of C-terminal domain Ser7 residues, promoter-proximal pausing, and termination by RNA polymerase II. Mol Cell Biol *29*, 5455-5464.

Goh, P.Y., and Surana, U. (1999). Cdc4, a protein required for the onset of S phase, serves an essential function during G(2)/M transition in Saccharomyces cerevisiae. Mol Cell Biol *19*, 5512-5522.

Gromak, N., West, S., and Proudfoot, N.J. (2006). Pause sites promote transcriptional termination of mammalian RNA polymerase II. Mol Cell Biol *26*, 3986-3996.

Gross, S., and Moore, C.L. (2001). Rna15 interaction with the A-rich yeast polyadenylation signal is an essential step in mRNA 3'-end formation. Mol Cell Biol *21*, 8045-8055.

Grunstein, M. (1992). Histones as regulators of genes. Sci Am *267*, 68-74B.

Grzechnik, P., and Kufel, J. (2008). Polyadenylation linked to transcription termination directs the processing of snoRNA precursors in yeast. Mol Cell *32*, 247-258.

Gudipati, R.K., Villa, T., Boulay, J., and Libri, D. (2008). Phosphorylation of the RNA polymerase II C-terminal domain dictates transcription termination choice. Nat Struct Mol Biol *15*, 786-794.

Harigaya, Y., Tanaka, H., Yamanaka, S., Tanaka, K., Watanabe, Y., Tsutsumi, C., Chikashige, Y., Hiraoka, Y., Yamashita, A., and Yamamoto, M. (2006). Selective elimination of messenger RNA prevents an incidence of untimely meiosis. Nature *442*, 45-50.

Harris, M.E., Bohni, R., Schneiderman, M.H., Ramamurthy, L., Schumperli, D., and Marzluff, W.F. (1991). Regulation of histone mRNA in the unperturbed cell cycle: evidence suggesting control at two posttranscriptional steps. Mol Cell Biol *11*, 2416-2424.

He, X., Khan, A.U., Cheng, H., Pappas, D.L., Jr., Hampsey, M., and Moore, C.L. (2003). Functional interactions between the transcription and mRNA 3' end processing machineries mediated by Ssu72 and Sub1. Genes Dev *17*, 1030-1042.

Helmling, S., Zhelkovsky, A., and Moore, C.L. (2001). Fip1 regulates the activity of Poly(A) polymerase through multiple interactions. Mol Cell Biol *21*, 2026-2037.

Hereford, L.M., Osley, M.A., Ludwig, T.R., 2nd, and McLaughlin, C.S. (1981). Cell-cycle regulation of yeast histone mRNA. Cell *24*, 367-375.

Hermand, D. (2006). F-box proteins: more than baits for the SCF? Cell Div *1*, 30.

Ho, M.S., Tsai, P.I., and Chien, C.T. (2006). F-box proteins: the key to protein degradation. J Biomed Sci *13*, 181-191.

Houseley, J., Kotovic, K., El Hage, A., and Tollervey, D. (2007). Trf4 targets ncRNAs from telomeric and rDNA spacer regions and functions in rDNA copy number control. EMBO J *26*, 4996-5006.

Houseley, J., LaCava, J., and Tollervey, D. (2006). RNA-quality control by the exosome. Nat Rev Mol Cell Biol *7*, 529-539.

Houser-Scott, F., Xiao, S., Millikin, C.E., Zengel, J.M., Lindahl, L., and Engelke, D.R. (2002). Interactions among the protein and RNA subunits of Saccharomyces cerevisiae nuclear RNase P. Proc Natl Acad Sci U S A *99*, 2684-2689.

Ito, H., Fukuda, Y., Murata, K., and Kimura, A. (1983). Transformation of intact yeast cells treated with alkali cations. J Bacteriol *153*, 163-168.

Kawauchi, J., Mischo, H., Braglia, P., Rondon, A., and Proudfoot, N.J. (2008). Budding yeast RNA polymerases I and II employ parallel mechanisms of transcriptional termination. Genes Dev *22*, 1082-1092.

Kaygun, H., and Marzluff, W.F. (2005). Regulated degradation of replication-dependent histone mRNAs requires both ATR and Upf1. Nat Struct Mol Biol *12*, 794-800.

Kessler, M.M., Henry, M.F., Shen, E., Zhao, J., Gross, S., Silver, P.A., and Moore, C.L. (1997). Hrp1, a sequence-specific RNA-binding protein that shuttles between the nucleus and the cytoplasm, is required for mRNA 3'-end formation in yeast. Genes Dev *11*, 2545-2556.

Kim, J.H., Zhao, Y., Pan, X., He, X., and Gilbert, H.F. (2009a). The unfolded protein response is necessary but not sufficient to compensate for defects in disulfide isomerization. J Biol Chem *284*, 10400-10408.

Kim, M., Krogan, N.J., Vasiljeva, L., Rando, O.J., Nedea, E., Greenblatt, J.F., and Buratowski, S. (2004). The yeast Rat1 exonuclease promotes transcription termination by RNA polymerase II. Nature *432*, 517-522.

Kim, M., Suh, H., Cho, E.J., and Buratowski, S. (2009b). Phosphorylation of the yeast Rpb1 C-terminal domain at serines 2, 5, and 7. J Biol Chem *284*, 26421-26426.

Kim, M., Vasiljeva, L., Rando, O.J., Zhelkovsky, A., Moore, C., and Buratowski, S. (2006a). Distinct pathways for snoRNA and mRNA termination. Mol Cell *24*, 723-734.

Kim, N., Yoon, H., Lee, E., and Song, K. (2006b). A new function of Skp1 in the mitotic exit of budding yeast Saccharomyces cerevisiae. J Microbiol *44*, 641-648.

Kipreos, E.T., and Pagano, M. (2000). The F-box protein family. Genome Biol *1*, REVIEWS3002.

Koepp, D.M., Kile, A.C., Swaminathan, S., and Rodriguez-Rivera, V. (2006). The F-box protein Dia2 regulates DNA replication. Mol Biol Cell *17*, 1540-1548.

Kolev, N.G., and Steitz, J.A. (2005). Symplekin and multiple other polyadenylation factors participate in 3'-end maturation of histone mRNAs. Genes Dev *19*, 2583-2592.

Komarnitsky, P., Cho, E.J., and Buratowski, S. (2000). Different phosphorylated forms of RNA polymerase II and associated mRNA processing factors during transcription. Genes Dev *14*, 2452-2460.

Krieg, P. (1996). A laboratory guide to RNA: Isolation, analysis and synthesis (New York).

Kuehner, J.N., and Brow, D.A. (2008). Regulation of a eukaryotic gene by GTP-dependent start site selection and transcription attenuation. Mol Cell *31*, 201-211.

Kyburz, A., Sadowski, M., Dichtl, B., and Keller, W. (2003). The role of the yeast cleavage and polyadenylation factor subunit Ydh1p/Cft2p in pre-mRNA 3'-end formation. Nucleic Acids Res *31*, 3936-3945.

LaBella, F., Sive, H.L., Roeder, R.G., and Heintz, N. (1988). Cell-cycle regulation of a human histone H2b gene is mediated by the H2b subtype-specific consensus element. Genes Dev *2*, 32-39.

LaCava, J., Houseley, J., Saveanu, C., Petfalski, E., Thompson, E., Jacquier, A., and Tollervey, D. (2005). RNA degradation by the exosome is promoted by a nuclear polyadenylation complex. Cell *121*, 713-724.

Lemay, J.F., D'Amours, A., Lemieux, C., Lackner, D.H., St-Sauveur, V.G., Bahler, J., and Bachand, F. (2010). The nuclear poly(A)-binding protein interacts with the exosome to promote synthesis of noncoding small nucleolar RNAs. Mol Cell *37*, 34-45.

Li, F.N., and Johnston, M. (1997). Grr1 of Saccharomyces cerevisiae is connected to the ubiquitin proteolysis machinery through Skp1: coupling glucose sensing to gene expression and the cell cycle. EMBO J *16*, 5629-5638.

Libri, D. (2010). Nuclear poly(a)-binding proteins and nuclear degradation: take the mRNA and run? Mol Cell *37*, 3-5.

Licatalosi, D.D., Geiger, G., Minet, M., Schroeder, S., Cilli, K., McNeil, J.B., and Bentley, D.L. (2002). Functional interaction of yeast pre-mRNA 3' end processing factors with RNA polymerase II. Mol Cell *9*, 1101-1111.

Lycan, D.E., Osley, M.A., and Hereford, L.M. (1987). Role of transcriptional and posttranscriptional regulation in expression of histone genes in Saccharomyces cerevisiae. Mol Cell Biol *7*, 614-621.

Lykke-Andersen, S., and Jensen, T.H. (2007). Overlapping pathways dictate termination of RNA polymerase II transcription. Biochimie *89*, 1177-1182.

Maillet, L., and Collart, M.A. (2002). Interaction between Not1p, a component of the Ccr4-not complex, a global regulator of transcription, and Dhh1p, a putative RNA helicase. J Biol Chem *277*, 2835-2842.

Mandel, C.R., Bai, Y., and Tong, L. (2008). Protein factors in pre-mRNA 3'-end processing. Cell Mol Life Sci *65*, 1099-1122.

Mandel, C.R., Kaneko, S., Zhang, H., Gebauer, D., Vethantham, V., Manley, J.L., and Tong, L. (2006). Polyadenylation factor CPSF-73 is the pre-mRNA 3'-end-processing endonuclease. Nature *444*, 953-956.

Marzluff, W.F., Wagner, E.J., and Duronio, R.J. (2008). Metabolism and regulation of canonical histone mRNAs: life without a poly(A) tail. Nat Rev Genet *9*, 843-854.

Millevoi, S., and Vagner, S. (2010). Molecular mechanisms of eukaryotic pre-mRNA 3' end processing regulation. Nucleic Acids Res *38*, 2757-2774.

Milligan, L., Torchet, C., Allmang, C., Shipman, T., and Tollervey, D. (2005). A nuclear surveillance pathway for mRNAs with defective polyadenylation. Mol Cell Biol *25*, 9996-10004.

Minvielle-Sebastia, L., Winsor, B., Bonneaud, N., and Lacroute, F. (1991). Mutations in the yeast RNA14 and RNA15 genes result in an abnormal mRNA decay rate; sequence analysis reveals an RNA-binding domain in the RNA15 protein. Mol Cell Biol *11*, 3075-3087.

Mischo, H.E., Gomez-Gonzalez, B., Grzechnik, P., Rondon, A.G., Wei, W., Steinmetz, L., Aguilera, A., and Proudfoot, N.J. (2011). Yeast Sen1 helicase protects the genome from transcription-associated instability. Mol Cell *41*, 21-32.

Miura, F., Kawaguchi, N., Sese, J., Toyoda, A., Hattori, M., Morishita, S., and Ito, T. (2006). A large-scale full-length cDNA analysis to explore the budding yeast transcriptome. Proc Natl Acad Sci U S A *103*, 17846-17851.

Moreira, M.C., Klur, S., Watanabe, M., Nemeth, A.H., Le Ber, I., Moniz, J.C., Tranchant, C., Aubourg, P., Tazir, M., Schols, L., *et al.* (2004). Senataxin, the ortholog of a yeast RNA helicase, is mutant in ataxia-ocular apraxia 2. Nat Genet *36*, 225-227.

Morlando, M., Greco, P., Dichtl, B., Fatica, A., Keller, W., and Bozzoni, I. (2002). Functional analysis of yeast snoRNA and snRNA 3'-end formation mediated by uncoupling of cleavage and polyadenylation. Mol Cell Biol *22*, 1379-1389.

Mullen, T.E., and Marzluff, W.F. (2008). Degradation of histone mRNA requires oligouridylation followed by decapping and simultaneous degradation of the mRNA both 5' to 3' and 3' to 5'. Genes Dev *22*, 50-65.

Narita, T., Yung, T.M., Yamamoto, J., Tsuboi, Y., Tanabe, H., Tanaka, K., Yamaguchi, Y., and Handa, H. (2007). NELF interacts with CBC and participates in 3' end processing of replication-dependent histone mRNAs. Mol Cell *26*, 349-365.

Nishimura, K., Fukagawa, T., Takisawa, H., Kakimoto, T., and Kanemaki, M. (2009). An auxin-based degron system for the rapid depletion of proteins in nonplant cells. Nature Methods *6*, 917-922.

Noble, C.G., Hollingworth, D., Martin, S.R., Ennis-Adeniran, V., Smerdon, S.J., Kelly, G., Taylor, I.A., and Ramos, A. (2005). Key features of the interaction between Pcf11 CID and RNA polymerase II CTD. Nat Struct Mol Biol *12*, 144-151.

Noble, C.G., Walker, P.A., Calder, L.J., and Taylor, I.A. (2004). Rna14-Rna15 assembly mediates the RNA-binding capability of Saccharomyces cerevisiae cleavage factor IA. Nucleic Acids Res *32*, 3364-3375.

Ohnacker, M., Barabino, S.M., Preker, P.J., and Keller, W. (2000). The WD-repeat protein pfs2p bridges two essential factors within the yeast pre-mRNA 3'-end-processing complex. Embo J *19*, 37-47.

Osley, M.A., and Hereford, L. (1982). Identification of a sequence responsible for periodic synthesis of yeast histone 2A mRNA. Proc Natl Acad Sci U S A *79*, 7689-7693.

Osley, M.A., and Hereford, L.M. (1981). Yeast histone genes show dosage compensation. Cell *24*, 377-384.

Osley, M.A., and Lycan, D. (1987). Trans-acting regulatory mutations that alter transcription of Saccharomyces cerevisiae histone genes. Mol Cell Biol *7*, 4204-4210.

Pandey, N.B., Sun, J.H., and Marzluff, W.F. (1991). Different complexes are formed on the 3' end of histone mRNA with nuclear and polyribosomal proteins. Nucleic Acids Res *19*, 5653-5659.

Park, N.J., Tsao, D.C., and Martinson, H.G. (2004). The two steps of poly(A)-dependent termination, pausing and release, can be uncoupled by truncation of the RNA polymerase II carboxyl-terminal repeat domain. Mol Cell Biol *24*, 4092-4103.

Pirngruber, J., and Johnsen, S.A. (2010). Induced G1 cell-cycle arrest controls replication-dependent histone mRNA 3' end processing through p21, NPAT and CDK9. Oncogene *29*, 2853-2863.

Pirngruber, J., Shchebet, A., Schreiber, L., Shema, E., Minsky, N., Chapman, R.D., Eick, D., Aylon, Y., Oren, M., and Johnsen, S.A. (2009). CDK9 directs H2B monoubiquitination and controls replication-dependent histone mRNA 3'-end processing. EMBO Rep *10*, 894-900.

Polevoda, B., Panciera, Y., Brown, S.P., Wei, J., and Sherman, F. (2006). Phenotypes of yeast mutants lacking the mitochondrial protein Pet20p. Yeast *23*, 127-139.

Proudfoot, N. (2004). New perspectives on connecting messenger RNA 3' end formation to transcription. Curr Opin Cell Biol *16*, 272-278.

Proudfoot, N.J., Furger, A., and Dye, M.J. (2002). Integrating mRNA processing with transcription. Cell *108*, 501-512.

Rasmussen, T.P., and Culbertson, M.R. (1998). The putative nucleic acid helicase Sen1p is required for formation and stability of termini and for maximal rates of synthesis and levels of accumulation of small nucleolar RNAs in Saccharomyces cerevisiae. Mol Cell Biol *18*, 6885-6896.

Recht, J., Dunn, B., Raff, A., and Osley, M.A. (1996). Functional analysis of histones H2A and H2B in transcriptional repression in Saccharomyces cerevisiae. Mol Cell Biol *16*, 2545-2553.

Reis, C.C., and Campbell, J.L. (2007). Contribution of Trf4/5 and the nuclear exosome to genome stability through regulation of histone mRNA levels in Saccharomyces cerevisiae. Genetics *175*, 993-1010.

Rondon, A.G., Mischo, H.E., Kawauchi, J., and Proudfoot, N.J. (2009). Fail-safe transcriptional termination for protein-coding genes in S. cerevisiae. Mol Cell *36*, 88-98.

Scharl, E.C., and Steitz, J.A. (1996). Length suppression in histone messenger RNA 3'-end maturation: processing defects of insertion mutant premessenger RNAs can be compensated by insertions into the U7 small nuclear RNA. Proc Natl Acad Sci U S A *93*, 14659-14664.

Sheldon, K.E., Mauger, D.M., and Arndt, K.M. (2005). A Requirement for the Saccharomyces cerevisiae Paf1 complex in snoRNA 3' end formation. Mol Cell *20*, 225-236.

Sive, H.L., Heintz, N., and Roeder, R.G. (1986). Multiple sequence elements are required for maximal in vitro transcription of a human histone H2B gene. Mol Cell Biol *6*, 3329-3340.

Spector, M.S., Raff, A., DeSilva, H., Lee, K., and Osley, M.A. (1997). Hir1p and Hir2p function as transcriptional corepressors to regulate histone gene transcription in the Saccharomyces cerevisiae cell cycle. Mol Cell Biol *17*, 545-552.

Stearns, T., Kahn, R.A., Botstein, D., and Hoyt, M.A. (1990). ADP ribosylation factor is an essential protein in Saccharomyces cerevisiae and is encoded by two genes. Mol Cell Biol *10*, 6690-6699.

Steinmetz, E.J., and Brow, D.A. (1996). Repression of gene expression by an exogenous sequence element acting in concert with a heterogeneous nuclear ribonucleoprotein-like protein, Nrd1, and the putative helicase Sen1. Mol Cell Biol *16*, 6993-7003.

Steinmetz, E.J., and Brow, D.A. (1998). Control of pre-mRNA accumulation by the essential yeast protein Nrd1 requires high-affinity transcript binding and a domain implicated in RNA polymerase II association. Proc Natl Acad Sci U S A *95*, 6699-6704.

Steinmetz, E.J., and Brow, D.A. (2003). Ssu72 protein mediates both poly(A)-coupled and poly(A)-independent termination of RNA polymerase II transcription. Mol Cell Biol *23*, 6339-6349.

Steinmetz, E.J., Conrad, N.K., Brow, D.A., and Corden, J.L. (2001). RNA-binding protein Nrd1 directs poly(A)-independent 3'-end formation of RNA polymerase II transcripts. Nature *413*, 327-331.

Steinmetz, E.J., Ng, S.B., Cloute, J.P., and Brow, D.A. (2006a). cis- and trans-Acting determinants of transcription termination by yeast RNA polymerase II. Mol Cell Biol *26*, 2688-2696.

Steinmetz, E.J., Warren, C.L., Kuehner, J.N., Panbehi, B., Ansari, A.Z., and Brow, D.A. (2006b). Genome-wide distribution of yeast RNA polymerase II and its control by Sen1 helicase. Mol Cell *24*, 735-746.

Sullivan, K.D., Steiniger, M., and Marzluff, W.F. (2009). A core complex of CPSF73, CPSF100, and Symplekin may form two different cleavage factors for processing of poly(A) and histone mRNAs. Mol Cell *34*, 322-332.

Suraweera, A., Becherel, O.J., Chen, P., Rundle, N., Woods, R., Nakamura, J., Gatei, M., Criscuolo, C., Filla, A., Chessa, L., *et al.* (2007). Senataxin, defective in ataxia oculomotor apraxia type 2, is involved in the defense against oxidative DNA damage. J Cell Biol *177*, 969-979.

Sutton, A., Bucaria, J., Osley, M.A., and Sternglanz, R. (2001). Yeast ASF1 protein is required for cell cycle regulation of histone gene transcription. Genetics *158*, 587-596.

Tacahashi, Y., Helmling, S., and Moore, C.L. (2003). Functional dissection of the zinc finger and flanking domains of the Yth1 cleavage/polyadenylation factor. Nucleic Acids Res *31*, 1744-1752.

Trautwein, M., Dengjel, J., Schirle, M., and Spang, A. (2004). Arf1p provides an unexpected link between COPI vesicles and mRNA in Saccharomyces cerevisiae. Mol Biol Cell *15*, 5021-5037.

Ursic, D., Chinchilla, K., Finkel, J.S., and Culbertson, M.R. (2004). Multiple protein/protein and protein/RNA interactions suggest roles for yeast DNA/RNA helicase Sen1p in transcription, transcription-coupled DNA repair and RNA processing. Nucleic Acids Res *32*, 2441-2452.

Vanacova, S., Wolf, J., Martin, G., Blank, D., Dettwiler, S., Friedlein, A., Langen, H., Keith, G., and Keller, W. (2005). A new yeast poly(A) polymerase complex involved in RNA quality control. PLoS Biol *3*, e189.

Vasiljeva, L., and Buratowski, S. (2006). Nrd1 interacts with the nuclear exosome for 3' processing of RNA polymerase II transcripts. Mol Cell *21*, 239-248.

Vasiljeva, L., Kim, M., Mutschler, H., Buratowski, S., and Meinhart, A. (2008). The Nrd1-Nab3-Sen1 termination complex interacts with the Ser5-phosphorylated RNA polymerase II C-terminal domain. Nat Struct Mol Biol *15*, 795-804.

Villa, T., Rougemaille, M., and Libri, D. (2008). Nuclear quality control of RNA polymerase II ribonucleoproteins in yeast: tilting the balance to shape the transcriptome. Biochim Biophys Acta *1779*, 524-531.

Viphakone, N., Voisinet-Hakil, F., and Minvielle-Sebastia, L. (2008). Molecular dissection of mRNA poly(A) tail length control in yeast. Nucleic Acids Res *36*, 2418-2433.

Wallace, R., Shaffer, J., Murphy, R., Bonner, J., Hirose, T. and Itakura, K. (1979). Hybridisation of synthetic oligodeoxyribonucleotides to phi chi 174 DNA: The effect of single base pair mismatch. Nucleic Acids Res *6*, 3543-3557.

West, S., Gromak, N., and Proudfoot, N.J. (2004). Human 5' --> 3' exonuclease Xrn2 promotes transcription termination at co-transcriptional cleavage sites. Nature *432*, 522-525.

Westmoreland, T.J., Marks, J.R., Olson, J.A., Jr., Thompson, E.M., Resnick, M.A., and Bennett, C.B. (2004). Cell cycle progression in G1 and S phases is CCR4 dependent following ionizing radiation or replication stress in Saccharomyces cerevisiae. Eukaryot Cell *3*, 430-446.

Whitelaw, E., and Proudfoot, N. (1986). Alpha-thalassaemia caused by a poly(A) site mutation reveals that transcriptional termination is linked to 3' end processing in the human alpha 2 globin gene. EMBO J *5*, 2915-2922.

Willems, A.R., Schwab, M., and Tyers, M. (2004). A hitchhiker's guide to the cullin ubiquitin ligases: SCF and its kin. Biochim Biophys Acta *1695*, 133-170.

Williams, A.S., and Marzluff, W.F. (1995). The sequence of the stem and flanking sequences at the 3' end of histone mRNA are critical determinants for the binding of the stem-loop binding protein. Nucleic Acids Res *23*, 654-662.

Wilusz, C.J., and Wilusz, J. (2008). New ways to meet your (3') end oligouridylation as a step on the path to destruction. Genes Dev *22*, 1-7.

Woolstencroft, R.N., Beilharz, T.H., Cook, M.A., Preiss, T., Durocher, D., and Tyers, M. (2006). Ccr4 contributes to tolerance of replication stress through control of CRT1 mRNA poly(A) tail length. J Cell Sci *119*, 5178-5192.

Xiao, S., Hsieh, J., Nugent, R.L., Coughlin, D.J., Fierke, C.A., and Engelke, D.R. (2006). Functional characterization of the conserved amino acids in Pop1p, the largest common protein subunit of yeast RNases P and MRP. RNA *12*, 1023-1037.

Xu, H.X., Johnson, L., and Grunstein, M. (1990). Coding and noncoding sequences at the 3' end of yeast histone H2B mRNA confer cell cycle regulation. Mol Cell Biol *10*, 2687-2694.

Yamanaka, S., Yamashita, A., Harigaya, Y., Iwata, R., and Yamamoto, M. (2010). Importance of polyadenylation in the selective elimination of meiotic mRNAs in growing S. pombe cells. EMBO J *29*, 2173-2181.

Yao, G., Chiang, Y.C., Zhang, C., Lee, D.J., Laue, T.M., and Denis, C.L. (2007). PAB1 self-association precludes its binding to poly(A), thereby accelerating CCR4 deadenylation in vivo. Mol Cell Biol *27*, 6243-6253.

Yin, Q.Y., de Groot, P.W., Dekker, H.L., de Jong, L., Klis, F.M., and de Koster, C.G. (2005). Comprehensive proteomic analysis of Saccharomyces cerevisiae cell walls: identification of proteins covalently attached via glycosylphosphatidylinositol remnants or mild alkali-sensitive linkages. J Biol Chem *280*, 20894-20901.

Yonaha, M., and Proudfoot, N.J. (1999). Specific transcriptional pausing activates polyadenylation in a coupled in vitro system. Mol Cell *3*, 593-600.

Yoshida, Y. (2007). F-box proteins that contain sugar-binding domains. Biosci Biotechnol Biochem *71*, 2623-2631.

Zhang, Z., Fu, J., and Gilmour, D.S. (2005). CTD-dependent dismantling of the RNA polymerase II elongation complex by the pre-mRNA 3'-end processing factor, Pcf11. Genes Dev *19*, 1572-1580.

Zhang, Z., and Gilmour, D.S. (2006). Pcf11 is a termination factor in Drosophila that dismantles the elongation complex by bridging the CTD of RNA polymerase II to the nascent transcript. Mol Cell *21*, 65-74.

Zhao, J., Hyman, L., and Moore, C. (1999). Formation of mRNA 3' ends in eukaryotes: mechanism, regulation, and interrelationships with other steps in mRNA synthesis. Microbiol Mol Biol Rev *63*, 405-445.

Appendixes

Appendix 1: Analysis of asynchronous cells

46a 30°C

Colony Number	Poly(A) Tail Length	Cleavage Site Used
colony 1	45nts	cleavage site 5 (+533)
colony 3	44nts	cleavage site 4 (+522)
colony 5	27nts	cleavage site 4 (+522)
colony 8	27nts	cleavage site 4 (+522)
colony 9	9nts	cleavage site 2 (+504)
colony 13	45nts	cleavage site 5 (+533)
colony 15	47nts	cleavage site 3 (+513)
colony 16	25nts	cleavage site 2 (+504)

46a 37°C

Colony Number	Poly(A) Tail Length	Cleavage Site Used
colony 4	15nts	cleavage site 1 (+487)
colony 6	32nts	cleavage site 4 (+522)
colony 10	34nts	cleavage site 4 (+522)
colony 11	32nts	cleavage site 4 (+522)
colony 12	32nts	cleavage site 2 (+504)
colony 13	32nts	cleavage site 4 (+522)
colony 19	33nts	cleavage site 3 (+513)
colony 34	33nts	cleavage site 4 (+522)
colony 45	31nts	cleavage site 4 (+522)
colony 48	87nts	cleavage site 4 (+522)

***sen1* 25°C**

Colony Number	Poly(A) Tail Length	Cleavage Site Used
colony 1	45nts	cleavage site 4 (+522)
colony 5	55nts	cleavage site 4 (+522)
colony 6	43nts	cleavage site 4 (+522)
colony 8	28nts	cleavage site 4 (+522)
colony 13	26nts	cleavage site 4 (+522)
colony 14	17nts	cleavage site 4 (+522)
colony 20	19nts	cleavage site 4 (+522)

***sen1* 37°C**

Colony Number	Poly(A) Tail Length	Cleavage Site Used
colony 1A	32nts	cleavage site 4 (+522)
colony 1B	11nts	cleavage site 1 (+487)
colony 1C	50nts	cleavage site 4 (+522)
colony 3	41nts	cleavage site 3 (+513)
colony 4	37nts	cleavage site 3 (+513)
colony 7	42nts	cleavage site 4 (+522)
colony 13	40nts	cleavage site B (+561)
colony 14	17nts	cleavage site 3 (+513)
colony 15	53nts	cleavage site 2 (+504)
colony 16A	17nts	cleavage site 4 (+522)
colony 16B	41nts	cleavage site 3 (+513)
colony 17	16nts	cleavage site 3 (+513)
colony 18	19nts	cleavage site 2 (+504)
colony 24	19nts	cleavage site 4 (+522)
colony 37	19nts	cleavage site 4 (+522)
colony 40	26nts	cleavage site 3 (+513)

***rna14-3/Δrrp6* 37°C**

Colony Number	Poly(A) Tail Length	Cleavage Site Used
colony 3	23nts	cleavage site 4 (+522)
colony 4	6nts	cleavage site 3 (+513)
colony 10	6nts	cleavage site 3 (+513)
colony 14	29nts	cleavage site 4 (+522)
colony 15	41nts	cleavage site 3 (+513)
colony 16	5nts	cleavage site 4 (+522)
colony 25	31nts	cleavage site 4 (+522)
colony 29	23nts	cleavage site 4 (+522)
colony 30	33nts	cleavage site 3 (+513)
colony 38	none	cleavage site 1 (+487)

***Δrrp6* 30°C**

Colony Number	Poly(A) Tail Length	Cleavage Site Used
colony 8	18nts	cleavage site 4 (+522)
colony 11	29nts	cleavage site 4 (+522)
colony 12	14nts	cleavage site 2 (+504)
colony 13	16nts	cleavage site A (+475)
colony 15	22nts	cleavage site 4 (+522)
colony 18	8nts	cleavage site 1 (+487)
colony 19A	24nts	cleavage site 4 (+522)
colony 19B	28nts	cleavage site 4 (+522)
colony 24	28nts	cleavage site 2 (+504)
colony 35	56nts	cleavage site 4 (+522)

Appendix 2: Analysis of synchronised wild type 46a cells

0 min

Colony Number	Poly(A) Tail Length	Cleavage Site Used
colony 10	39nts	cleavage site 4 (+522)
colony 13	20nts	cleavage site 4 (+522)
colony 18	56nts	cleavage site 4 (+522)
colony 23	57nts	cleavage site 4 (+522)
colony 26	58nts	cleavage site 4 (+522)
colony 27	59nts	cleavage site 4 (+522)
colony 29	53nts	cleavage site 4 (+522)
colony 31	26nts	cleavage site 4 (+522)

15 min

Colony Number	Poly(A) Tail Length	Cleavage Site Used
colony 1	0nts	cleaving at +439
colony 4	52nts	cleavage site 4 (+522)
colony 5	57nts	cleavage site 4 (+522)
colony 14	28nts	cleavage site 4 (+522)
colony 17	0nts	cleaving at +142
colony 26	53nts	cleavage site 4 (+522)
colony 29A	51nts	cleavage site 4 (+522)
colony 29B	15nts	cleavage site 1 (+487)
colony 31	25nts	cleavage site 4 (+522)

30 min

Colony Number	Poly(A) Tail Length	Cleavage Site Used
colony 1	16nts	cleavage site 2 (+522)
colony 3	18nts	cleavage site 4 (+522)
colony 4	28nts	cleavage site 4 (+522)
colony 6	0nts	cleavage site 3 (+513)
colony 9	38nts	cleavage site 4 (+522)
colony 15	39nts	cleavage site 4 (+522)
colony 23	38nts	cleavage site 2 (+504)
colony 24	0nts	cleaving at +412

45 min

Colony Number	Poly(A) Tail Length	Cleavage Site Used
colony 1A	18nts	cleavage site 4 (+522)
colony 1B	28nts	cleavage site 4 (+522)
colony 3	16nts	cleavage site 4 (+522)
colony 8	19nts	cleavage site 4 (+522)
colony 11	29nts	cleavage site 4 (+522)
colony 13	16nts	cleavage site 4 (+522)
colony 15	17nts	cleavage site 3 (+513)
colony 14	26nts	cleavage site 1 (+487)
colony 17	56nts	cleavage site 4 (+522)

60 min

Colony Number	Poly(A) Tail Length	Cleavage Site Used
colony 4	0nts	cleaving at +418
colony 3	12nts	cleavage site 4 (+522)
colony 5	49nts	cleavage site 3 (+513)
colony 18	31nts	cleavage site 3 (+513)
colony 21	30nts	cleavage site 3 (+513)
colony 36	0nts	cleaving at +418
colony 37	20nts	cleavage site 4 (+522)
colony 39	35nts	cleavage site 3 (+513)

75 min

Colony Number	Poly(A) Tail Length	Cleavage Site Used
colony 1	2nts	cleaving at +375
colony 7A	32nts	cleavage site 3 (+513)
colony 7B	31nts	cleavage site 3 (+513)
colony 8	24nts	cleavage site 4 (+522)
colony 11	0nts	cleaving at +252
colony 12	0nts	cleaving at +439
colony 14	0nts	cleaving at +378
colony 15	26nts	cleavage site 2 (+504)
colony 18	24nts	cleavage site 4 (+522)
colony 19	0nts	cleaving at +378
colony 24A	50nts	cleavage site 4 (+522)
colony 24B	53nts	cleavage site 4 (+522)
colony 25A	36nts	cleavage site 4 (+522)
colony 25B	36nts	cleavage site 4 (+522)
colony 32	0nts	cleaving at +143
colony 38	0nts	cleaving at +143

90 min

Colony Number	Poly(A) Tail Length	Cleavage Site Used
colony 1	48nts	cleavage site 4 (+522)
colony 3	33nts	cleavage site 4 (+522)
colony 5	24nts	cleavage site 4 (+522)
colony 21	19nts	cleaving at +478
colony 23	18nts	cleavage site 3 (+513)
colony 27	44nts	cleavage site 2 (+504)
colony 35	0nts	cleaving at +281
colony 42A	15nts	cleavage site 4 (+522)
colony 42B	15nts	cleavage site 4 (+522)
colony 44A	17nts	cleavage site 3 (+513)
colony 44B	17nts	cleavage site 3 (+513)

120 min

Colony Number	Poly(A) Tail Length	Cleavage Site Used
colony 3	45nts	cleavage site 4 (+522)
colony 5	47nts	cleavage site 4 (+522)
colony 7	29nts	cleavage site 4 (+522)
colony 8	48nts	cleavage site 1 (+487)
colony 11	29nts	cleavage site 4 (+522)
colony 13	22nts	cleavage site 4 (+522)
colony 15	21nts	cleavage site 4 (+522)
colony 16	20nts	cleavage site 4 (+522)
colony 19	26nts	cleavage site 4 (+522)
colony 20	28nts	cleavage site 4 (+522)

Supplementary Data